

UC Davis

UC Davis Electronic Theses and Dissertations

Title

CHARACTERIZATION OF THE GLYCOME AND GLYCOPROTEOME IN ALZHEIMER'S DISEASE PATIENTS BY LIQUID CHROMATOGRAPHY-MASS SPECTROMETRY

Permalink

<https://escholarship.org/uc/item/3q13x8v7>

Author

Tena, Jennyfer

Publication Date

2021

Peer reviewed|Thesis/dissertation

CHARACTERIZATION OF THE GLYCOME AND GLYCOPROTEOME IN ALZHEIMER'S DISEASE
PATIENTS BY LIQUID CHROMATOGRAPHY-MASS SPECTROMETRY

By

JENNYFER TENA

DISSERTATION

Submitted in partial satisfaction of the requirements for the degree of

DOCTOR OF PHILOSOPHY

in

CHEMISTRY

in the

OFFICE OF GRADUATE STUDIES

of the

UNIVERSITY OF CALIFORNIA

DAVIS

Approved:

Carlito B. Lebrilla, Chair

Sheila S. David

Andrew J. Fisher

Committee in Charge

2022

DEDICATION

In memory of my father.

To my mother, brother, and sisters
for their unconditional love and support.

ACKNOWLEDGEMENTS

I will forever be grateful to my Ph.D. advisor Prof. Carlito B. Lebrilla. His continuous support and mentorship were essential to my growth as a scientist. I could not have made it without his guidance. The opportunities he provided me such as attending national conferences strengthen my communication skills as a scientist. He taught me how to write scientific papers and how to critically design and execute projects. Conducting my Ph.D. studies under his guidance is one of the best decisions I have made in my life, thank you Carlito.

I am also thankful to the entire Lebrilla Lab. Special thanks to Dr. Mariana Barboza, for her endless teaching and support when I recently joined the lab. Many thanks to Dr. Maurice Wong for helping me tremendously when I joined the lab. I will always be thankful for his mass spectrometry teaching and patience. I would also like to thank our former lab manager Diane Tu and our current lab manager Winnie Chen for always being helpful and creating an enjoyable lab environment. Thanks to Dave Zhou, Juan Castillo, Chris Ranque and Ying Sheng for their friendship and all the good and fun memories together. In addition, I would like to thank previous lab members for offering great advice: Matthew Amicucci, Ace Galermo, Eshani Nandita, Qiongyu Li, and Yixuan Xie. I also want to thank Xinyu Tang, Chenghao Zhu and Russel Alvarez for their help on different aspects of my research and my undergraduate research assistants Shira Tikofsky and Maria Barajas for all their help in performing experiments. To all the current group members, Cathy Chen, Garret Couture, Nikko Bacalzo, Anita Vinjamuri, Armin Oloumi, Ryan Schindler, Yasmine Bouchibti, Cheng-Yu Weng and Aaron Stacy thank you for your support and friendship.

I would also like to thank our collaborators Professor Lee-Way Jin, Professor Izumi Maezawa, Professor Daniela Harvey and Professor Angela Zivkovic for all their great input, great discussions, helping me move the projects forward and teaching me new scientific techniques.

Special thanks to my dissertation committee members, Professor Sheila David and Professor Andy Fisher for their guidance and advise on my qualifying exam and dissertation.

Lastly, thanks to my sisters Stephanie, Arismel, Fabiola and Nancy for their encouragement during my graduate studies. My best friends Sandrine Kyane, Sandra Valdivia and Tracy Aguilar for always cheering me on. My undergraduate mentors Yuli Ortega, Dr. Bakthan Singram, Dr. Indranil Chakraborty and Professor Ted Holman – thank you all from the bottom of my heart.

ABSTRACT

Chapter I introduces the importance and challenges of studying glycosylation. The chapter describes the long-term associations between glycosylation and brain development. However, emphasis is placed in the interplay between protein glycosylation and Alzheimer's Disease. The chapter further discusses the key aspects of employing mass spectrometry techniques for glycomic and glycoproteomic analysis.

In **Chapter II**, a comprehensive map of the N-glycome and glycoproteome of the human brain is presented. The study involved four subjects, two with confirmed Alzheimer Disease neuropathology and the remaining two termed non-cognitive impaired. This map involved 11 functional human brain regions per subject. The research described in **Chapter III**, resulted from the human brain glycome map findings. This study only focused on three functional brain regions affected differently in the Alzheimer's Disease pathology. The study design involved higher biological replicates per region and was characterized using a novel nano-liquid chromatography chip-quadrupole-time of flight mass spectrometry (nanoLC-Chip-Q-ToF MS) platform.

The motivation behind **Chapter IV**, involved the increased demand for the development of novel blood-based biomarkers for early detection, prevention, or intervention in Alzheimer's Disease. This research sought out to determine whether serum glycopeptide analysis holds potential for identifying novel diagnostics and prognostics of Alzheimer's Disease. This work used an ultra-high-performance liquid-chromatography triple quadrupole mass spectrometry (UHPLC-QqQ-MS) operated in dynamic multiple reaction monitoring (dMRM) mode to monitor glycopeptides alterations in Alzheimer's Disease patients.

Together these chapters highlight the powerful application of mass spectrometry techniques in biological and biomarker research discovery.

ABBREVIATIONS

A β : amyloid beta

AD: Alzheimer's Disease

C: Complex

CID: Collision Induced Dissociation

CV: Coefficient of Variation

ECC: Extracted Compound Chromatogram

EIC: Extracted Ion Chromatogram

ESI: Electrospray Ionization

FA: Formic Acid

Fuc: Fucose

Gal: Galactose

GalNAc: N-Acetyl-D-galactosamine

Glc: Glucose

GlcNAc: N-Acetyl-D-glucosamine

GSL: Glycosphingolipid

H: Hybrid

Hex: Hexose

HexNAc: N-Acetyl-hexosamine

HILIC: Hydrophilic Interaction Liquid Chromatography

HM: High Mannose

HMO: Human Milk Oligosaccharide

HPLC: High Performance Liquid Chromatography

MALDI: Matrix-Assisted Laser Desorption/Ionization

Man: Mannose

MRM: Multiple Reaction Monitoring

MS: Mass Spectrometry

Nano-LC: Nanoflow-Liquid Chromatography

NCAM: Neuronal Cell Adhesion Molecule

NeuAc: N-Acetylneuraminic Acid

PGC: Porous Graphitized Carbon

PNGase F: Peptide N-Glycosidase F

PTM: Post-translational Modification

RSD: Relative Standard Deviation

SPE: Solid-Phase Extraction

TIC: Total Ion Chromatogram

TOF: Time-of-Flight

UHPLC: Ultra-High Performance Liquid Chromatograph

Table of Contents

Title Page	i
Dedication	ii
Acknowledgements	iii
Abstract	v
Abbreviations	vii
Chapter I. Introduction to Glycans, Alzheimer’s Disease, and Liquid Chromatography-Mass Spectrometry	1
Overview	2
Monosaccharides in the Human Glycome	4
N-Glycans	5
O-Glycans	6
Glycosphingolipids	7
Important Biological Function of Glycans	9
Glycosylation in Alzheimer’s Disease	11
Glycomic Profiling and the Mammalian Brain	12
Glycan Analysis using LC-MS	19
References	23
Chapter II. Regio-Specific N-Glycome and N-Glycoproteome Map of the Elderly Human Brain with and without Alzheimer’s Disease	27
Abstract	28
Introduction	29
Results	32
Human brain global N-glycome profiling in a region-specific manner	32
N-Glycomic variations in the brain regions	38
Glycoproteomic analysis of the brain regions	42

Discussion	53
Conclusion	56
Methods	57
Cell membrane extraction from human brain tissue	57
Enzymatic Release and Purification of N-Glycans	57
Glycoproteomics Enzymatic Digestion and Purification	58
Glycomics Analysis by LC-MS/MS	58
Data Analysis	60
References	61
Supplementary Data	64

Chapter III. Glycosylation alterations across three pathological stages in the human brain of Alzheimer’s disease patients81

Abstract	82
Introduction	83
Results and Discussion	84
N-Glycome alterations across three pathological stages in AD	84
Glycosphingolipid (GSL) alterations across three pathological stages in AD	88
Conclusion	91
Methods	92
Cell membrane extraction from human brain tissue	92
Enzymatic Release and Purification of N-Glycans	92
Release and Purification of Glycosphingolipids	93
Glycomics Analysis by LC-MS/MS	93
References	96
Supplementary Data	98

Chapter IV. Glycosylation alterations in serum of Alzheimer’s disease patients show widespread changes in N-glycosylation of proteins related to immune function, inflammation, and lipoprotein metabolism.....102

Abstract	103
Introduction	105
Experimental	106
Study Design	106
Sample Preparation	108
UPLC–ESI-QqQ–MS Analysis of Serum Glycoproteomic	108
Data Processing and Statistical Analysis	109
Results	111
Fucosylated and Sialylated Glycopeptides in AD	111
Identification of Aberrant Fucosylated or Sialylated Glycopeptides in AD	113
Glycopeptide Signatures of AD	113
Identification of Aberrant Glycopeptides in AD	115
Potential Confounders	117
Associations Between Glycopeptides and Clinical Cognitive Scores	117
Discussion	119
Conclusion	121
References	123
Supplementary Data	126

Chapter I

Introduction to Glycans, Alzheimer's Disease, and Liquid Chromatography-Mass Spectrometry

Overview

Every cell in the human body such as immune cells, blood cells, neurons, and all others are covered by a dense layer of glycans. These glycans are covalently attached to lipids and to the polypeptide of proteins to form the “glycocalyx.” For many decades, the glycocalyx has been known to be a protective layer to cells. Current work shows that the glycocalyx is an organelle of vital importance actively involved in many cellular process that can aid in therapeutic contexts (1). The biosynthesis for glycoproteins and glycolipids is performed in the Endoplasmic Reticulum (ER) and the Golgi apparatus. The glycans are metabolically synthesized to yield a suite of structures that vary heterogeneously by linkage, length, number of antennae, and composition. Efforts into depicting these complicated structures has hindered our understanding of the glycocalyx. For such reasons, glycomics and glycoproteomic alterations caused in disease state have not advanced at the rate of other -omic analysis such as genomics or proteomics.


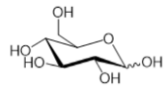

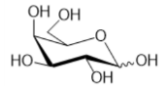

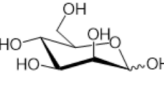

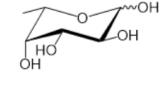

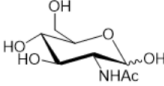

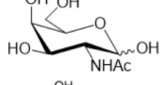

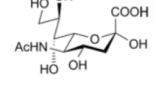
Development of comprehensive analytical methods to depict the fine structure of these glycoconjugates is of great importance. Mass spectrometry has been at the center of this effort. Utilizing novel mass spectrometry tools, the work presented in this thesis focuses on mapping and profiling three types of glycoconjugates including N- and O- glycans, glycosphingolipids, and their corresponding glycoproteins. Mass spectrometry methods are employed as they yield, structurally informative fragments, accurate mass, and can be coupled to separation methods such as high-performance liquid chromatography (HPLC). Using both approaches, glycans can then be separated chromatographically and analyzed using mass spectrometry. This chapter will focus on discussing the important biological functions of glycans their role in a

neurodegenerative disease like Alzheimer's disease as well as the mass spectrometry techniques utilized for their characterization.

Monosaccharides in the human glycome

Monosaccharides are the most basic form of carbohydrates. In nature they exist as free or linked through glycosidic bonds to form larger carbohydrates as oligosaccharide or polysaccharides. Monosaccharides including D-glucose (Glc), D-galactose (Gal), D-mannose (Man), *N*-acetyl-D-glucosamine (GlcNAc), *N*-acetyl-D-galactosamine (GalNAc), L-fucose (Fuc), and *N*-acetylneuraminic acid (Neu5Ac) are the most common components in N-glycans, O-glycans and glycolipids, **Table 1**.

Table 1: Monosaccharide Structures.

Symbol	Name	Abbreviation	Monosaccharide Structure
	D-glucose	Glc	
	D-galactose	Gal	
	D-mannose	Man	
	L-fucose	Fuc	
	<i>N</i> -acetyl-D-glucosamine	GlcNAc	
	<i>N</i> -acetyl-D-galactosamine	GalNAc	
	<i>N</i> -acetylneuraminic acid	Neu5Ac	

N-Glycans

N-Glycosylation begins in the endoplasmic reticulum with the addition of a precursor oligo-saccharide $\text{Glc}_3\text{Man}_9\text{GlcNAc}_2$, which is transferred from the lipid dolichyl-pyrophosphate (dolichyl-PP) to the luminal side of a polypeptide chain (2). The N-glycans are covalently attached to an asparagine sharing a common sequence, $\text{Man}\alpha 1-6(\text{Man}\alpha 1-3)\text{Man}\beta 1-4\text{GlcNAc}\beta 1-4\text{GlcNAc}\beta 1-\text{Asn-X-Ser/Thr}$, and are classified into three general types: oligomannose, complex and hybrid (3). The complex and hybrid N-glycans can then be further structurally understood by grouping them into neutral, fucosylated-only, sialylated-only and sialofucosylated **Figure 1**.

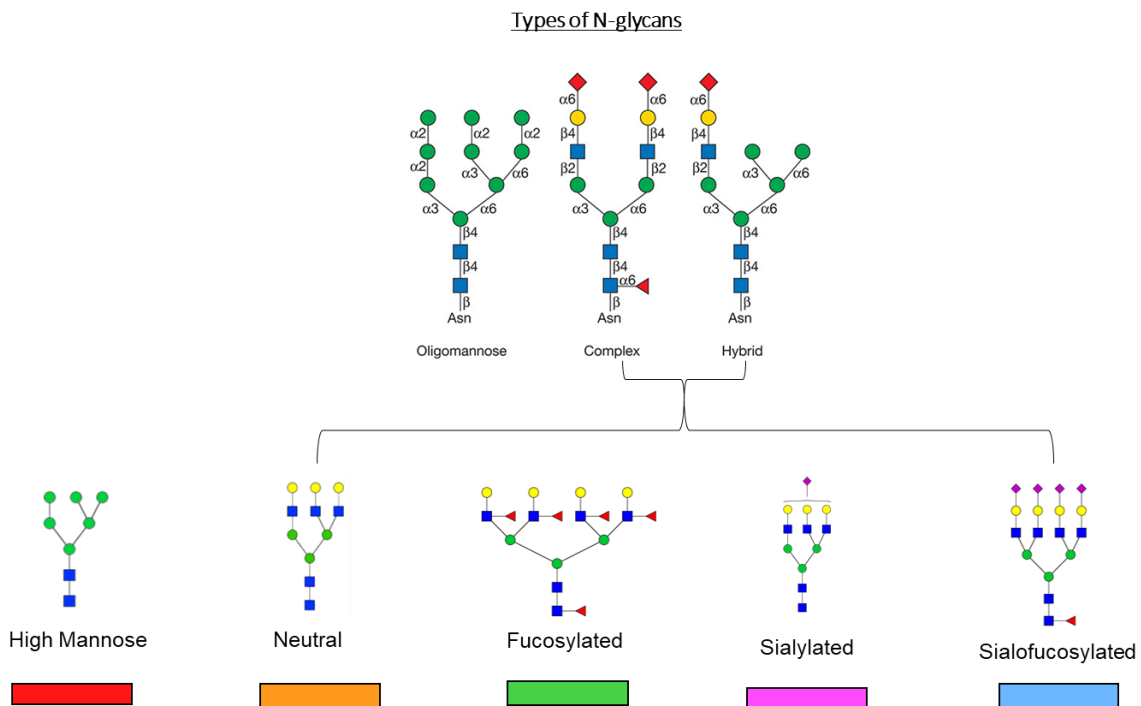


Figure 1: Types of N-glycans.

Neutral type N-glycans refer to glycans not containing fucose or sialic acid moieties. While sialofucosylated contain both fucose and sialic acid. Fucosylated-only and sialylated-only contain only fucose or sialic acid, respectively.

O-Glycans

Another common posttranslational modification in glycoproteins is O-glycosylation. Glycoproteins carry glycans initiated by GalNAc attached to the hydroxyl groups of serine or threonine. The monosaccharides found in O-glycans include GalNAc, GlcNAc, Gal, Fuc and Sia where Man is not present unlike in N-glycans. O-Glycans fall into four major core structures, **Figure 2**. The extension of O-GalNAc by a β 1-3Gal forms the most common (core 1) O-GalNAc glycan. Core 2 is formed by the addition of β 1-6GlcNAc to the GalNAc of core 1. Less common core structures are core 3, in which β 1-3GlcNAc is added to O-GalNAc, and core 4, in which core 3 is branched by the addition of β 1-6GlcNAc (4, 5). Core 1 and 2 glycans have been reported in glycoproteins and mucins, however core 3 and 4 are less common and present in mucins and glycoproteins specifically found in gastrointestinal and bronchial tissues (6). Challenges in the isolation and purification of O-glycans have made it difficult to study. Unlike with N-glycan analysis where an enzymatic release is used, there is no commercial enzyme to release O-glycans for analysis (5, 7).

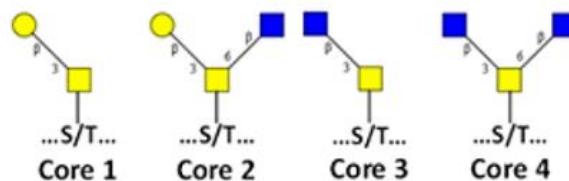


Figure 2. The four common core structures of O-glycans, adapted from ref. (8).

Despite the importance of N- and O- glycosylation in biological process, it is still not completely understood how the specific decorations of these glycan affect the biological fate and function of glycoproteins (9). Nonetheless, recent efforts towards analyzing the protein and site-

specific occupancy in proteins and glycolipids have advanced considerably employing novel mass spectrometry methods.

Glycosphingolipids

Glycosphingolipids (GSL's) are composed of a monosaccharide such as glucose or galactose attached directly to a ceramide molecule. Glycosphingolipids play an important role in the cell surface glycosylation of the central nervous system. The first GSLs characterized and the most abundant in the vertebrate brain are the galactosylceramides (GalCer) (10, 11). Gangliosides, glycosphingolipids with one or more sialic acid moieties present, are found in high concentration in the grey matter of the human brain (10). Efforts into correlating the gangliosides and neural development and function have been of great interest. The ceramide lipid component of GSL's consist of a spingoid base with a fatty acid amide at C-2 amine, which can vary in length ranging from C14 to C40. Both the ceramide and glycan component of GSL's structure add great diversity to the final structure. Understanding the complexity of these molecules is eased by knowing the biosynthetic pathway of GSL's in the brain. In this pathway ceramide (cer) is the acceptor for UDP-Gal:ceramide β -galactosyltransferase or UDP-Glc:ceramide β -glucosyltransferase. The action of UDP-Gal:GlcCer β 1-4 galactosyltransferase and then CMP-Neu5Ac:lactosylceramide α 2-3 sialyltransferase converts GlcCer into GM3. GM3 can then generate a-series gangliodies or b-series gangliosides, by accepting UDP-GalNAc:GM3/GD3 β 1-4 N-acetylgalactosaminyltransferase or CMP-Neu5Ac:GM3 α 2-8 sialyltransferase, respectively, **Figure 3.** Mass spectrometry when coupled with high performance liquid chromatography is the

method of choice when characterizing structural complexity and heterogeneity of GSL's structures and assisted with the known biosynthetic pathway.

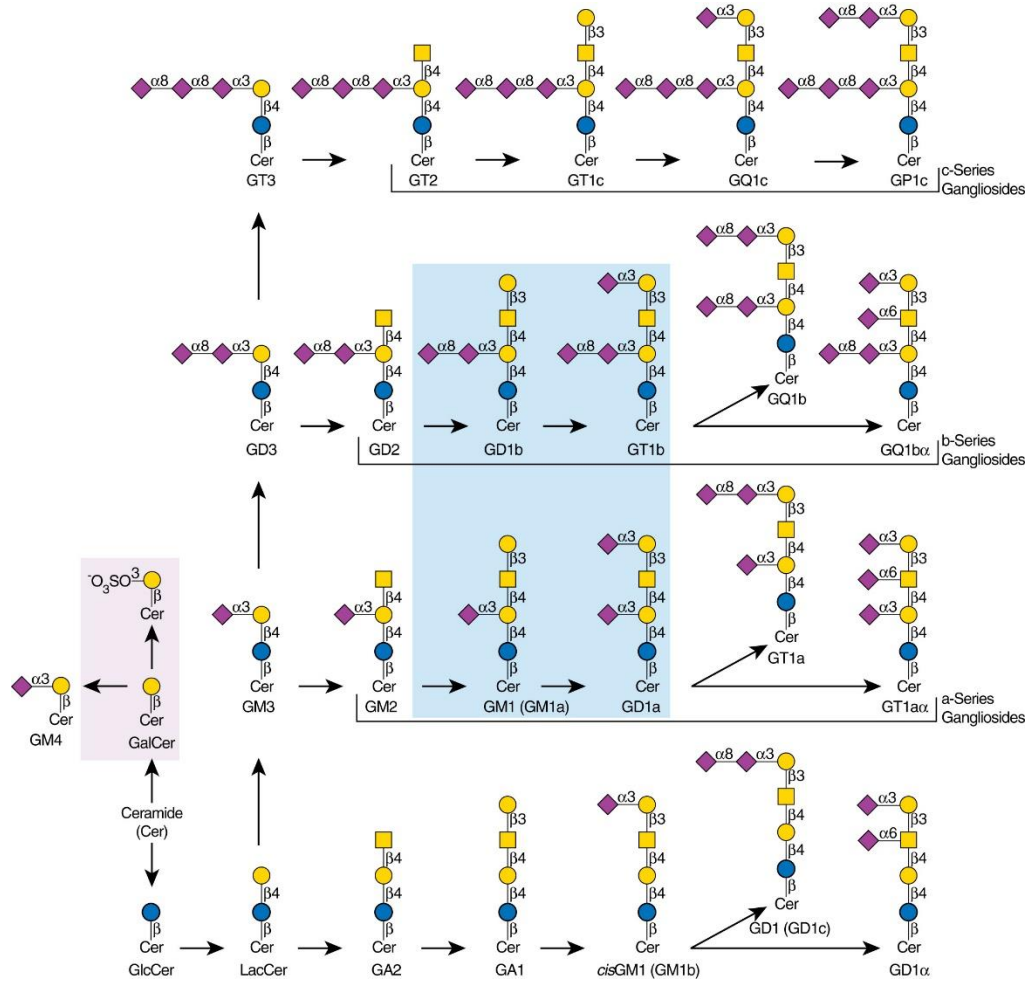


Figure 3: The stepwise addition of the most abundant brain GSLs is shown. Adapted from Essentials of Glycobiology, Chapter 11, Figure 3., Third Edition.

Important Biological function of Glycans

Glycans in the nervous system carry important roles during development, synaptic plasticity and regeneration (12). Glycans can mediate interactions between each other and within nearby proteins creating a dynamic and extensive set of molecular interactions. Evolution has been consistently synthesizing these glycans for more than three billion year therefore their biological functions should be as important as the major macromolecular building blocks of life (13). General classifications of the biological roles of glycans involve organism-intrinsic and organism-extrinsic glycan-binding proteins in recognizing glycans. Interestingly, glycans can also interact with microorganism or toxins, extrinsic recognitions of glycans involve bacterial, fungal and parasite adhesins. While structural and modulatory roles include physical structure, glycoprotein folding, gradient generation, and protection from immune recognition to name a few (13). The ABO blood group antigens are among the most known fucosylated glycans, **Figure 4**. The ABO system is an important determinate during blood donation and transfusions highlighting the importance of glycosylation on blood cells (14).

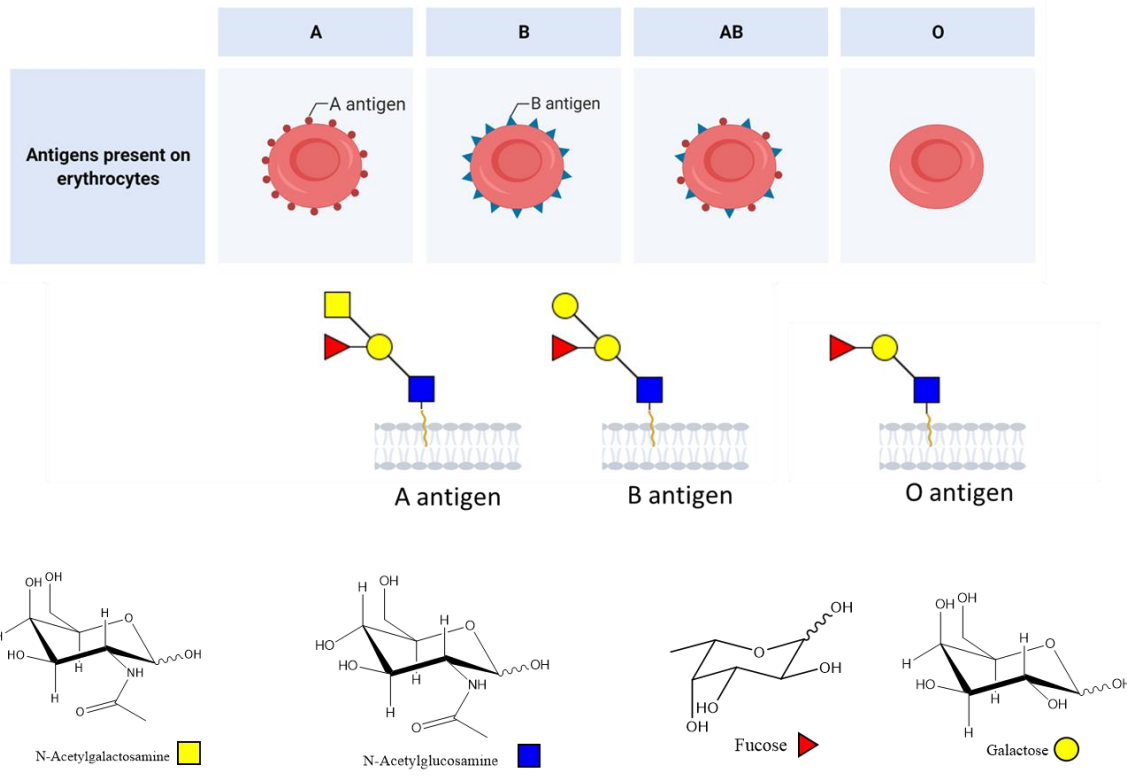


Figure 4: ABO blood types with their corresponding specific glycan structures.

Glycosylation in Alzheimer’s Disease

Alzheimer’s Disease (AD) is an incurable, progressive, neurodegenerative disorder and the most common cause of dementia affecting millions of people worldwide (15). The major pathological hallmark in AD are neurofibrillary tangles and amyloid plaques. Abnormalities are first detected in the frontal and temporal lobes and slowly progress to the neocortex where at this point AD affects individuals differently (3, 15). The primary cause of this neurodegenerative disease is still unknown although diagnosis is based on medical history and clinical findings. While therapies are available, they are only symptomatic and do not affect the progression of the disease.

<i>Gene</i>	<i>Glycosylation Type</i>	<i>Comment</i>
<i>APP</i>	N-glycosylation	Defects in glycosylation alter APP processing.
<i>Tau</i>	N-glycosylation O-glycosylation	N-glycosylation only reported in AD patients.
<i>Nicastrin</i>	N-glycosylated	Highly N-glycosylated but functions remain poorly understood
<i>TREM2</i>	N-glycosylation	Altered glycosylation can lead to dysregulated molecular affecting AD pathogenesis

Table 2: Glycosylation in Alzheimer’s Disease

The amyloid cascade hypothesis has led the research field of AD. For more than 20 years, researchers have used extensive efforts in lowering the production of A β monomers and oligomers aggregates as well as plaques (16–19). While the initial step in AD is the accumulation of amyloid plaques, for more than 15 years several drugs have targeted to decrease the levels of A β aggregates; however, they have not been successful. Top biopharmaceutical companies have invested billions of dollars in anti-A β drugs to halt the progression of AD, however there has been no success in early stages to late clinical stages (20). This raised the concern that the amyloid

cascade hypothesis leading the field of AD has failed. There is now an imperative need for alternative approaches in combating this disease.

Implication of glycosylation in AD have been observed in amyloid precursor protein (APP) processing and tau proteins directly connected to the two pathological hallmarks of AD (21). Several studies have shown that defects in glycosylation of APP and tau have been reported in AD (16, 22–24). Interestingly, while APP is known to have two glycosylation sites, tau which is found in the cytosol is also N-glycosylated. Tau has three potential N-glycosylation sites and only known to be glycosylated in AD, but not in control brain. Alterations in glycosylation on other proteins related to AD pathogenesis have also been reported, **Table 2** (3, 21) . As more than 70% of all cells in the human body are glycosylated it is important to understand the alterations of glycosylation in a neurodegenerative disease. Major AD-related proteins have been shown to have altered glycosylation, however the effects of such alterations are still poorly understood.

Glycomic Profiling and the Mammalian Brain

Recent advances in glycomic analysis has provided deep structural characterization of glycan subtypes in human and mice brains (25). Despite all existing evidence suggesting glycosylation is important in brain development, recent research represents only the first comprehensive glycomic analysis of N-glycans or any glycan subtypes in the brain. N-Glycans are generally the most abundant type, easiest to localize on proteins, and most mechanistically understood. Remarkable advances in analytical methods for the genome and the proteome have been made, where sequence defines the molecule. However, glycomic analysis has been

considerably more constrained because every molecule must be structurally identified, and elucidated.

Glycosylation is indeed a key and common post-translational modification of brain proteins and lipids. Over 70% of brain proteins are glycosylated, and a large fraction of the lipids are glycolipids. It is the most structurally complicated and diverse type of post-translational modification in proteins. The limitations in the ability to profile glycans with quantitation have similarly limited our ability to obtain a deeper understanding of the role of glycosylation. Unlike the genome and the proteome, there is no template for the creation of the glycome (the totality of glycan structures). Glycans are metabolically synthesized to yield a host of structures that vary heterogeneously by linkage, length, degree of branching (number of antennae), and composition. The glycome differs with gender(26), however their biological variability remain generally constant over time(27) but changes with increasing age(25, 26, 28, 29), and in health status (30). They are therefore strong indicators of phenotypes and are arguably closer to the disease states.

Glycosylation has long been associated with brain development. In early nutrition, glycans in human milk are known to affect the infant's brain development (31). Sialic acid, a key component in human milk oligosaccharides (HMO's), and neural tissues, is a crucial nutrient during periods of rapid brain growth (32). Piglets, with brain that develop similarly to infant in structure and function, fed with increasing amounts of sialic acids were able to learn and complete the most difficult tasks in a shorter period of time. Brain gangliosides (sialylated glycolipids) and sialylated glycoproteins were reportedly higher in breastfed compared to formula-fed human infants in the grey matter region of the frontal cortex (33). Thus, proper nutrition during brain development affects the content of sialic acids in brain glycoconjugates. In

another study, similar feeding studies of sialylated oligosaccharides such as 6'-sialyllactose affected rat behavior and cognitive function leading to enhanced learning, memory, and behavioral assessments (34). These studies, even while focused on a single monosaccharide such as sialic acids, provide valuable information regarding brain development and functionalities.

When structures of glycans are determined, often lectins are used for their analysis. Lectins are non-immunoglobulin proteins that recognize structural glycan motifs. Lectin microarrays have, for example, been used to study the systematic variation in protein N-glycosylation of Alzheimer's Disease (AD). The N-glycoproteomic analysis of AD (APP/PS1 transgenic) and wild-type mouse brains were studied using lectins revealing highly complicated site-specific heterogeneity in AD mouse brains (35). A lectin array assay was also used on serum samples from patients with AD, mild-cognitive impairment (MCI), and healthy controls. Several lectins, especially VVA, exhibited increased signals in AD and MCI relative to controls. The VVA lectins putatively recognize the monosaccharide N-aceylgalactosamine (GalNAc), which are commonly present in O-linked glycans (36). Lectins are typically labeled with chromophore tags and, when coupled with confocal microscopy, provide visual information regarding the distribution of various structural motifs (37). Despite the broad utility and accessibility of lectins, they have several limitations. They provide information that are either too specific (such as a sialic acid linkage) or too broad (such as a glycan type), but never the complete glycan structure. Lectins provide some quantitative information; however one lectin cannot be directly compared to the response of another. Furthermore, many lectins have not been validated with glycomic methods as to their broad glycan specificity or sensitivity. For example, *Hippeastrum hybrid* (HHL) is commonly used for monitoring high mannose glycans. However, when the glycans and the

underlying polypeptide backbone were examined through oxidative labeling, the lectin was found to have poor sensitivity and specificity compared to lectins that selected for either sialic acids or fucoses (37).

Glycoproteomic methods are more recent additions to the glycomic toolbox with the focus on glycosite analysis of proteins rather than the glycans themselves. For example, ¹⁸O-labeling was used to mark N-glycosylation sites in a large-scale, site-specific N-glycoproteomic study of human AD and control brain (38). Even when comprehensive glycoproteomic methods are used, they rely on input of glycan libraries, which when limited may not completely represent the broad structural variations of the glycome.

All of these techniques represent attempts to recapitulate the nature of the glycome. Employing advanced liquid chromatography – mass spectrometry (LC-MS) methods that provided extensive separation of isomers is important. Other MS based profiling methods such as matrix-assisted laser desorption/ionization (MALDI) provide limited information as it does not produce isomer separation and yield only compositional monosaccharide information. Furthermore, because MALDI has generally poorer sensitivity for oligosaccharides compared to nanospray ionization, it often requires derivatization such as permethylation, which increases the complexity of the analysis by producing partially derivatized compounds that severely limit the potential dynamic range of the MS.

The LC-MS analysis of native glycans provides valuable information regarding the spatial and temporal glycome expression in human and mice brains. Researchers have shown that the glycome expression among different brain regions in mouse were generally spatially well-

conserved. Additionally, the temporal diversity of glycans in the prefrontal cortex (PFC) in humans ranging in age from 39 days to 49 years and in mice at different time points corresponding to six postnatal stages has been explored. Both mammalian brains revealed highly regulated glycan expression patterns. Remarkably, the temporal diversity of glycan expression in mammalian PFC revealed that the glycosylation pattern at an early developmental stage is generally conserved between the two species. The authors further demonstrated that development-specific traits were prominent in early developmental stages regardless of species, whereas species-specific traits became more pronounced in later development (25). Additionally, glycans that were highly expressed in both groups at the older stages yielded positive correlations with ageing, while those more abundant glycans in the younger age groups had negative correlation with ageing.

This research will lead to more effective use of bio-orthogonal methods for producing non-native glycans *in situ*. The ability to profile the incorporation of unnatural monosaccharides will enhance, for example, metabolic labeling studies. Introduction of unnatural monosaccharides to mice results in the incorporation of activated sialylated glycans that was used for the fluorescence imaging of the brain (39). The studies further showed that sialylation was spatially regulated. The turnover rates of these glycans were significantly lower in the hippocampus than in other brain regions, thereby revealing region-specific biosynthesis of the glycans.

The work could also lead to glycan and glyconjugate biomarkers in the blood for brain-related diseases. Glycan biomarkers in the brain have been previously explored such as polysialic acids in glioblastoma (40), as well as general alterations in sialylation and fucosylation in N- and

O-glycans of brain cancer (41). These studies have been limited to brain tissues. However, recent studies on cancer have shown that rather than being localized in specific tissues, glycomic changes can be system-wide (30). Indeed, glycomic changes in the blood are associated with many types of cancers including esophageal, gastric, colon, gallbladder, pancreatic, liver, ovarian, and breast cancer (30). A recent study showed that the high mannose glycans induce specific interactions in distinct glycoproteins that enhance the metastatic properties of cancer (42).

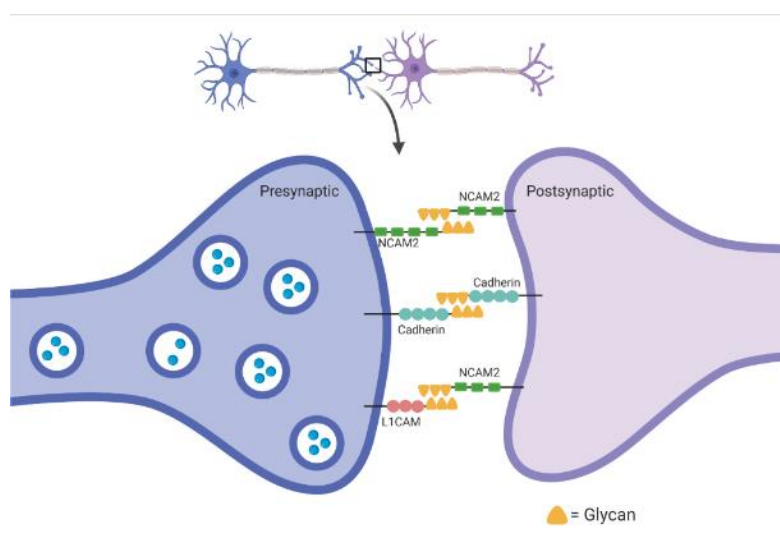


Figure 5. Schematic diagram illustrating synaptic CAMs accumulation in synaptic membranes to form homophilic (e.g., NCAM2-NCAM2, Cadherin-Cadherin) or heterophilic (e.g., L1-NCAM2) adhesion bonds important in forming stabilized interactions between synaptic membranes. These interactions of synaptic glycoproteins may be mediated by glycosylation type. Adapted from reference (43).

Glycan maps of brains with neurological diseases such as Alzheimer's and Parkinson's could lead to better therapies. Highly glycosylated membrane proteins such as NCAM and cadherin are known to interact in the synaptic membrane (43). These interactions are potentially

mediated by glycans that may be affected by aberrant glycosylation (**Figure 5**). Additionally, adeno associated virus (AAV) used in gene therapy employs terminal galactose binding for transduction and gene delivery. Brain regions with terminal galactoses serve as receptor for AAV9 binding (44). It has been suggested that age related changes in the glycan receptors such as heparan sulfate proteoglycans and/or N-glycans can result in poor AAV binding thereby affecting treatment for the elderly. It is therefore crucial to fully elucidate the N-glycans structures as they may guide the improvement of viral vectors for gene therapies.

The potential roles glycans play in the spatial and temporal stages of normal brain development and disease progression remain underexplored. Despite these analytical advancements, there are still limitations that will need to be addressed. Elucidating the structures to provide complete N-glycome profiles, such as those that have been performed for serum glycans (45) and HMOs in breast milk (31), will further improve our understanding of the role of glycosylation in the brain. Additionally, to obtain more complete and comprehensive glycomic brain profiles, the O-glycome and the glycolipidome will also be needed. As our knowledge of glycosylation in mammalian brains continues to grow the development of much needed biomarkers and therapeutics will advance with it.

Glycan Analysis using LC-MS

Liquid chromatography (LC)

Liquid chromatography is a technique used to separate compounds in a complex mixture. The separation occurs based on the interaction of the analyte with the mobile and stationary phase. LC is currently the best chromatography separation for a glycome mixture due to the efficient isomeric separation. The sensitivity is further improved when employing ultra-high-performance liquid chromatography (UHPLC) or nano liquid chromatography (nanoLC) systems. The most widely used stationary phase in glycome research is porous graphitized carbon (PGC) (46). Native reducing-end and reduced glycans are strongly retained by PGC, but not hardly retained on C18 reversed-phase. However, for the separation of glycolipids and glycopeptides C18 columns are more efficient in separation (47).

Porous graphitized carbon (PGC)

The chromatographic performance of PGC in the purification and separation of underivatized glycans has been proven excellent (48). PGC has been widely used for the separation in N-glycans as its retention greatly depends on the monosaccharide composition and linkage. When separating a di-sialylated bi-antennary N-glycans with PGC isomeric separation is beautifully achieved, **Figure 6** (27, 49). The exact mechanism of PGC is not fully understood however both dipole-induced-dipole and hydrophobic interactions are known to occur between the stationary phase and oligosaccharides (46).

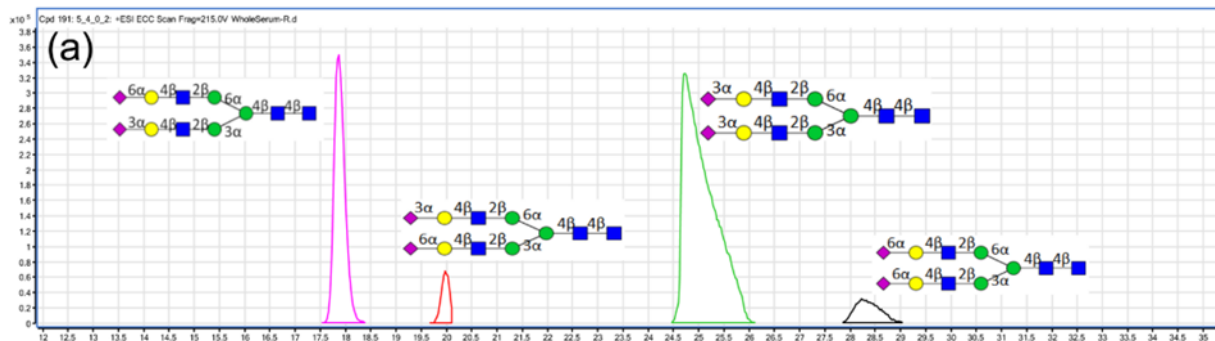


Figure 6: Extracted compound chromatograph of di-sialylated bi-antennary N-glycans with mass 2222.80 Da. Adapted from reference (27).

Mass spectrometry (MS)

Mass spectrometers can be categorized into three fundamental parts: the ionization source, the analyzer, and the detector. The analyte of interest is first introduced into the ionization source of the instrument. The analytes are ionized and extracted into the analyzer region where they are analyzed according to their mass-to-charge (m/z) ratios. The analyzer and detector are maintained under high vacuum to avoid any hindrance from air molecules onto the traveling ions (50). Tandem mass spectrometry is a mass spectrum of a mass spectrum raised to the power of n , (MS^n) where n is the number of MS/MS spectra obtained per molecular ion. Tandem MS has been on the forefront of characterizing complex mixtures (50, 51). Important features that make MS ideal for glycomic and glycoproteomic analysis include the extent of structural information generated on limited amount of sample. Limits of detection have reached femtomolar to attomolar levels for glycans, while the dynamic range is typically 4 or 5 orders of magnitude (7, 47, 50). The most common sources of ionization are MALDI and ESI (52, 53). The mass analyzers include Time-of-flight (ToF), quadrupole, ion trap, orbitrap and Fourier transform

ion cyclotron resonance (FTICR). The best mass resolution accuracy is offered by FTICR and orbitrap mass analyzers (54–56).

Comprehensive glycoproteomic analysis have been the most recent addition to the glycomic toolbox. There is a need for understanding the global and site-specific analysis of glycoprotein, however there are challenges in the low abundance of the native target glycoprotein. The analysis of site-specific glycopeptide requires simultaneous profiling of protein sequence, glycosite occupancy and glycan structural composition. The glycan structure found on the glycosite only increases the complexity and heterogeneity of the glycopeptide structural elucidation. Thus, highly sensitive and quantitative methods are needed to detect site-specific alterations in glycoproteins.

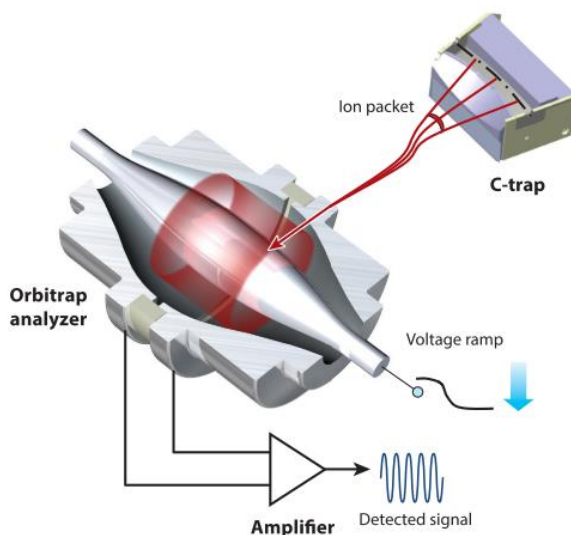


Figure 7: The C-trap ion accumulation device and the Orbitrap mass analyzer with an example of an ion trajectory. Image adapted from ref. (57).

The combination of high resolution, accurate mass analyzers and multiple dissociation techniques (CID, ETD, HCD) on Orbitrap mass spectrometer have been able to profile peptide sequence, glycosylation sites and glycan moieties of glycopeptides. The Orbitrap mass analyzer, **Figure 7**, is a high-performance mass analyzer that employs trapping of ions in electrostatic fields. The Quadro-logarithmic field employs orbital trapping in an electrostatic field with potential distribution (58). Tight integration with the ion injection process enables the high-resolution, mass accuracy, and sensitivity that have become essential for site-specific glycopeptide profiling (57).

References

1. L. Möckl, The Emerging Role of the Mammalian Glycocalyx in Functional Membrane Organization and Immune System Regulation. *Front. Cell Dev. Biol.* **8**, 1–14 (2020).
2. E. Bieberich, Synthesis, Processing, and Function of N-glycans in N-glycoproteins. *Adv Neurobiol* **9**, 47–70 (2014).
3. S. Schedin-Weiss, B. Winblad, L. O. Tjernberg, The role of protein glycosylation in Alzheimer disease. *FEBS J.* **281**, 46–62 (2014).
4. B. López-Gutiérrez, R. R. Dinglasan, L. Izquierdo, Sugar nucleotide quantification by liquid chromatography tandem mass spectrometry reveals a distinct profile in *Plasmodium falciparum* sexual stage parasites. *Biochem. J.* **474**, 897–905 (2017).
5. G. Xu, E. Goonatileke, S. Wongkham, C. B. Lebrilla, Deep Structural Analysis and Quantitation of O-Linked Glycans on Cell Membrane Reveal High Abundances and Distinct Glycomic Profiles Associated with Cell Type and Stages of Differentiation. *Anal. Chem.* **92**, 3758–3768 (2020).
6. Inka Brockhausen, P. Stanley, Chapter 10 O-GalNAc Glycans. *Essentials Glycobiol. 3rd Ed.* (2017) <https://doi.org/10.1101/glycobiology.3e.010>.
7. M. J. Kailemia, *et al.*, Recent Advances in the Mass Spectrometry Methods for Glycomics and Cancer. *Anal. Chem.* **90**, 208–224 (2018).
8. L. R. Ruhaak, G. Xu, Q. Li, E. Goonatileke, C. B. Lebrilla, Mass Spectrometry Approaches to Glycomic and Glycoproteomic Analyses. *Chem. Rev.* **118**, 7886–7930 (2018).
9. J. Stadlmann, *et al.*, Comparative glycoproteomics of stem cells identifies new players in ricin toxicity. *Nature* **549**, 538–542 (2017).
10. C. L. Schengrund, Gangliosides: Glycosphingolipids essential for normal neural development and function. *Trends Biochem. Sci.* **40**, 397–406 (2015).
11. M. Wong, G. Xu, D. Park, M. Barboza, C. B. Lebrilla, Intact glycosphingolipidomic analysis of the cell membrane during differentiation yields extensive glycan and lipid changes. *Sci. Rep.* **8**, 1–10 (2018).
12. R. Kleene, M. Schachner, Glycans and neural cell interactions. *Nat. Rev. Neurosci.* **5**, 195–208 (2004).
13. A. Varki, Biological roles of glycans. *Glycobiology* **27**, 3–49 (2017).
14. D. J. Becker, J. B. Lowe, Fucose: Biosynthesis and biological function in mammals. *Glycobiology* **13** (2003).
15. C. L. Masters, *et al.*, Alzheimer’s disease. *Nat. Rev. Dis. Prim.* **1**, 1–18 (2015).
16. M. A. Deture, D. W. Dickson, The neuropathological diagnosis of Alzheimer’s disease.

- Mol. Neurodegener.* **14**, 1–18 (2019).
17. F. Panza, M. Lozupone, D. Seripa, B. P. Imbimbo, Amyloid- β immunotherapy for alzheimer disease: Is it now a long shot? *Ann. Neurol.* **85**, 303–315 (2019).
 18. C. P. Boix, I. Lopez-Font, I. Cuchillo-Ibañez, J. Sáez-Valero, Amyloid precursor protein glycosylation is altered in the brain of patients with Alzheimer’s disease. *Alzheimer’s Res. Ther.* **12**, 1–15 (2020).
 19. J. Wang, B. J. Gu, C. L. Masters, Y. J. Wang, A systemic view of Alzheimer disease - Insights from amyloid- β metabolism beyond the brain. *Nat. Rev. Neurol.* **13**, 612–623 (2017).
 20. F. Panza, M. Lozupone, G. Logroscino, B. P. Imbimbo, A critical appraisal of amyloid- β -targeting therapies for Alzheimer disease. *Nat. Rev. Neurol.* **15**, 73–88 (2019).
 21. H. Haukedal, K. K. Freude, Implications of Glycosylation in Alzheimer’s Disease. *Front. Neurosci.* **14** (2021).
 22. J. L. Molinuevo, *et al.*, Current state of Alzheimer’s fluid biomarkers. *Acta Neuropathol.* (2018) <https://doi.org/10.1007/s00401-018-1932-x>.
 23. R. Tarawneh, Biomarkers: Our Path Towards a Cure for Alzheimer Disease. *Biomark. Insights* **15** (2020).
 24. Y. Sato, Y. Naito, I. Grundke-Iqbal, K. Iqbal, T. Endo, Analysis of N-glycans of pathological tau: Possible occurrence of aberrant processing of tau in Alzheimer’s disease. *FEBS Lett.* **496**, 152–160 (2001).
 25. J. Lee, *et al.*, Spatial and temporal diversity of glycome expression in mammalian brain. *Proc. Natl. Acad. Sci.* **117**, 28743–28753 (2020).
 26. A. A. Merleev, *et al.*, A site-specific map of the human plasma glycome and its age and gender-associated alterations. *Sci. Rep.* **10**, 1–11 (2020).
 27. T. Song, D. Aldredge, C. B. Lebrilla, A Method for In-Depth Structural Annotation of Human Serum Glycans That Yields Biological Variations. *Anal. Chem.* **87**, 7754–7762 (2015).
 28. R. Raghunathan, *et al.*, Glycomic and proteomic changes in aging brain nigrostriatal pathway. *Mol. Cell. Proteomics* **17**, 1778–1787 (2018).
 29. J. Krištić, *et al.*, Glycans are a novel biomarker of chronological and biological ages. *Journals Gerontol. - Ser. A Biol. Sci. Med. Sci.* **69**, 779–789 (2014).
 30. M. J. Kailemia, D. Park, C. B. Lebrilla, Glycans and glycoproteins as specific biomarkers for cancer. *Anal. Bioanal. Chem.* **409**, 395–410 (2017).
 31. M. R. Ninonuevo, *et al.*, A strategy for annotating the human milk glycome. *J. Agric. Food Chem.* **54**, 7471–7480 (2006).
 32. B. Wang, Sialic acid is an essential nutrient for brain development and cognition. *Annu.*

- Rev. Nutr.* **29**, 177–222 (2009).
33. B. Wang, P. McVeagh, P. Petocz, J. Brand-Miller, Brain ganglioside and glycoprotein sialic acid in breastfed compared with formula-fed infants. *Am. J. Clin. Nutr.* **78**, 1024–1029 (2003).
 34. E. Oliveros, *et al.*, Sialic acid and sialylated oligosaccharide supplementation during lactation improves learning and memory in rats. *Nutrients* **10**, 1519 (2018).
 35. P. Fang, *et al.*, Multilayered N-Glycoproteome Profiling Reveals Highly Heterogeneous and Dysregulated Protein N-Glycosylation Related to Alzheimer's Disease. *Anal. Chem.* **92**, 867–874 (2020).
 36. M. Frenkel-Pinter, *et al.*, Interplay between protein glycosylation pathways in Alzheimer's disease. *Sci. Adv.* **3**, e1601576 (2017).
 37. Y. Xie, *et al.*, Determination of the glycoprotein specificity of lectins on cell membranes through oxidative proteomics. *Chem. Sci.* **11**, 9501–9512 (2020).
 38. Q. Zhang, C. Ma, L. S. Chin, L. Li, Integrative glycoproteomics reveals protein n-glycosylation aberrations and glycoproteomic network alterations in Alzheimer's disease. *Sci. Adv.* **6**, 1–19 (2020).
 39. R. Xie, *et al.*, In vivo metabolic labeling of sialoglycans in the mouse brain by using a liposome-assisted bioorthogonal reporter strategy. *Proc. Natl. Acad. Sci. U. S. A.* **113**, 5173–5178 (2016).
 40. M. C. Amoureux, *et al.*, Polysialic acid neural cell adhesion molecule (psa-ncam) is an adverse prognosis factor in glioblastoma, and regulates olig2 expression in glioma cell lines. *BMC Cancer* **10** (2010).
 41. L. Veillon, C. Fakih, H. Abou-El-Hassan, F. Kobeissy, Y. Mechref, Glycosylation Changes in Brain Cancer. *ACS Chem. Neurosci.* **9**, 51–72 (2018).
 42. D. D. Park, *et al.*, Metastasis of cholangiocarcinoma is promoted by extended high-mannose glycans. *Proc. Natl. Acad. Sci. U. S. A.* **117**, 7633–7644 (2020).
 43. I. Leshchyn'sKa, V. Sytnyk, Synaptic Cell Adhesion Molecules in Alzheimer's Disease. *Neural Plast.* **2016**, 6427537 (2016).
 44. R. Raghunathan, J. D. Hogan, A. Labadorf, R. H. Myers, J. Zaia, A glycomics and proteomics study of aging and Parkinson's disease in human brain. *Sci. Rep.* **10**, 12804 (2020).
 45. C. Kirmiz, *et al.*, A serum glycomics approach to breast cancer biomarkers. *Mol. Cell. Proteomics* **6**, 43–55 (2007).
 46. L. Pereira, Porous graphitic carbon as a stationary phase in HPLC: Theory and applications. *J. Liq. Chromatogr. Relat. Technol.* **31**, 1687–1731 (2008).
 47. Q. Li, Y. Xie, M. Wong, M. Barboza, C. B. Lebrilla, Comprehensive structural glycomic

- characterization of the glycocalyxes of cells and tissues. *Nat. Protoc.* **15** (2020).
48. C. West, C. Elfakir, M. Lafosse, Porous graphitic carbon: A versatile stationary phase for liquid chromatography. *J. Chromatogr. A* **1217**, 3201–3216 (2010).
 49. M. Anugraham, *et al.*, Specific Glycosylation of Membrane Proteins in Epithelial Ovarian Cancer Cell Lines : Glycan Structures Reflect Gene Expression and DNA Methylation Status * □. *Mol. Cell. Proteomics*, 2213–2232 (2014).
 50. S. Tilvi, M. S. Majik, K. S. Singh, *Mass spectrometry for determination of bioactive compounds* (Elsevier B.V., 2014).
 51. N. M. Riley, S. A. Malaker, M. D. Driessen, C. R. Bertozzi, Optimal Dissociation Methods Differ for N- and O-Glycopeptides. *J. Proteome Res.* **19**, 3286–3301 (2020).
 52. T. Kasumov, *et al.*, Quantification of ceramide species in biological samples by liquid chromatography electrospray ionization tandem mass spectrometry. *Anal. Biochem.* **401**, 154–161 (2010).
 53. D. J. Harvey, *et al.*, Identification of high-mannose and multiantennary complex-type N-linked glycans containing α -galactose epitopes from Nurse shark IgM heavy chain. *Glycoconj. J.* **26**, 1055–1064 (2009).
 54. K. Strupat, O. Scheibner, M. Bromirski, High-Resolution, Accurate-Mass Orbitrap Mass Spectrometry -- Definitions, Opportunities, and Advantages. *Thermo Sci. Tech. Note* **64287**, 1–5 (2013).
 55. Crawford, *Mass Spectrometry Fundamental LC-MS Orbitrap Mass Analyzers.* *Crawford Sci.* (2011).
 56. M. Scigelova, M. Hornshaw, A. Giannakopoulos, A. Makarov, Fourier transform mass spectrometry. *Mol. Cell. Proteomics* **10**, 1–19 (2011).
 57. S. Eliuk, A. Makarov, Evolution of Orbitrap Mass Spectrometry Instrumentation. *Annu. Rev. Anal. Chem.* **8**, 61–80 (2015).
 58. A. Makarov, Electrostatic axially harmonic orbital trapping: A high-performance technique of mass analysis. *Anal. Chem.* **72**, 1156–1162 (2000).

Chapter II

Regio-Specific N-Glycome and N-Glycoproteome Map of the Elderly Human Brain with and without Alzheimer's Disease

ABSTRACT

The proteins in the cell membrane of the brain are modified by glycans in highly interactive regions. The glycans and the glycoproteins are involved in cell-cell interactions that are of fundamental importance to the brain. In this study, the comprehensive N-glycome and glycoproteome of the brain were determined in eleven functional brain regions some of them known to be affected with the progression of Alzheimer's Disease (AD). N-Glycans throughout the regions were generally highly branched and highly sialofucosylated. Regional variations were also found with regards to the glycan types including high mannose and complex-type structures. Glycoproteomic analysis identified the proteins that differed in glycosylation in the various regions. To obtain the broader representation of glycan compositions, four subjects with two in their seventies and two in their nineties representing two Alzheimer disease subjects, one hippocampal sclerosis subject, and one subject with no cognitive impairment were analyzed. The four subjects were all glycomically mapped across 11 brain regions. Marked differences were observed between disease states in the glycomic profiles of the four subjects.

INTRODUCTION

Glycans on proteins create an extensive interactive network on the cell surface known as the glycocalyx. In the brain and other tissues, they are found in the extracellular matrix facilitating cell-cell and cell-matrix interactions resulting in intercellular signaling and adhesion (1–3). While glycosylation is indeed a common post-translational modification of proteins, they are also the most structurally complicated. Until recently, the limitations in our ability to determine and quantitate structures have challenged our ability to obtain a deeper understanding of the role of glycosylation. Unlike the genome and the proteome, there is no template for the creation of the glycome (the totality of glycan structures). Glycans are metabolically synthesized to yield a suite of structures that vary heterogeneously by linkage, length, number of antennae, and composition.

The glycocalyx plays a crucial role in maintaining brain homeostasis (4). Protein N-glycosylation is a specific type of glycosylation where N-glycans are covalently attached to an asparagine by an N-glycosidic bond. N-Glycosylation is also the most abundant type of glycosylation, with approximately 90% of all eukaryotic cells carrying N-glycosylated glycoproteins (5). The crucial role of N-glycosylation is highlighted in the central nervous system where alterations in N-glycosylation have been linked to different neuropathological symptoms such as mental retardation and epilepsy (6). As a result, N-glycans and N-glycoproteins make compelling targets for therapeutics and as biomarkers for diseases. Although the importance of N-glycans for neural development has been documented (7), understanding how the N-glycome is altered in response to a disease state is of importance and remains to be thoroughly studied. Most efforts have focused specifically on cancer (8) where glycosylation has been shown to be

altered during cancer progression and metastasis (9). Similarly, in brain cancer, aberrant alterations in glycosylation have been reported pertaining to sialylation and fucosylation of N-glycans (10).

Recent studies have indicated glycomic profiles of the mammalian brain in neurological disorders such as Alzheimer's disease (AD) and Parkinson's disease (PD) (11–13). Alzheimer's Disease is an irreversible neurodegenerative disorder characterized by the loss of neurons in a region-specific manner particularly in the cortex and hippocampus. Nearly all of the important brain proteins associated with AD pathogenesis are glycosylated (14). Changes in glycosylation for several key proteins including amyloid precursor protein (APP) (15), β -site amyloid precursor protein-cleaving enzyme (BACE1) (16), and tau (17) among others have been reported. The glycosylation changes observed on the key proteins involved sialylation and the presence of bisecting GlcNAc (16, 18, 19). In Parkinson's disease, which is characterized by the progressive loss of functional dopaminergic neurons, changes in the region- and age-specific N-glycan compositional profiles have also been observed (20).

A comprehensive glycan map of the human brain representing various functional regions can yield a better understanding of the roles of glycans as well as provide potential therapeutic targets for brain diseases. Presently, studies on brain glycosylation have focused on limited structural features with even more limited regions. The efforts have employed primarily lectins, which are glycan recognizing proteins on selected brain tissues (11). More structurally intensive analyses have been performed using liquid chromatography-mass spectrometry (21). In a recent study, glycan profiles of nine regions of mouse brain a single region of human brain across different ages were examined (21). In general, human brain studies have focused on the brain

as a whole (22) or a very limited number such two (23). Rodent brain, which are more accessible, have been more widely studied in terms of their spatial and temporal variations (24–26). However, to our best knowledge, there have been no reported glycomic profiling of the elderly human brain.

Neurodegenerative disorders such as AD have an estimated prevalence of 10-30% in the population of 65 years and older (27). The brain regions first affected include the frontal and temporal lobes and then slowly progresses to impact other areas of the neocortex. To study the glycosylation of the brain of elderly patients, we determined the extent of glycan variations associated with various brain regions. In this report, we describe a limited pilot study to examine the variation in the N-glycome and N-glycoproteome of post-mortem human brain tissues from four different individuals across 11 functional brain regions. The cell membrane-associated N-glycans and glycoproteins from the regions were determined using nanoflow LC-MS/MS platform (28). The brain regions included the frontal, temporal, parietal, occipital, cingulate, lateral cerebellar and orbitofrontal cortex, posterior hippocampus, thalamus, caudate nucleus, and pons. Two patients in their 70s and two in their 90s some with confirmed neurodegenerative diagnosis were examined with the goal of illustrating the utility of glycomic and glycoproteomic tools and to define the general breadth of the variations in glycans associated with the elderly brain and some neuropathological conditions.

RESULTS

Human brain global N-glycome profiling in a region-specific manner

The samples included post-mortem tissues from two sets of donors: two males in their 70's and two males in their 90's. The subjects were chosen to represent two disease pathologies. Among the 70-year-olds, one had pathologically confirmed AD (**AD-74**), and the other had no cognitive impairment (**NCI-72**) (**Table 1**).

Subjects	Labeled	ApoE	BRAAK	Age	Sex
Subject 1	NCI-72	E3/E3	1	72	M
Subject 2	AD-74	E3/E4	6	74	M
Subject 3	AD-93	E3/E4	5	93	M
Subject 4	HS-95	E3/E3	1	95	M

Table 1. Human brain tissue samples of NCI and AD cases used in this study. Detailed list of brain regions analyzed per subject are found in Table S1.

Among the 90-year-olds, one had pathology confirmed AD (**AD-93**), and the other was diagnosed with hippocampal sclerosis (**HS-95**) or a subtype of neuropathological changes of limbic-predominant age-related TDP-43 encephalopathy (LATE-NC + HS). The brain from the four subjects was separated into 11 functional regions including the frontal, temporal, parietal, occipital, cingulate, lateral cerebellar and orbitofrontal cortex, posterior hippocampus, thalamus, caudate nucleus, and pons as shown in **Table S1**. From these regions, the cell membrane fractions were enriched, processed, and analyzed for the glycome and the glycoproteome.

Brain sample preparation involved tissue homogenization, a series of ultracentrifugation for cell membrane enrichment, and glycan release with the enzyme PNGase F (**Figure 1**).

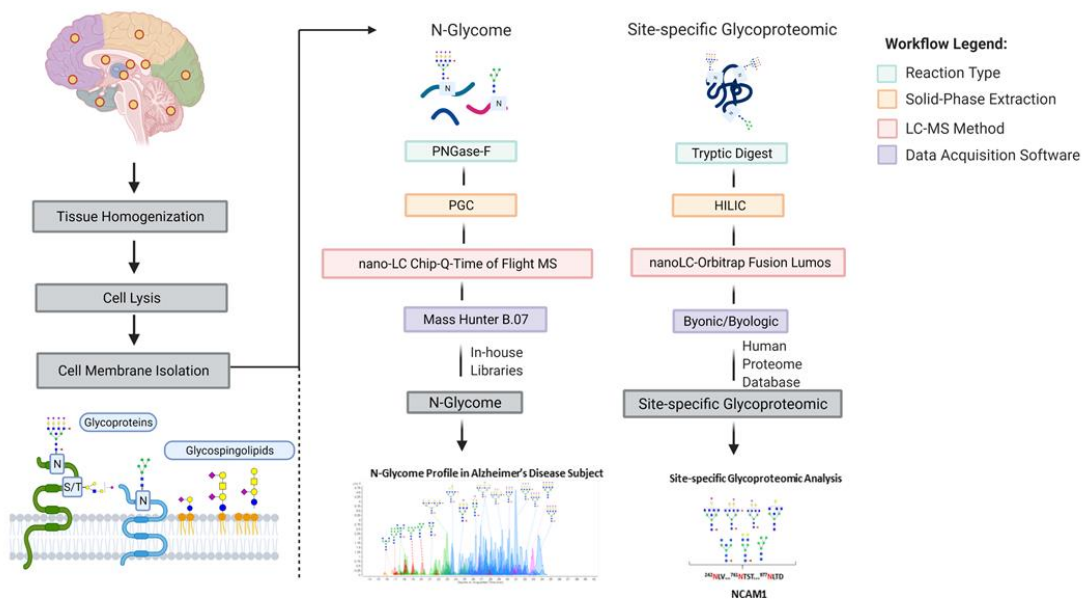
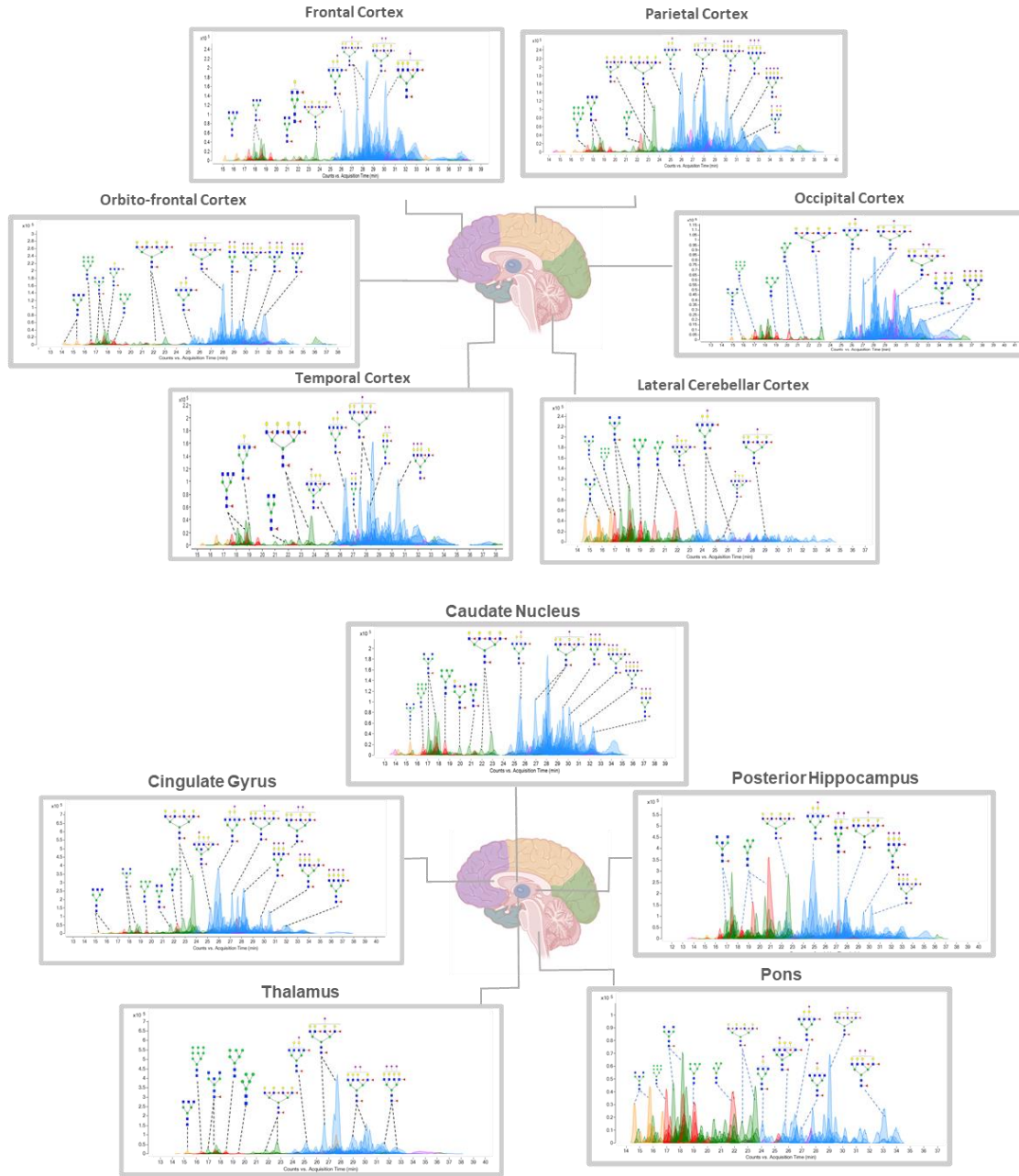


Figure 1. Summary of the workflow for comprehensive LC-MS/MS analysis of the human brain. Tissue region of interest was subjected to tissue homogenization followed by cell lysis to obtain cell membrane fraction. Two cell membrane fractions were isolated from the same brain region, one for N-glycome analysis and the other for site-specific glycoproteomic analysis. The reaction type, solid phase extraction, LC-MS method and data-acquisition software are shown.

A separate sample set was similarly prepared without the N-glycan release for glycoproteomic analyses. Representative nanoLC-MS chromatograms of glycans associated with the different regions for the 72-year-old NCI subject (**NCI-72**) are presented in **Figure 2**. The outer brain regions were grouped in the upper presentation (**Figure 2a**), while the inner regions were in the lower (**Figure 2b**). In each chromatogram, over 200 compositions were observed across four orders of magnitude in dynamic range. The figures were color-coded according to their

structural features with the most common glycoform corresponding to sialofucosylated species (blue in **Figure 2**).



Chromatogram Legend

■ High Mannose
 ■ Undecorated
 ■ Fucosylated
 ■ Sialylated
 ■ Sialofucosylated

Monosaccharide Legend

● Galactose
 ● Mannose
 ■ GlcNac
 ▲ Fucose
 ◆ NeuAc

Figure 2. N-Glycome map of the 11 functional brain regions for **NCI-72**. Representative total compound chromatograms of N-glycans from the temporal cortex, orbito-frontal cortex, frontal cortex, parietal cortex, occipital cortex, lateral cerebellar cortex, thalamus, cingulate gyrus, caudate nucleus posterior hippocampus and pons obtained by PGC-chip-Q-ToF MS/MS. Representative N-glycan structures were assigned to each peak.

The other glycoforms included undecorated (orange), high mannose-type (red) sialylated-only (pink), and fucosylated-only (green). Non-high mannose type glycans may be either hybrid or complex types, however the latter are far more abundant. Based on the chromatogram, spatial (or regional) variations were readily observed even with casual visual inspections. Closer inspection of the **NCI-72** brain N-glycome reveals that sialofucosylated species account for more than 70% of the entire N-glycome with eight of the brain regions including the frontal, temporal, parietal, occipital, cingulate, and orbitofrontal cortex, caudate nucleus, and thalamus. The remaining three brain regions, which include the posterior hippocampus, lateral cerebellar cortex, and pons displayed lower levels of sialofucosylated compositions with relative abundances of 55%, 29%, and 28%, respectively (**Figure S1A-S1K**). Fucosylated-only type N-glycans were the second most abundant glycoform in **NCI-72**. The highest levels of fucosylated-only N-glycans ranged from 29% to 38% and were found in the posterior hippocampus, lateral cerebellar cortex, and pons. The remaining eight brain regions had lower levels of fucosylated-only species ranging from 5% to 12%. The lateral cerebellar cortex and pons contained 23% of the high-mannose structures, which are the highest levels compared to the other regions of **NCI-72**.

Variations between the four subjects were examined in the different regions. LC-MS chromatograms of the occipital cortex, a brain region important in vision and visual

interpretation, showed wide variations in N-glycan compositions among the four subjects **NCI-72**, **AD-74**, **AD-93**, and **HS-95** (Figure 3A).

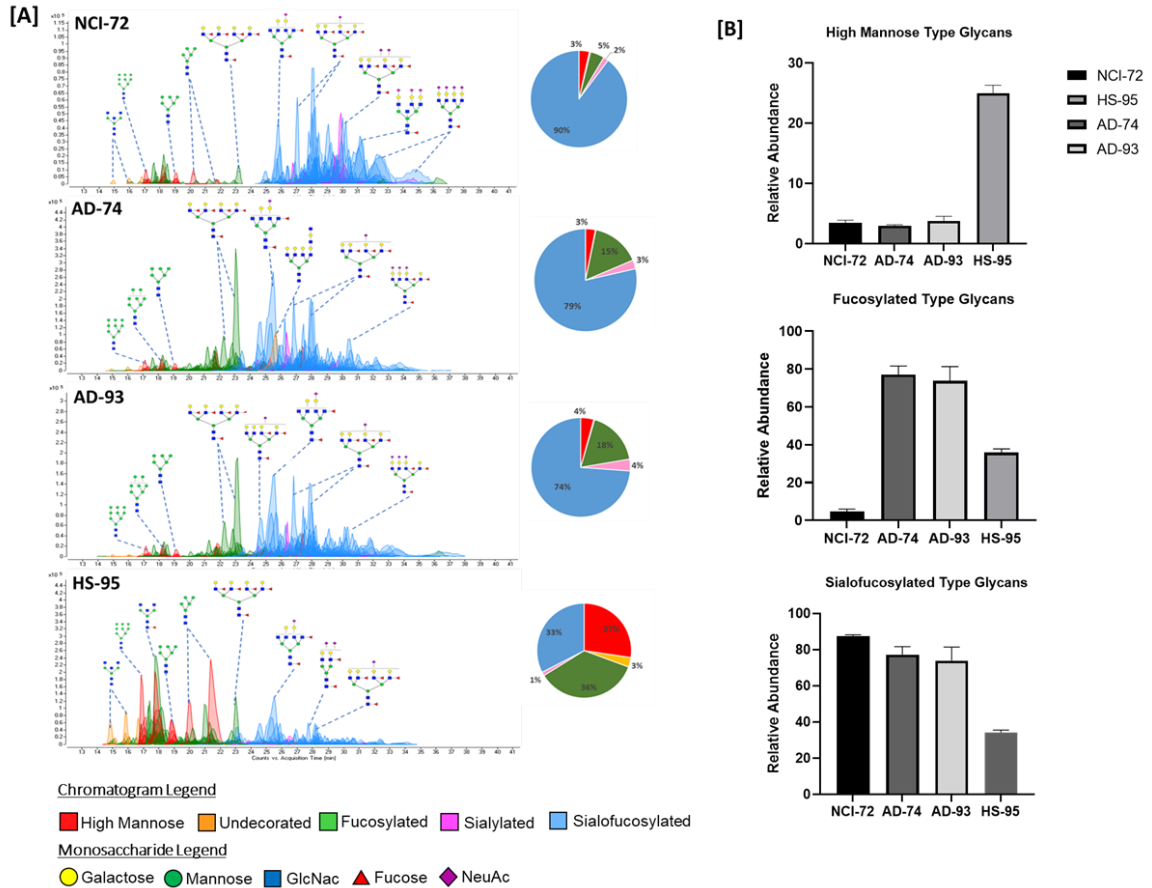


Figure 3. (A) Representative total compound chromatograms of N-glycome from the occipital cortex from subjects **NCI-72** (top), **AD-74**, **AD-93**, and **HS-95** (bottom). Representative N-glycan structures were assigned to each peak. Monosaccharide schematic symbols: yellow circle, galactose; green circle, mannose; blue square, N-acetyl glucosamine; red triangle, fucose; and purple diamond, N-Acetylneuraminic acid. High mannose glycans correspond to peaks in red. N-glycans without fucose or sialic acid termed undecorated correspond to peaks in orange. Peaks in green correspond to N-glycans that are fucosylated only with no sialic acid. Peaks in blue corresponds to N-glycans with both fucose and sialic acid moiety termed sialofucosylated. (B) Bar graphs representing abundances of high mannose, fucosylated and sialofucosylated type N-glycans. Relative abundance of subjects **NCI-72**, **AD-74**, **AD-93**, and **HS-95** from the occipital cortex brain region. Error bars indicate instrumental replicates.

Variations were observed in the two non-AD subjects (**NCI-72** and **HS-95**) which had widely different types of glycans, with **NCI-72** having very little high mannose abundances and primarily complex-types structure that were sialofucosylated. **HS-95** had very high levels of high mannose-type glycans and low levels of complex-type sialofucosylated structures. The N-glycome of **HS-95** showed a more varied distribution of high mannose (27%), fucosylated-only (36%), and sialofucosylated (33%) species (**Figure 3B**). Interestingly, the two AD subjects (**AD-74** and **AD-93**) yielded highly similar chromatograms. For example, the N-glycan composition Hex₃HexNAc₅Fuc₁NeuAc₀ have similar abundances in **AD-74** and **AD-93** but were six-fold higher between **NCI-72** and **HS-95**. In addition, large variations were also observed in the frontal cortex, a region primarily responsible for controlling executive functions including working memory and cognitive flexibility (29). Comparison of **AD-74** and **NCI-72** showed that sialofucosylated N-glycans were of lesser abundance in **AD-74** (**Figure S1**). Interestingly, the sialofucosylated glycans that decreased contained high degrees of terminal sialylation represented by compositions such as Hex₇HexNAc₆Fuc₂NeuAc₄, Hex₇HexNAc₆Fuc₃NeuAc₃, Hex₇HexNAc₆Fuc₄NeuAc₂, and Hex₇HexNAc₆Fuc₃NeuAc₃. A similar comparison of the other regions was presented in **Figure S1** with more in-depth analyses provided below.

N-Glycomic variations in the brain regions

N-Glycans detected in the individual brain regions ranged in numbers between 200 and 900 (including isomers), revealing the large number of N-glycan compositions across the brain (**Figure S2**). All glycan species were grouped into the five subgroups that included undecorated (complex and hybrid -types lacking in fucose or sialic acid), high mannose, fucosylated-only, sialylated-only, and sialofucosylated (glycans containing both sialic acid and fucose moieties) (**Figure 2, Figure S1A**). To monitor the total levels of fucosylation, both fucosylated-only and sialofucosylated types were grouped (**Figure 4**). Similarly, total levels of sialylation involved grouping sialylated-only and sialofucosylated species. Brain N-glycans were generally high in fucose and sialic acids, and in nearly all regions fucosylated N-glycans represented over 90% of the total abundances (**Figure 4a**). Similarly, sialylated glycans represented 70-90% of all brain N-glycans (**Figure 4b**). As both sialylation and fucosylation were abundant, most of the N-glycans in nearly all the regions were sialofucosylated. The exceptions were the lateral cerebral cortex and pons where sialofucosylation was lower in comparison to the other nine brain regions but still high at 60-70% (relative abundances). The lower abundant N-glycan were high mannose and undecorated (**Figure 4c and 4d**). High mannose glycans were generally low in abundances (below 10%) except in the lateral cerebral cortex and pons, where they represent 25% of the total glycan species. Those that were non-high mannose type glycans were composed primarily of over 65% complex-types with lower abundances (around 15%) for hybrid-type structures (**Figure S3**).

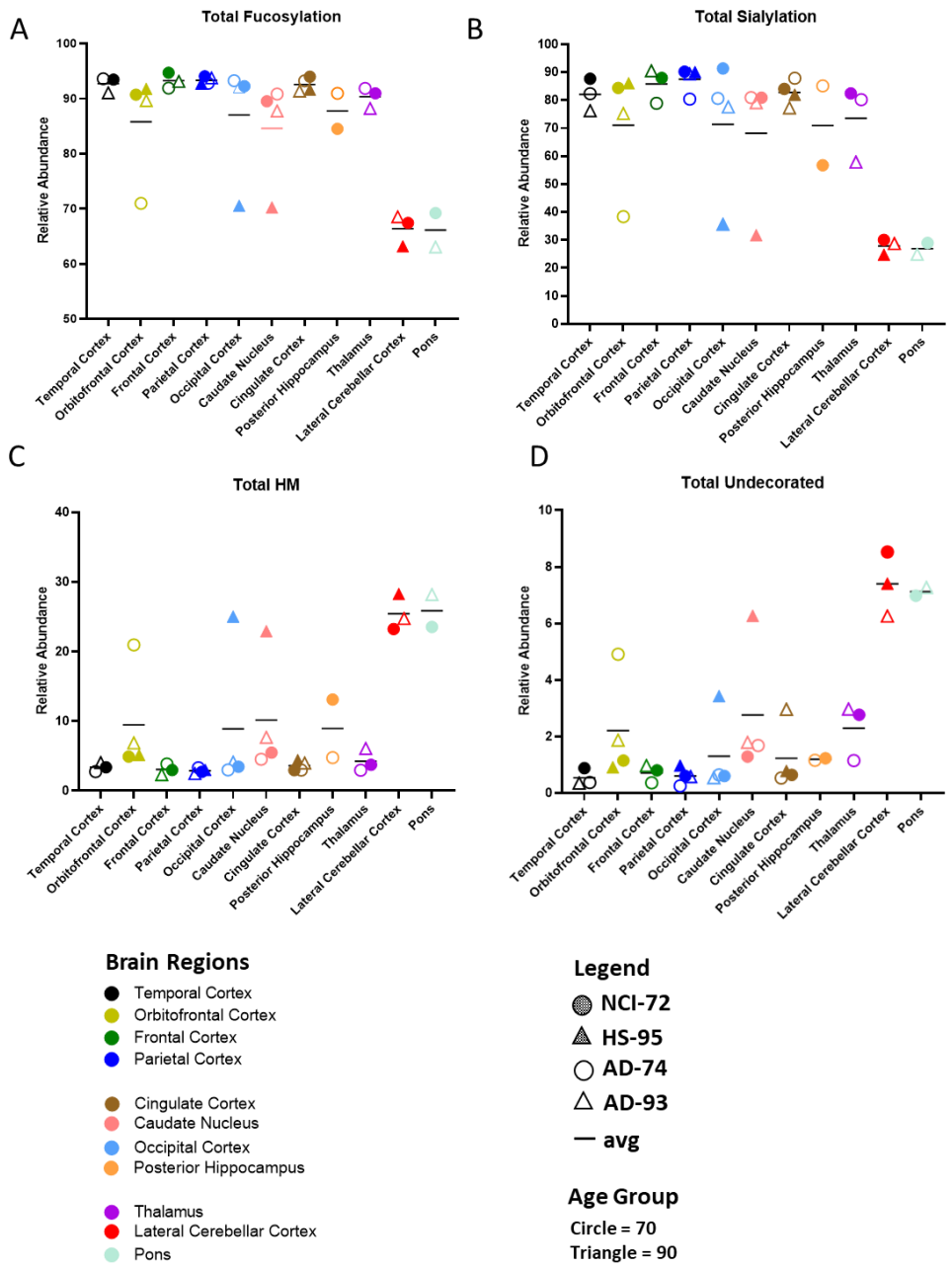


Figure 4. The relative abundances of the total amounts of (A) fucosylation, (B) sialylation, (C) high mannose, and (D) undecorated across the 11 brain regions from the four subjects. Each brain region is distinctly color coded where circles denote age group 70 and triangles denote age group 90. Shaded shapes represent subject with no cognitive impairment (NCI) while unshaded shapes represent subject with Hippocampal sclerosis (HS).

We also evaluated the level of branching in the N-glycans across all the brain regions (**Figure 5**). The N-glycans were generally highly branched with tetra-antennary type glycans being the most abundant with relative intensities ranging from 22% to 60% (**Figure 5c**). However, in the lateral cerebellar cortex and pons, similar abundances of bi-, tri-, and tetra-antennary structures were observed. The highest abundances of tetra-antennary glycans were in the parietal cortex for all four subjects. Bi-antennary glycans were found to be highest in the lateral cerebellar cortex with almost 20% in relative abundances (**Figure 5a**). Tri-antennary glycans ranged from 16% to 24% with the highest percentages observed in the orbitofrontal cortex and caudate nucleus (**Figure 5b**).

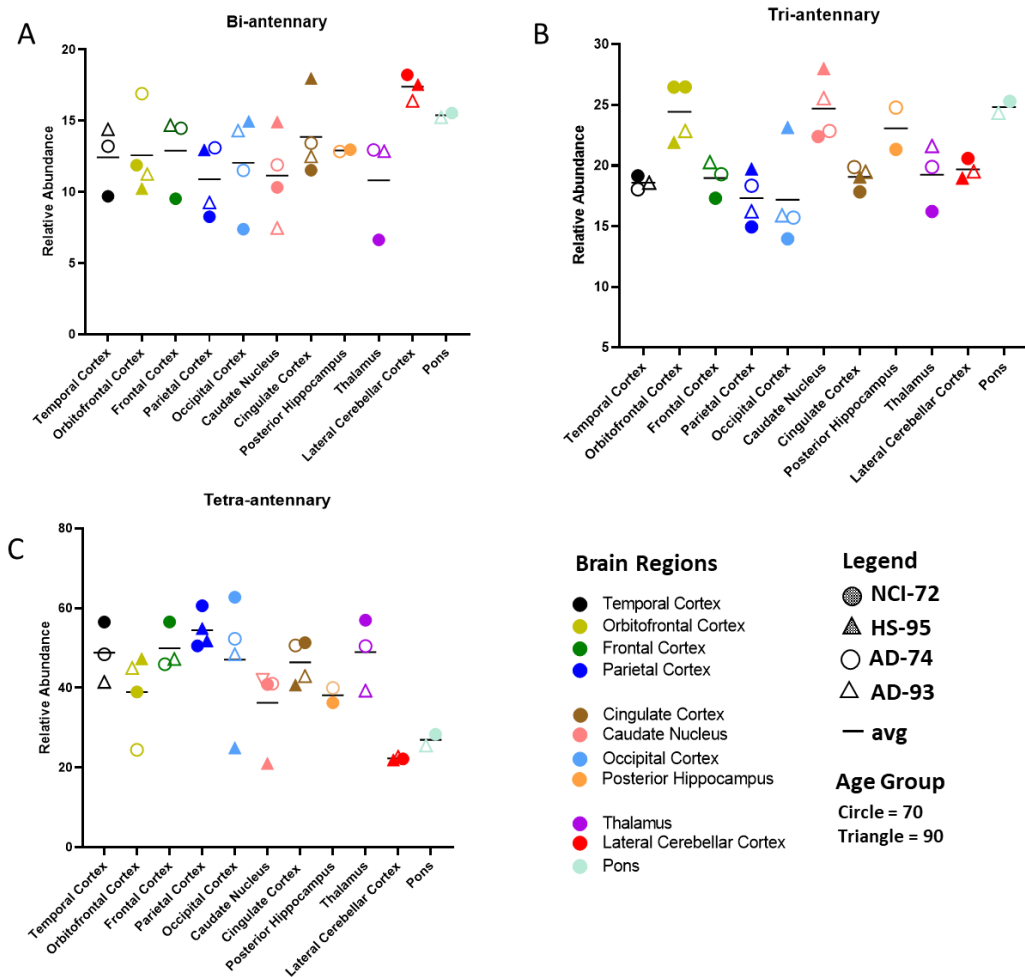


Figure 5. Comparison of the level of branching for (A) bi-antennary, (B) tri-antennary, and (C) tetra-antennary across the temporal cortex, orbitofrontal cortex, frontal cortex, parietal cortex, cingulate cortex, caudate nucleus, occipital cortex, posterior hippocampus, thalamus, lateral cerebellar cortex, and pons.

A comprehensive representation of all detected N-glycans in the brain regions was summarized (**Figure S4**). The results indeed showed that sialofucosylated N-glycans were the most abundant in almost all brain regions. The exceptions were again noted in the occipital cortex and caudate nucleus of **NC-95**, and the orbitofrontal of **AD-74**. For all the subjects, the lateral cerebellar cortex and pons differed from the rest of the regions. It should be noted that there were specific N-glycans that were abundant in the samples, regardless of age, disease, and brain region. Notably, the sialofucosylated tetraantennary species with composition $\text{Man}_3\text{Gal}_3\text{GlcNAc}_7\text{Fuc}_4\text{NeuAc}$, was abundant across 78% of all the samples (**Figure S4**).

A nontargeted analysis of the four subjects using principal component analysis (PCA) and all detected N-glycan compositions with their relative abundances was performed (**Figure S5**). The results showed brain regions clustered into three distinct groups (**Figure S5**). Samples from **NCI-72** clustered in three different groups. One group (*Cluster 1*) was composed of the orbital frontal cortex, caudate nucleus, temporal cortex, frontal cortex, thalamus, occipital cortex, parietal cortex, and cingulate cortex. The posterior hippocampus of **NCI-72** grouped into *Cluster 2*. The remainder, lateral cerebellar cortex, and pons, of **NCI-72** associated with a third group (*Cluster 3*). For the 95-year-old with hippocampal sclerosis (**HS-95**), *Cluster 1* also contained the orbital frontal cortex, temporal cortex, frontal cortex, and parietal cortex, however the caudate nucleus and occipital cortex grouped with *Cluster 3* while the cingulate cortex grouped with *Cluster 2*. Due to difficulties in obtaining all the brain regions, some such as the thalamus were

not obtained for all subjects. The lateral cerebellar cortex, which was previously in *Cluster 3*, remained unchanged. **AD-74** showed large differences compared to **NCI-72**. The caudate nucleus, thalamus, and cingulate cortex remained in *Cluster 1*, while the temporal cortex, occipital cortex, frontal cortex, and parietal cortex, which were previously grouped in *Cluster 1* and are the four major sections of the outer brain lobes, now grouped with *Cluster 2*. *Cluster 3* only included the orbitofrontal cortex for **AD-74**. Lastly, for the 94-year-old with AD (**AD-94**), *Cluster 1* was composed of the orbitofrontal cortex, caudate nucleus, and the frontal cortex. *Cluster 2* consisted of the cingulate cortex, temporal cortex, occipital cortex, and thalamus. Interestingly, *Cluster 3*, which included the pons and the lateral cerebellar cortex for all subjects, showed the strongest glycan diversity containing high levels of high mannose type species. Changes in glycosylation were apparent in some brain regions. Namely, the caudate nucleus of **HS-95** was found in *Cluster 3*, while for the other subjects this brain region grouped in *Cluster 1*. Similarly, for the occipital cortex, **HS-95** grouped in *Cluster 3*, while **AD-74** and **AD-95** grouped in *Cluster 2*, and **NCI-72** grouped in *Cluster 1*.

Glycoproteomic analysis of the brain regions

A glycoproteomic analysis of the membrane proteins in the select brain regions (frontal, temporal, parietal, occipital, cingulate, lateral cerebellar and orbitofrontal cortex, posterior hippocampus, thalamus, caudate nucleus, and pons) was also performed. Because the glycans were primarily on the membrane, membrane proteins were enriched and also analyzed using standard proteomic analysis. This yielded approximately 1000 proteins in each of the regions. An additional digested membrane fraction was passed through HILIC SPE to enrich for glycopeptides. The region-specific cell membrane glycoproteins were identified, and site-specific glycosylation

was determined and quantified. The number of site-specific glycopeptides varied with each region, accounting for a total of more than 500 unique membrane glycoproteins identified when all regions were combined.

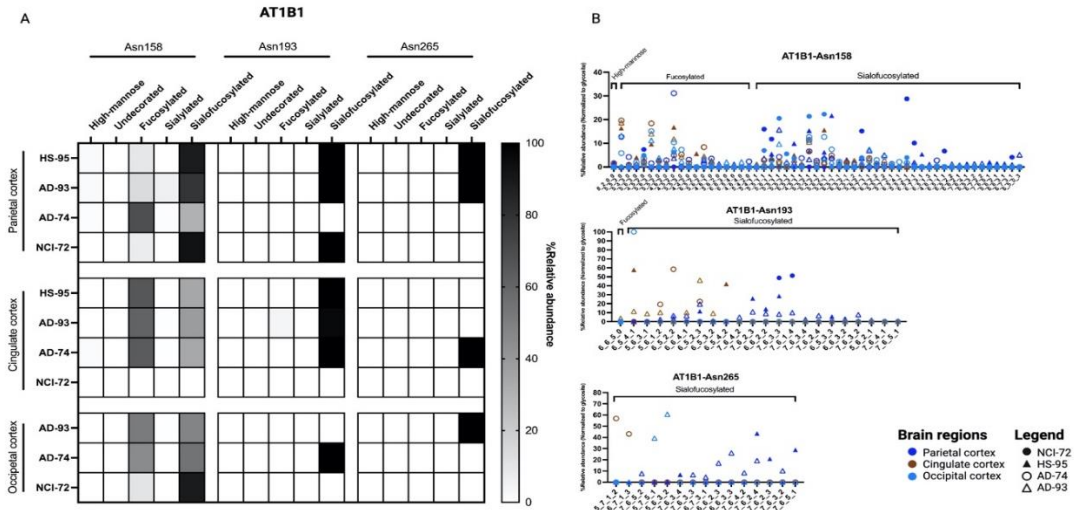


Figure 6. (A) Site-specific glycosylation pattern of AT1B1 (Sodium/Potassium-transporting ATPase subunit B1) across three brain regions – Parietal, Cingulate, and Occipital cortex – and across its three known glycosylation sites: Asn158, Asn193, and Asn265. (B) Distribution of glycoforms and glycan type across the three brain regions and three glycosylation sites.

The glycoproteins in each region were compared across all 11 regions. All glycoproteins detected in a specific region for the four subjects were grouped together (**Figure S6**). Comparisons yielded similarities in the membrane glycoproteins between the regions. Comparing the temporal cortex and the frontal cortex yielded a 47% similarity. The similarities between the regions differed considerably from as low as 9% between the parietal cortex and pons to as high as 60% for the orbitofrontal cortex and caudate nucleus. Interestingly, the geographic location does not seem to correlate with glycoprotein similarities. For example, the

parietal cortex which sits near the top and center of the cerebral cortex has low glycoprotein similarities with the pons which is not part of the cerebral cortex but the brainstem. Remarkably, a very high overlap in membrane proteins is observed in the orbitofrontal cortex which sits in the front of the cerebral cortex, and the caudate nucleus which lies deep inside the brain.

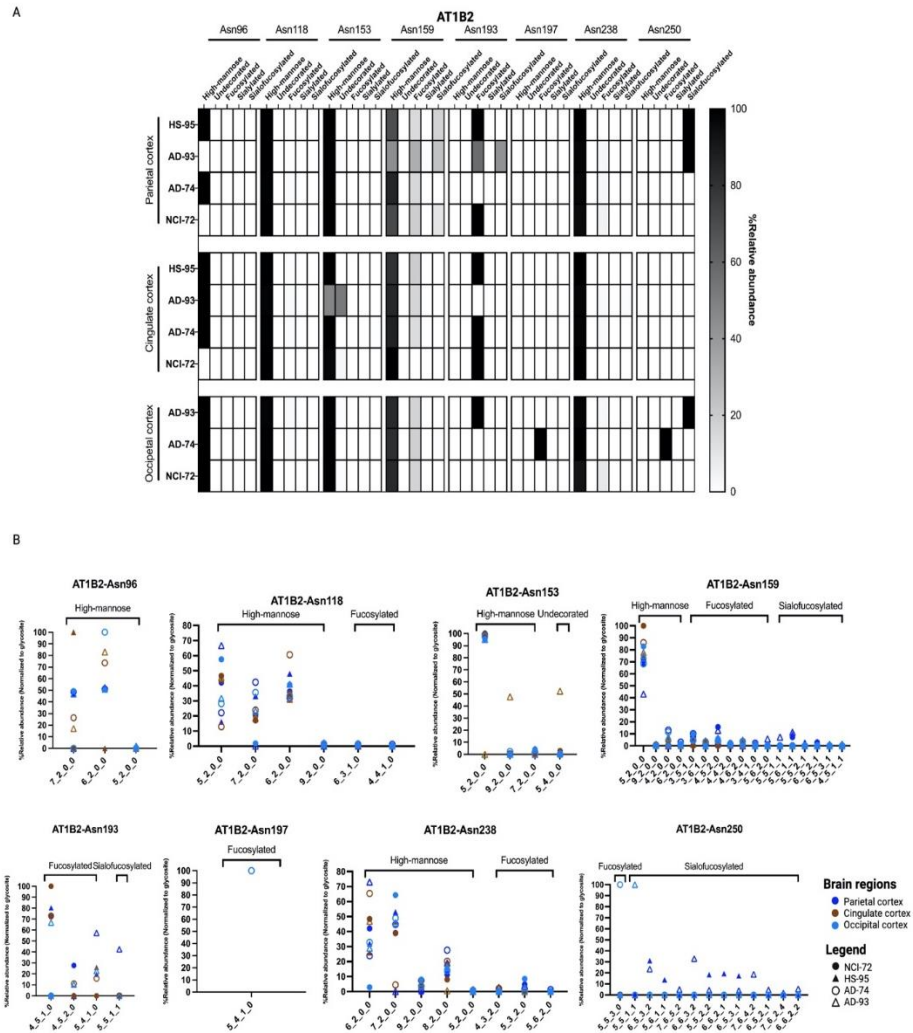


Figure 7. (A) Site-specific glycosylation pattern of AT1B2 (Sodium/Potassium-transporting ATPase subunit B2) across three brain regions – Parietal, Cingulate, and Occipital cortices – and across its eight known glycosylation sites: Asn96, Asn118, Asn153, Asn159, Asn193, Asn197, Asn238, and Asn250. (B) Distribution of glycoforms and glycan type across the three brain regions and eight glycosylation sites.

Glycoproteins varied in glycosylation between different glycosites. The proteins sodium/potassium-transporting ATPase subunits beta-1 (AT1B1), beta-2 (AT1B2), and beta-3 (AT1B3) were found to be abundant in all regions and illustrated the diversity between glycosylation sites and brain regions. AT1B1 had three putative N-glycosites corresponding to N158, N193, and N265. AT1B1-N158 was found to be both fucosylated and sialofucosylated, while N193 and N265 were solely sialofucosylated (**Figure 6A**). The most abundant N-glycan compositions in N158 were found to be sialofucosylated (mainly monosialylated) with compositions corresponding to Hex₅HexNAc₅Fuc₁NeuAc₁, Hex₅HexNAc₅Fuc₂NeuAc₁, and Hex₅HexNAc₆Fuc₂NeuAc₁. N193 and N265 bore similar compositions but were more highly sialylated with di-, tri-, and tetra-sialylated to include Hex₆HexNAc₅Fuc₂NeuAc₃, Hex₇HexNAc₆Fuc₃NeuAc₃, and Hex₇HexNAc₆Fuc₂NeuAc₄ (**Figure 6B**). For comparison, the relative abundance of each N-glycan composition was normalized to all the glycoforms associated with the site.

To determine whether site-specific occupancy of proteins varied across regions, selected glycoproteins were compared across three randomly selected regions, namely the parietal-, occipital- and cingulate cortex. N-Glycans in the three proteins AT1B1, AT1B2, and AT1B3 were found to be primarily fucosylated and sialofucosylated complex-type glycans and high mannose types. For AT1B1, there were only minor changes in glycosylation between the three regions. However, AT1B2 with eighth detected glycosites, the glycoforms varied between regions and between subjects. The glycosites N96, N118, N153, N159, and N238 were primarily mannosylated, while N193 and N250 were mainly fucosylated and sialofucosylated (**Figure 7A**). Interestingly, site N197 was only glycosylated in the occipital cortex of **AD-74** and was not found

to be glycosylated in the other two regions. In glycosite N159, Man5 was the most abundant glycoform however fucosylated and sialofucosylated composition were still present in lower abundances (**Figure 7B**). AT1B3 was found to be least glycosylated among the three ATPase beta subunits, with only one N-glycosylation site, N124. In the three brain regions, AT1B3-N124 was found to be primarily sialofucosylated and fucosylated (**Figure 8A**).

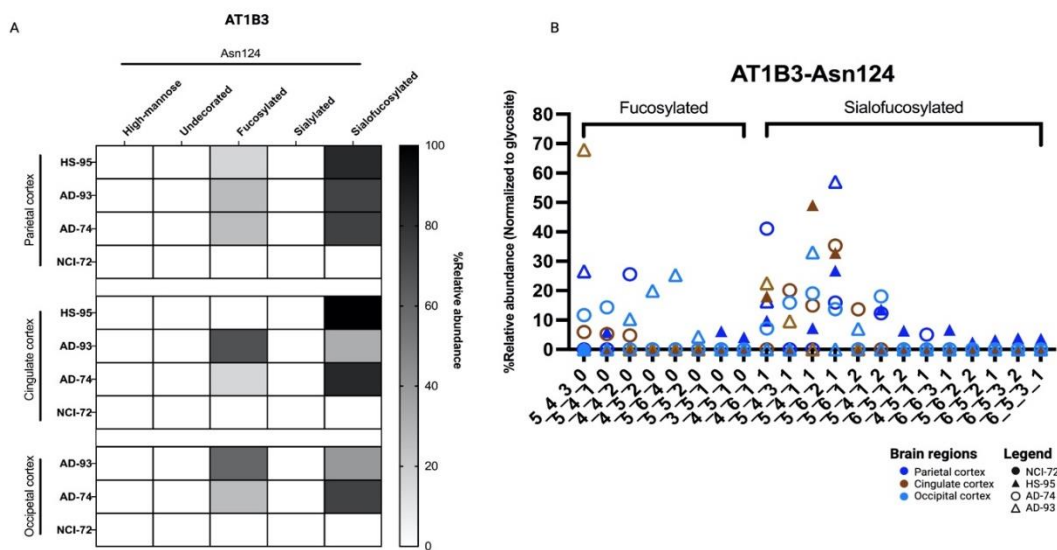


Figure 8. (A) Site-specific glycosylation pattern of AT1B3 (Sodium/Potassium-transporting ATPase subunit B3) across three brain regions – Parietal, Cingulate, and Occipital cortices – and across one of its known glycosylation sites: Asn124. (B) Distribution of glycoforms and glycan type across the three brain regions and glycosylation site.

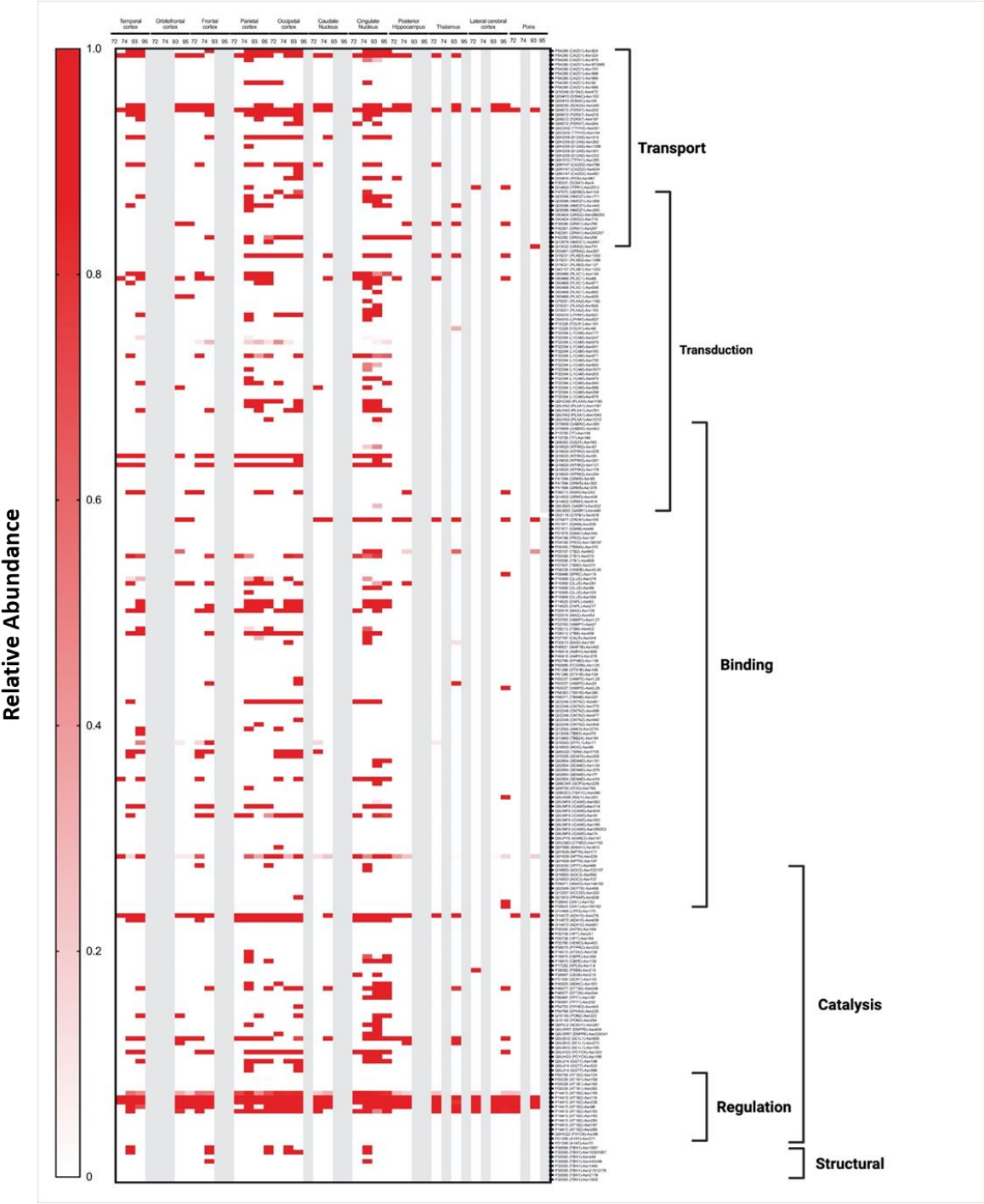
To obtain a comprehensive view of the glycans associated with the glycoproteins in the different regions, heat maps were constructed corresponding to each glycosite across different regions (**Figure 9A**). Each horizontal line represented a specific glycosite, with the glycosites for the same proteins grouped together. The proteins were further grouped according to their function as determined by the gene ontology. The results were separated for the different

glycans with the high mannose-type glycans illustrated in **Figure 9A**, complex-type undecorated (**Figure 9B**), complex-type sialylated-only (**Figure 9C**), complex-type fucosylated-only (**Figure 9D**), and complex-type sialofucosylated (**Figure 9E**).

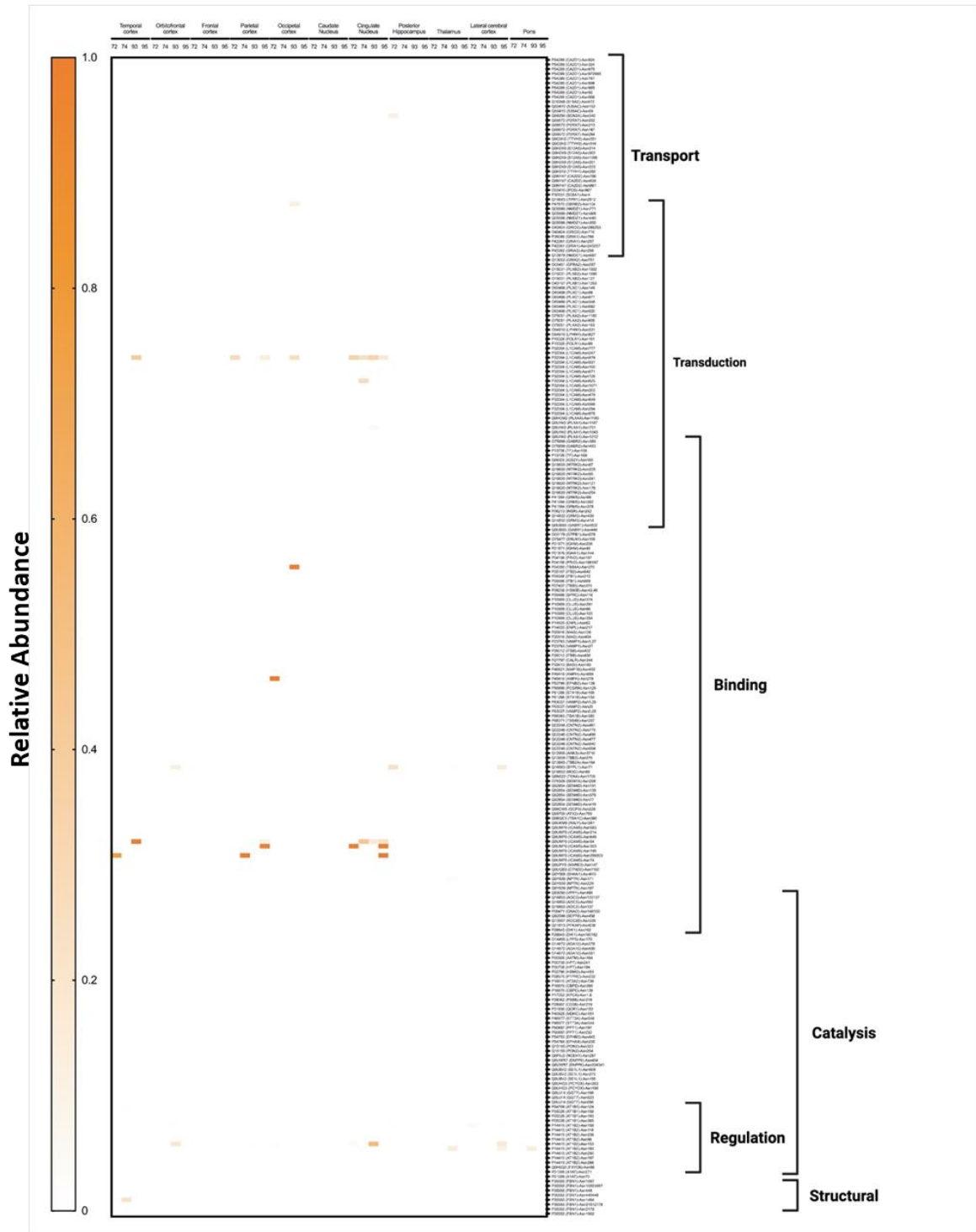
The high mannose-type glycans were found in most of the glycoproteins (**Figure 9A**). Interestingly, the glycomic data showed that this glycan type was not particularly abundant in the brain. However, they appear to be widely distributed on several protein sites with some maintained throughout all subjects and brain regions (solid red lines). Glycoprotein AT1B2 glycosite N96, N118 and N238, disintegrin and metalloproteinase domain-containing protein 10 (ADA10) at N278 and P2X purinoceptor 7 (P2RX7) at N202 followed similar behavior (**Figure 9A**). The least abundant subtype in the glycomic profile was the undecorated N-glycans (**Figure 4C**), which correlated well with the glycoproteomic analysis (**Figure 9B**). There were no glycosites observed that maintained this glycan across all regions and all subjects. However, Intercellular adhesion molecule 5 (ICAM5) at glycosite N303 was identified to contain the highest abundance of undecorated glycans in the cingulate cortex in subjects **NCI-72** and **HS-95**, temporal and parietal cortex in subject **AD-93**. Similarly, the sialylated-only glycans (**Figure 9C**) were not broadly present but found in several more sites. However, these glycan subtypes were generally not found in the same glycosites among all regions and subjects. The most abundant sialylated-only glycopeptide was found on N241 of glycoprotein Haptoglobin (HPT), which was present in more than 50% of the brain regions. Interestingly, the fucosylated-only (**Figure 9D**) glycans were found in more sites than the undecorated and sialylated-only glycans. This glycan type was maintained among several regions and found on the majority of the glycoproteins. The most common complex type-structures were the sialofucosylated species (**Figure 9E**). These were

similarly found in many glycosylation sites, some with presence across several regions and all subjects.

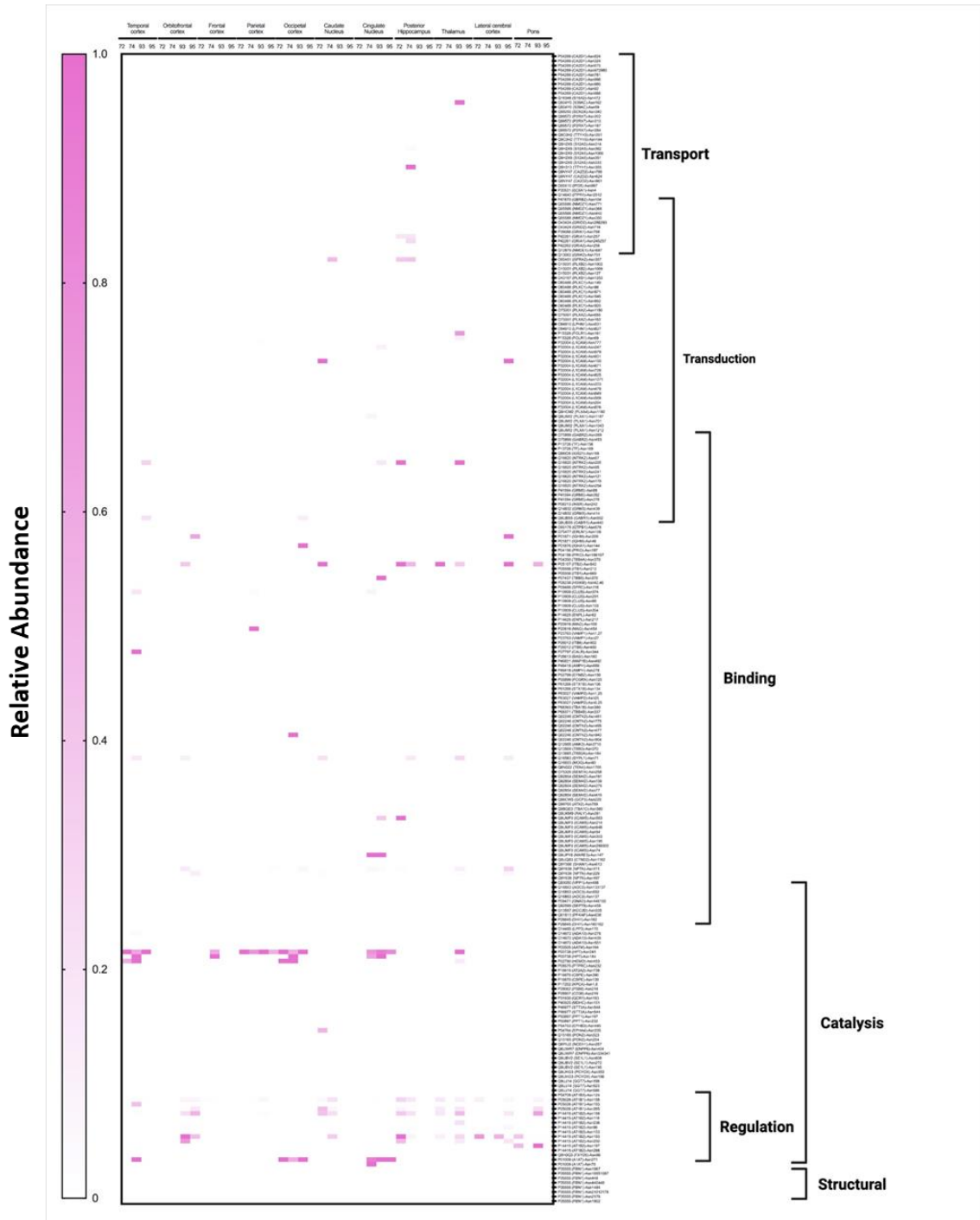
[A]



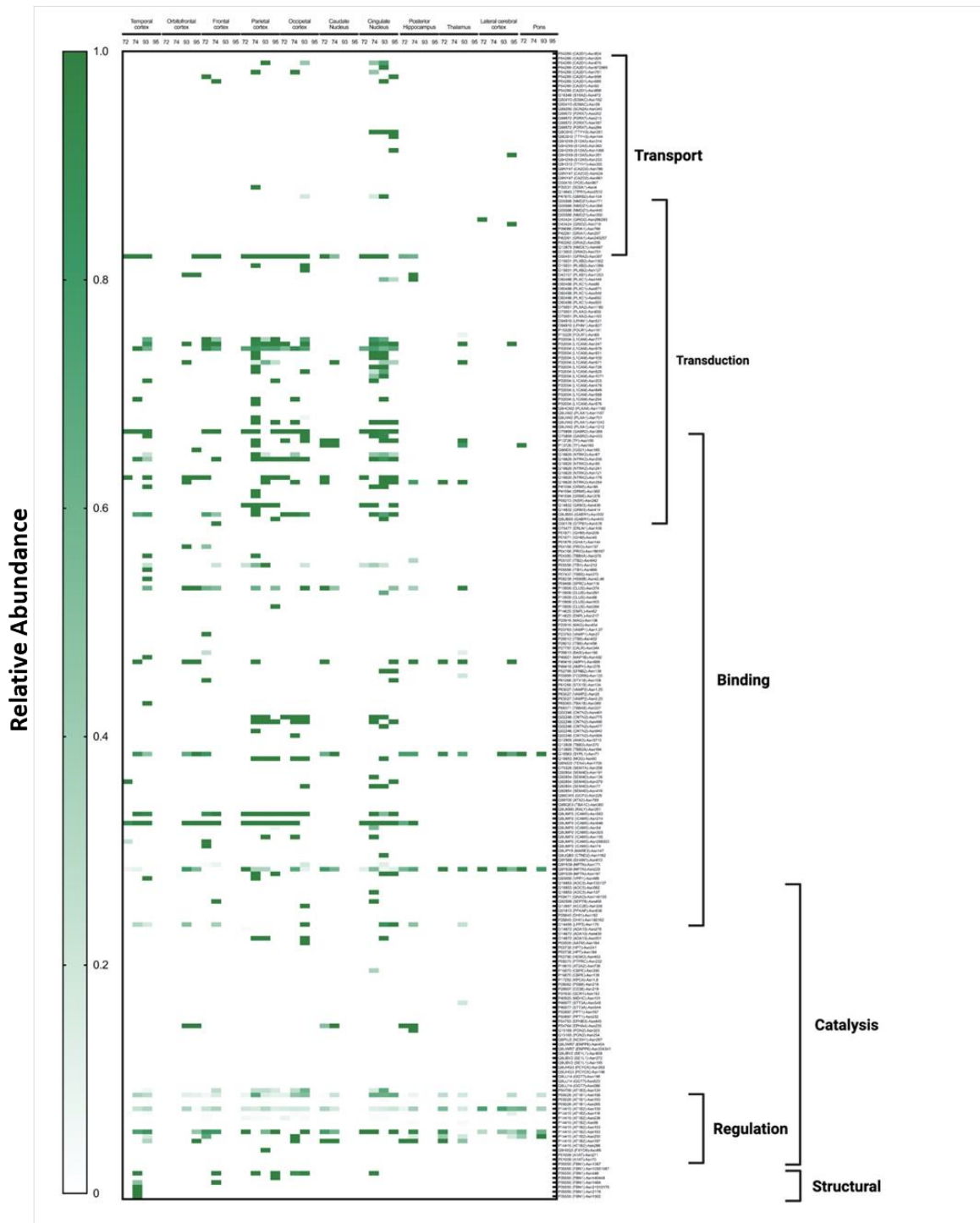
[B]



[C]



[D]



[E]

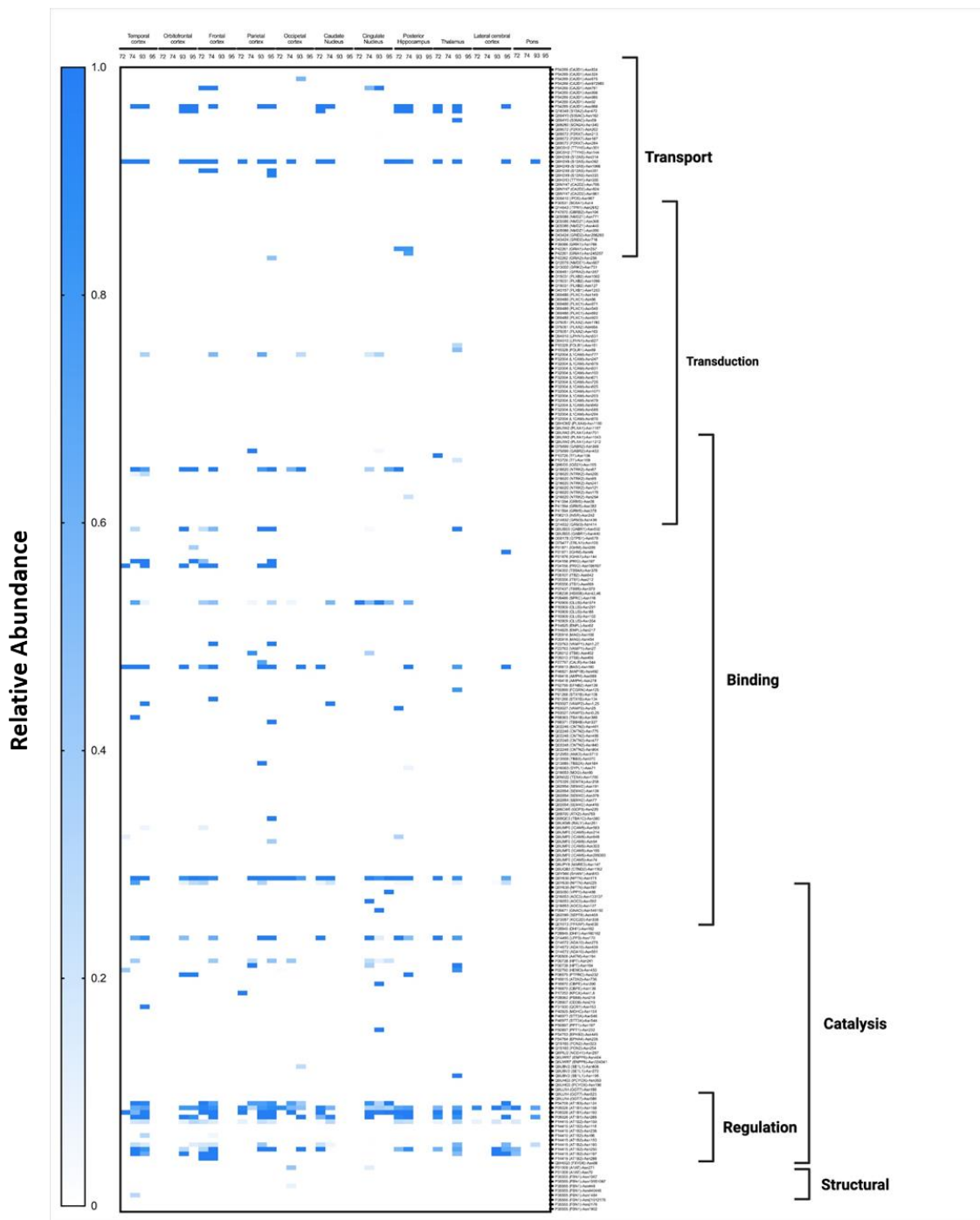


Figure 9. Heat maps displaying the characterization of the N-glycoproteome in the human brain separated by their glycotypes including A) high mannose, B) undecorated, C) sialylated-only, D) fucosylated-only and E) sialofucosylated. The heat map displays low to high relative abundances. More intense color correlated with higher glycan abundances on the specific glycosite. Molecular processes which include transport, transduction, binding, structural, regulation, and catalysis are shown on the right.

DISCUSSION

The N-glycans are typically the most abundant of the glycoconjugate with the largest structural diversity. They provide a convenient yet extensive view of the brain glycome. Similarly, as many brain glycans are N-glycosylated, the geographical survey provides both glycomic and glycoproteomic distribution of the brain. Large glycomic variations were readily observed in different functional parts of the brain. The most notable observation in the N-glycome of the brain was the high abundance of sialofucosylated N-glycans as well as the presence of large multi-antennary structures. Previous reports noted similarly multi-antennary structures for brain glycans with as high as four and five antennae (21). These results contrast with N-glycans in the blood, the most glycomically characterized tissue, which yielded primarily biantennary structures with more sialylated but fewer sialofucosylated species (30). These large multi-antennary structures and the high levels of sialofucosylation are appropriate given the highly interactive nature of brain cells and tissues (14). Studies performed both in rodents and pigs have also shown the primacy of sialic acid in improving cognitive functions (31–33). Fucose has been reported to play important roles in neural development (34, 35). Neuronal synapses have been shown to have enriched levels of fucose, and indeed increase levels of fucosyltransferases have also been reported during synaptogenesis (1, 36). Previous studies on brain glycosylation have focused primarily on sialylation (7, 31, 32, 37), but clearly fucosylation is an abundant and therefore an important structural component. Indeed, high levels of fucosylation are found in most of the brain regions (**Figure 4C**). When correlated with the glycoproteomic and gene ontology data, the fucosylated glycoproteins functionally align more with molecular transduction (**Figure S9**) suggesting that high levels of fucosylated type glycan present in the brain are crucial in regulating

many important cellular functions such as cell signaling. Additionally, most of the fucose is in the core structures, which has been shown to promote trans rather than cis protein-protein interactions through the glycan (38). There are two regions that are glycomically very dissimilar from the remaining brain regions and contain significantly lower sialofucosylated species. The lateral cerebellar cortex and pons are both low in complex-type structures and abundant in high-mannose type structures.

The variations between the subjects point to possible differences between disease states that could be revealed with more samples. For example, a comparison of the frontal cortex between **NCI-72** and **AD-74** (**Figure 4C**, **Figure S1B**) showed a decrease in sialofucosylated species. This result is in agreement with previous reports where a significant decrease in sialyltransferase (ST) activity was similarly observed in serum, postmortem brains, and cerebrospinal fluid (CSF) proteins of AD patients (39–41). Genomic studies have also associated the gene Siglec 33, a sialic acid binding receptor, with late-onset AD (39). In these experiments, in the occipital cortex, and temporal cortex a decrease in sialofucosylated N-glycans was also observed when comparing **NCI-72** with both AD subjects (**AD-74** and **AD-93**). As the N-glycans were enriched from proteins on the cell membrane, the loss of these species specifically the sialic acid moieties, may mean the loss of intracellular interactions on the cell surface of the brain cells. Studies involving polysialylated-neural cell adhesion molecules (PSA-NCAM) showed that the loss of PSA was associated with the disruption of several NCAM-dependent neurodevelopmental processes (42). A large body of work on brain sialylation has focused primarily on PSA (32, 37, 43, 44), however, the large abundances of sialofucosylated species should encourage the examination of sialofucosylated NCAMs in axonal guidance.

The glycoproteomic analysis yielded site-specific information of proteins allowing direct comparison across brain regions and between patients (**Figure 9**). The glycans most preserved across sites are the high mannose types. These glycans are unique among the various types as some sites maintain them among all subjects and across many regions of the brain. Comparison of the other glycans shows that neither the sialylated (only), fucosylated (only), nor sialofucosylated species maintain the glycans across all samples uniformly. Closer inspection of the sites showed that AT1B2 (site N118) and (site N238) were two examples of sites that contain high mannose in nearly all samples. AT1B2 is a functionally important molecule at synapses as part of the ion pump Na⁺/K⁺ -ATPase. Earlier studies have shown that 80% of its glycans are high mannose (2, 45). Another high mannose site that was found occupied by the same glycan type across nearly all samples was ADA10 (Site N278). Further inspections of the heat maps showed that sialylated (only) and fucosylated (only) sites were preserved in some regions, but not consistently as with high mannose type. Interestingly, when focusing on all the glycopeptides containing fucose-only (**Figure 9D**), N-glycans, the signal transduction type glycoproteins, show high relative abundances in comparison to other molecular functions such as transport type glycoproteins. However, the fucosylation is not preserved among all subjects. This is of importance as such processes are known to be mediated by cell surface glycosylation and potential perturbation could result in a dysfunctional cell membrane. Sialofucosylated compositions were much more common across many regions and some subjects. For example, AT1B1 (Site N158) maintained sialofucosylated glycans among nearly all regions and subjects. Interestingly, sialofucosylated N-glycans were most abundant on glycoproteins corresponding to regulatory processes as seen in **Figure 9E**. The glycan maps further showed the breadth of

variations in the glycosites across different regions associated with different pathological conditions.

We note the limitations of this study, which is the small number of subjects prohibiting any conclusions regarding glycan specific clinical indicators. However, these brain samples are difficult to obtain, but efforts are underway to increase the number of subjects. To increase the sample size further, we plan to focus the collection to a limited number of brain regions. Other limitations include the lack of comprehensive structural analysis of the glycans. The linkages, for example, are important component of the structures and strongly affect the function and the specificity of the glycan interactions. The lack of glycan standards also prohibits absolute quantitation, however the low coefficient of variations in the measurements allow accurate relative quantitation.

CONCLUSION

In summary, our study demonstrated the most comprehensive glycan map of the brain of elderly adult males and showed that protein glycosylation could be altered by disease conditions. Some glycosites may be more affected than others, while glycosites containing high mannose-type structures were more persistent and less variable compared to other glycoforms. While the biological significance of the glycomic variation in the regions needs to be further resolved, the glycans appear to be primarily sialofucosylated species that are multi-antennary with a high degree of branching. Sialic acids have been the primary focus of brain glycosylation, but the large abundance of fucosylation indicates that fucose should also be considered of great importance.

The results further showed the broad compositional ranges of glycans between regions and between subjects suggesting potential targets for biomarkers and therapeutics.

METHODS

Cell membrane extraction from human brain tissue

All tissue samples were obtained from the UC Davis Alzheimer's Disease Research Center brain bank. Tissue samples were homogenized and resuspended in homogenization buffer containing 0.25 M sucrose, 20 mM HEPES-KOH (pH 7.4), and a 1:100 protease inhibitor cocktail. Cells were lysed on ice using a probe sonicator operated with alternating on and off pulses of 5 and 10 s, respectively. Lysates were pelleted by centrifugation at 9000xg for 10 min to remove the nuclear fraction and cell debris. The supernatant was transferred to high-speed tubes, loaded onto a Beckman Optima TLX Ultra-centrifuge at 4°C, and centrifuged at 200,000 x g for 45 min in series to remove other nonmembrane subcellular fractions. The resulting cell membrane pellet was stored at - 20°C until further processing. Optimizations to this approach has been shown to generate a purified cell membrane pellet (28).

Enzymatic Release and Purification of N-Glycans

Proteins were suspended with 100 µL of 100 mM NH_4HCO_3 in 5 mM dithiothreitol and heated at 100°C for 10s to thermally denature the proteins. To release the glycans, 2 µL of peptide N-glycosidase F were added to the samples, followed by incubation in a microwave reaction at 60°C for 10 min to accelerate N-glycans release. Samples were incubated for 18 h at 37°C to hydrolyze the N-glycans. The reaction was quenched with 350 µL of water followed by

ultracentrifugation at 200,000 x g to separate the N-glycans and the membrane fraction (MF) containing our lipids and de-glycosylated proteins. The released N-glycans were purified by solid-phase extraction using porous graphitized carbon (PGC) packed cartridges. The cartridges were first equilibrated with nanopure water and a solution of 80% (v/v) acetonitrile and 0.05% (v/v) trifluoroacetic acid in water. The dried samples were solubilized, loaded onto the cartridge, and washed with nanopure water to remove salts and buffer. N-Glycans were eluted with a solution of 40% (v/v) acetonitrile and 0.05% (v/v) trifluoroacetic acid in water, dried and reconstituted in 30µl of water prior to mass spectrometric analysis.

Glycoproteomics Enzymatic Digestion and Purification

Specific brain region of interest was homogenized and then cell lysis in a buffer containing 0.25 M sucrose, 20 mM HEPES-KOH (pH 7.4) using a probe sonicator. Subcellular fractionation was performed to isolate cell membrane fraction. Cell membrane proteins were dissolved and denatured with 8M urea for optimal digestion followed by dithiothreitol (DTT) and alkylated with iodoacetamide (IAA). Protein concentration was determined using BCA Protein Assay Kit. Samples were then digested with trypsin at 37°C for 18h. Enrichment of glycopeptides was necessary to avoid ion suppression effects from coeluting peptides. The high enrichment efficiency was done using iSPE HILIC cartridges.

Glycomics Analysis by LC-MS/MS

Purified brain N-glycans were analyzed using an Agilent nano-LC/chip Q-ToF MS system. The nano-LC system employs a binary solvent consisting of A (0.1% formic acid in 3% acetonitrile in water (v/v)) and B (0.1% formic acid in 90% acetonitrile in water (v/v)). Samples were enriched

and separated on the Agilent HPLC-Chip comprised of a 40 nL enrichment column and a 75 μm x 43 mm ID analytical column both packed with porous graphitized carbon in 5 μm particle size. The sample was delivered by the capillary pump to the enrichment column at a flow rate of 3 $\mu\text{L min}^{-1}$ and separated on the analytical column by the nano-pump at a flow rate of 0.3 $\mu\text{L min}^{-1}$ with a gradient that was previously optimized for N-glycans: 0% B, 0-2.5 min; 0-16% B, 2.5-20 min; 16-44% B, 20-30 min; 44-100% B, 30-35 min; and 100% B, 35-45 min followed by pure A for 20 min of equilibration. MS spectra were acquired at 1.5 s per spectrum over a mass range of m/z 600–2000 in positive ionization mode. Mass inaccuracies were corrected with reference mass m/z of 1221.991.

N-Glycan compositions were identified using MS and MS/MS data as well as an in-house retrosynthetic library based on the mammalian N-glycan biosynthetic pathway. Deconvoluted masses were compared to theoretical masses using a mass tolerance of 20 ppm and a false discovery rate of 0.5% on the Agilent MassHunter software version B.7. Relative abundances were determined by integrating peak areas for observed glycan masses, averaging abundances from instrumental triplicates and normalizing to the summed peak areas of all glycans detected.

Enriched glycopeptides were subjected to nanoLC-Orbitrap Fusion Lumos for MS/MS analysis. 1 μL of samples was injected and the analytes were separated on an Acclaim PepMap C18 LC column (3 μm , 0.075 mm x 500 mm, ThermoFisher Scientific) at a flow rate of 300 nL min^{-1} . Binary mobile phase containing 0.1% formic acid in water and 80% acetonitrile containing 0.1% formic acid were used as solvents A and B, respectively. MS spectra was acquired at a rate of 1.5 s per spectrum over a mass range of m/z 600-2000 in positive ionization mode. The filtered

precursor ions in each MS spectrum were subjected to fragmentation through 30% higher-energy C-trap dissociation (HCD) with nitrogen gas.

Data Analysis

Glycoproteins were identified using the Byonic v. 3.5.0 software (Protein Metrics, CA) against the human protein database (UniProt). Alkylation of cysteine with carbamidomethylation was assigned as a fixed modification. Deamidation of asparagine and glutamine and oxidation of methionine was selected as common variable modification. Acetylation of the protein N-terminus and methylation of lysine and arginine were assigned as rare variable modifications. An in-house human N-glycan database was applied for site-specific in asparagine N-glycosylation. A DeltaMod threshold of 10.0 was used and a $|\text{Log Prob}| < 2$ (error probabilities > 0.01) were removed.

Glycopeptides were quantified using Byologic Version: v3.11-1 (Protein Metrics, CA) after identification using Byonic. Glycopeptide intensities were normalized to each specific protein glycosite, allowing for comparison between glycoproteins having varying degrees of expression across brain regions. Glycans attached to each glycosite were categorized based on the N-glycan subtypes – high mannose, undecorated, fucosylated, sialylated, and sialofucosylated N-glycan types. Relative abundances of each N-glycan subtype attached to protein glycosites were summed and summarized into heatmaps generated by GraphPad Prism version 9 (CA). The heatmaps were further annotated by mapping the gene ontologies – biological processes of the glycoproteins in PantherDB (<http://pantherdb.org/>) (46). This allows us to view the N-glycosylation of proteins participating in specific biological processes for each brain region.

REFERENCES

1. H. E. Murrey, L. C. Hsieh-Wilson, The chemical neurobiology of carbohydrates. *Chem. Rev.* **108**, 1708–1731 (2008).
2. R. Kleene, M. Schachner, Glycans and neural cell interactions. *Nat. Rev. Neurosci.* **5**, 195–208 (2004).
3. A. Varki, Biological roles of glycans. *Glycobiology* **27**, 3–49 (2017).
4. F. Zhao, L. Zhong, Y. Luo, Endothelial glycocalyx as an important factor in composition of blood-brain barrier. *CNS Neurosci. Ther.* **27**, 26–35 (2021).
5. N. S. Rolf Apweiler a, Henning Hermjakob, On the frequency of protein glycosylation, as deduced from analysis of the SWISS-PROT database1. *Biochim. Biophys. Acta* **1**, 4–8 (1999).
6. J. Paprocka, A. Jezela-Stanek, A. Tylki-Szymańska, S. Grunewald, Congenital disorders of glycosylation from a neurological perspective. *Brain Sci.* **11**, 1–25 (2021).
7. H. Scott, V. M. Panin, N-Glycosylation in Regulation of the Nervous System. *Adv Neurobiol*, 367–394 (2014).
8. L. R. Ruhaak, S. Miyamoto, C. B. Lebrilla, Developments in the identification of glycan biomarkers for the detection of cancer. *Mol. Cell. Proteomics* **12**, 846–855 (2013).
9. M. J. Kailemia, D. Park, C. B. Lebrilla, Glycans and glycoproteins as specific biomarkers for cancer. *Anal. Bioanal. Chem.* **409**, 395–410 (2017).
10. L. Veillon, C. Fakih, H. Abou-El-Hassan, F. Kobeissy, Y. Mechref, Glycosylation Changes in Brain Cancer. *ACS Chem. Neurosci.* **9**, 51–72 (2018).
11. M. Frenkel-Pinter, *et al.*, Interplay between protein glycosylation pathways in Alzheimer’s disease. *Sci. Adv.* **3**, e1601576 (2017).
12. Q. Zhang, C. Ma, L. S. Chin, L. Li, Integrative glycoproteomics reveals protein n-glycosylation aberrations and glycoproteomic network alterations in Alzheimer’s disease. *Sci. Adv.* **6**, 1–19 (2020).
13. R. Raghunathan, J. D. Hogan, A. Labadorf, R. H. Myers, J. Zaia, A glycomics and proteomics study of aging and Parkinson’s disease in human brain. *Sci. Rep.* **10**, 1–9 (2020).
14. H. Haukedal, K. K. Freude, Implications of Glycosylation in Alzheimer’s Disease. *Front. Neurosci.* **14** (2021).
15. C. P. Boix, I. Lopez-Font, I. Cuchillo-Ibañez, J. Sáez-Valero, Amyloid precursor protein glycosylation is altered in the brain of patients with Alzheimer’s disease. *Alzheimer’s Res. Ther.* **12**, 1–15 (2020).

16. S. Schedin-Weiss, B. Winblad, L. O. Tjernberg, The role of protein glycosylation in Alzheimer disease. *FEBS J.* **281**, 46–62 (2014).
17. Y. Sato, Y. Naito, I. Grundke-Iqbal, K. Iqbal, T. Endo, Analysis of N-glycans of pathological tau: Possible occurrence of aberrant processing of tau in Alzheimer's disease. *FEBS Lett.* **496**, 152–160 (2001).
18. K. Akasaka-Manyá, *et al.*, Protective effect of N-glycan bisecting GlcNAc residues on β -amyloid production in Alzheimer's disease. *Glycobiology* **20**, 99–106 (2010).
19. Y. Kizuka, S. Kitazume, N. Taniguchi, N-glycan and Alzheimer's disease. *Biochim. Biophys. Acta - Gen. Subj.* **1861**, 2447–2454 (2017).
20. R. Raghunathan, *et al.*, Glycomic and proteomic changes in aging brain nigrostriatal pathway. *Mol. Cell. Proteomics* **17**, 1778–1787 (2018).
21. J. Lee, *et al.*, Spatial and temporal diversity of glycome expression in mammalian brain. *Proc. Natl. Acad. Sci.* **117**, 28743–28753 (2020).
22. P. Fang, *et al.*, Multilayered N-Glycoproteome Profiling Reveals Highly Heterogeneous and Dysregulated Protein N-Glycosylation Related to Alzheimer's Disease. *Anal. Chem.* **92**, 867–874 (2020).
23. S. Gaunitz, L. O. Tjernberg, S. Schedin-Weiss, The N-glycan profile in cortex and hippocampus is altered in Alzheimer disease. *J. Neurochem.*, 1–13 (2020).
24. J. Samal, R. Saldova, P. M. Rudd, A. Pandit, R. O'Flaherty, Region-Specific Characterization of N-Glycans in the Striatum and Substantia Nigra of an Adult Rodent Brain. *Anal. Chem.* **92**, 12842–12851 (2020).
25. A. L. Rebelo, *et al.*, Complete spatial characterisation of N-glycosylation upon striatal neuroinflammation in the rodent brain. *J. Neuroinflammation* **18**, 1–19 (2021).
26. M. Barboza, *et al.*, Region-Specific Cell Membrane N-Glycome of Functional Mouse Brain Areas Revealed by nanoLC-MS Analysis. *Mol. Cell. Proteomics*, 100130 (2021).
27. C. L. Masters, *et al.*, Alzheimer's disease. *Nat. Rev. Dis. Prim.* **1**, 1–18 (2015).
28. Q. Li, Y. Xie, M. Wong, M. Barboza, C. B. Lebrilla, Comprehensive structural glycomic characterization of the glycocalyxes of cells and tissues. *Nat. Protoc.* **15** (2020).
29. P. De Jager, *et al.*, A multi-omic atlas of the human frontal cortex for aging and Alzheimer's disease research. *Data Descr. A multi-omic atlas Hum. Front. cortex aging Alzheimer's Dis. Res.*, 251967 (2018).
30. T. Song, D. Aldredge, C. B. Lebrilla, A Method for In-Depth Structural Annotation of Human Serum Glycans That Yields Biological Variations. *Anal. Chem.* **87**, 7754–7762 (2015).
31. B. Wang, *et al.*, Dietary sialic acid supplementation improves learning and memory in piglets. *Am. J. Clin. Nutr.* **85**, 561–569 (2007).

32. E. Oliveros, *et al.*, Sialic acid and sialylated oligosaccharide supplementation during lactation improves learning and memory in rats. *Nutrients* **10** (2018).
33. B. Wang, J. Brand-Miller, The role and potential of sialic acid in human nutrition. *Eur. J. Clin. Nutr.* **57**, 1351–1369 (2003).
34. D. J. Becker, J. B. Lowe, Fucose: Biosynthesis and biological function in mammals. *Glycobiology* **13** (2003).
35. J. Li, H. C. Hsu, J. D. Mountz, J. G. Allen, Unmasking Fucosylation: from Cell Adhesion to Immune System Regulation and Diseases. *Cell Chem. Biol.* **25**, 499–512 (2018).
36. H. E. Murrey, *et al.*, Protein fucosylation regulates synapsin Ia/Ib expression and neuronal morphology in primary hippocampal neurons. *Proc. Natl. Acad. Sci. U. S. A.* **103**, 21–26 (2006).
37. A. Dityatev, *et al.*, Polysialylated neural cell adhesion molecule promotes remodeling and formation of hippocampal synapses. *J. Neurosci.* **24**, 9372–9382 (2004).
38. Y. Xie, *et al.*, Determination of the glycoprotein specificity of lectins on cell membranes through oxidative proteomics. *Chem. Sci.* **11**, 9501–9512 (2020).
39. L. R. Fodero, *et al.*, Wheat germ agglutinin-binding glycoproteins are decreased in Alzheimer’s disease cerebrospinal fluid. *J. Neurochem.* **79**, 1022–1026 (2001).
40. T. M. Maguire, A. M. Gillian, D. O’Mahony, C. M. Coughlan, K. C. Breen, A decrease in serum sialyltransferase levels in Alzheimer’s disease. *Neurobiol. Aging* **15**, 99–102 (1994).
41. T. M. Maguire, K. C. Breen, A decrease in neural sialyltransferase activity in Alzheimer’s disease. *Dement. Geriatr. Cogn. Disord.* **6**, 185–190 (1995).
42. S. P. Mutalik, S. L. Gupton, Glycosylation in axonal guidance. *Int. J. Mol. Sci.* **22** (2021).
43. S. E. Williams, R. G. Mealer, E. M. Scolnick, J. W. Smoller, R. D. Cummings, Aberrant glycosylation in schizophrenia: a review of 25 years of post-mortem brain studies. *Mol. Psychiatry* (2020) <https://doi.org/10.1038/s41380-020-0761-1>.
44. M. C. Amoureux, *et al.*, Polysialic acid neural cell adhesion molecule (psa-ncam) is an adverse prognosis factor in glioblastoma, and regulates olig2 expression in glioma cell lines. *BMC Cancer* **10** (2010).
45. V. Sytnyk, I. Leshchyns’ka, M. Schachner, Neural glycomics: the sweet side of nervous system functions. *Cell. Mol. Life Sci.* **78**, 93–116 (2021).
46. H. Mi, *et al.*, PANTHER version 7: Improved phylogenetic trees, orthologs and collaboration with the Gene Ontology Consortium. *Nucleic Acids Res.* **38**, D204–D210 (2009).

Supplementary Data

Fig. S1A.

N-Glycome of the Occipital Cortex.

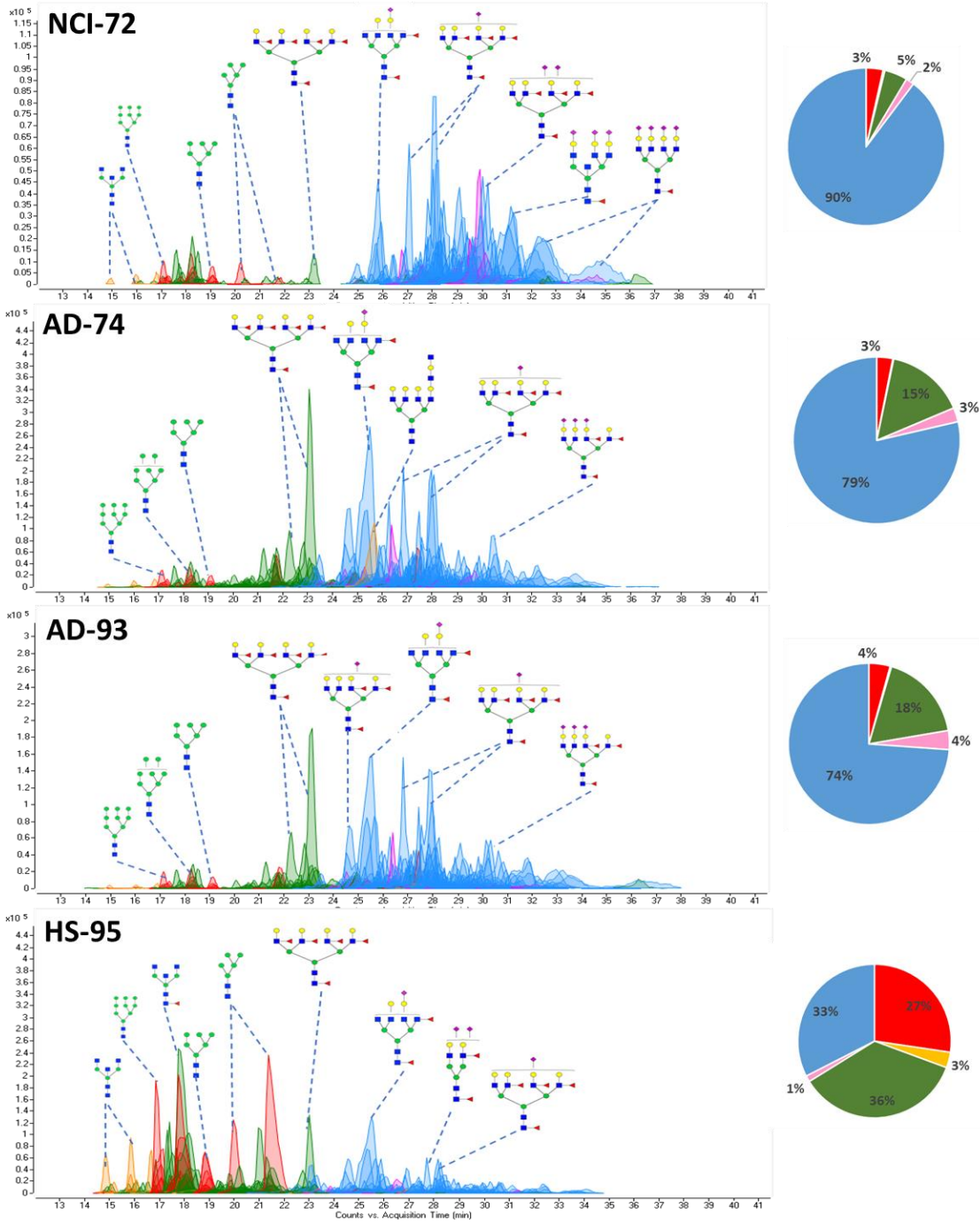


Fig. S1B.

N-Glycome of the Frontal Cortex.

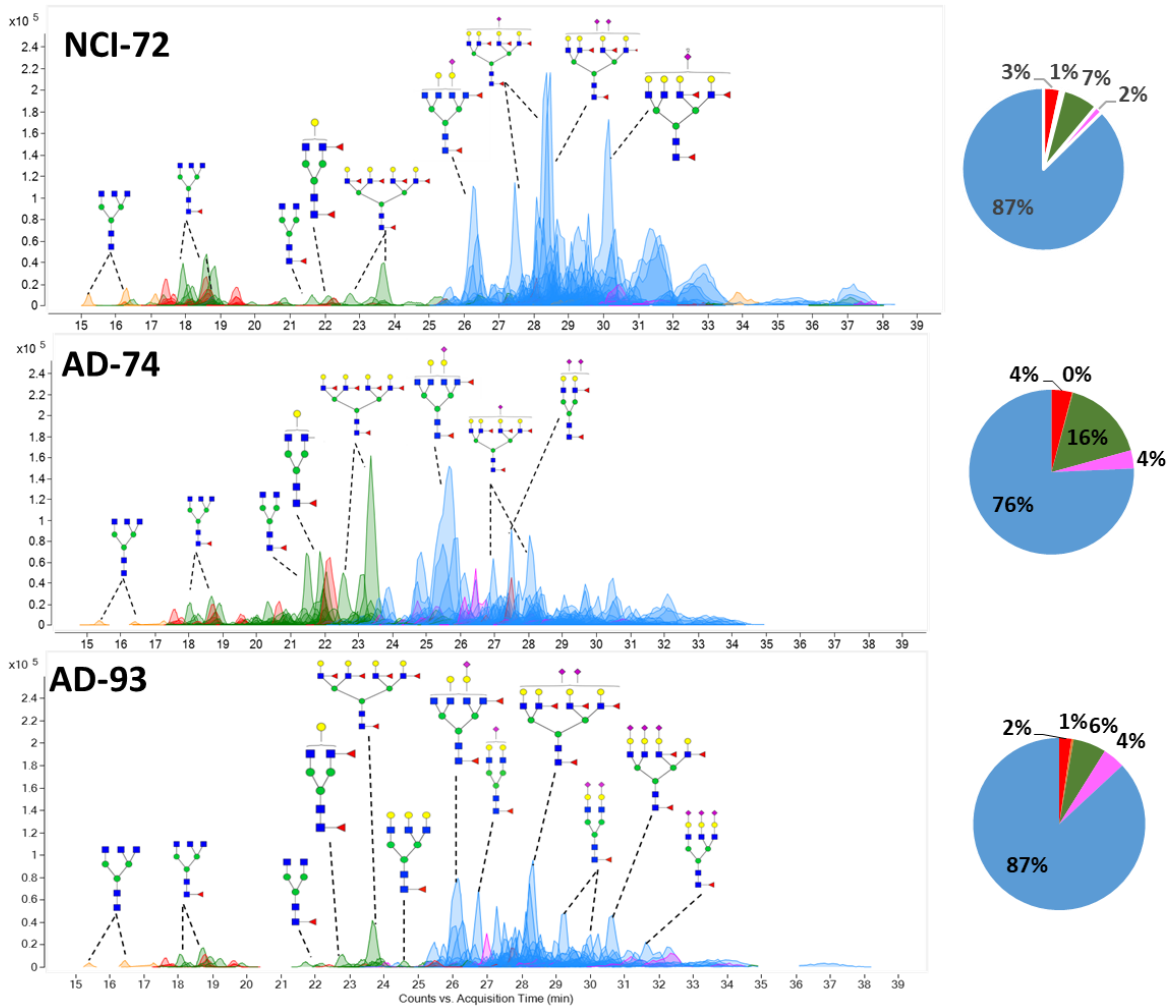


Fig. S1C.

N-Glycome of the Temporal Cortex.

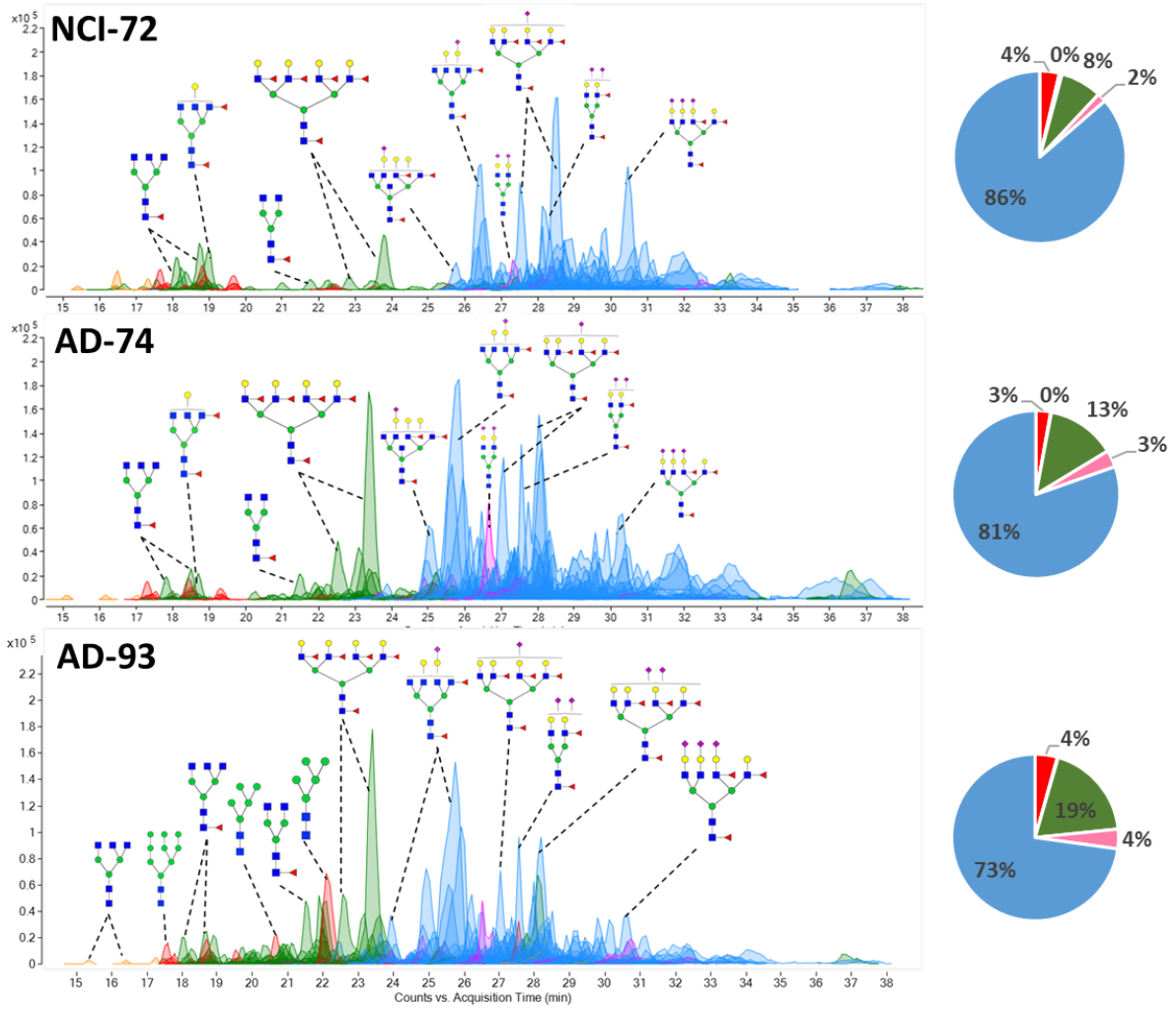


Fig. S1D.

N-Glycome of the Parietal Cortex.

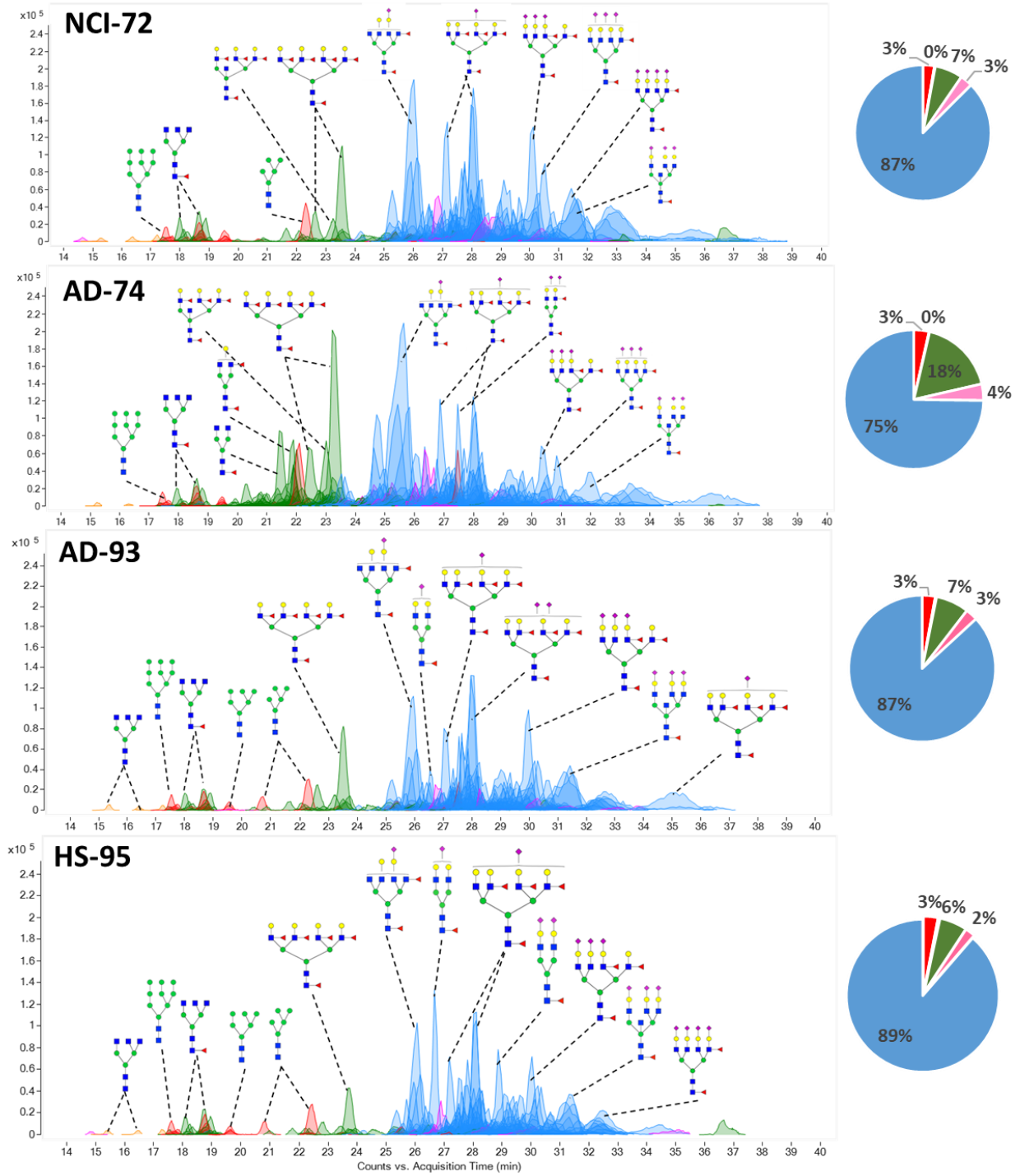


Fig. S1E.

N-Glycome of the Cingulate Cortex.

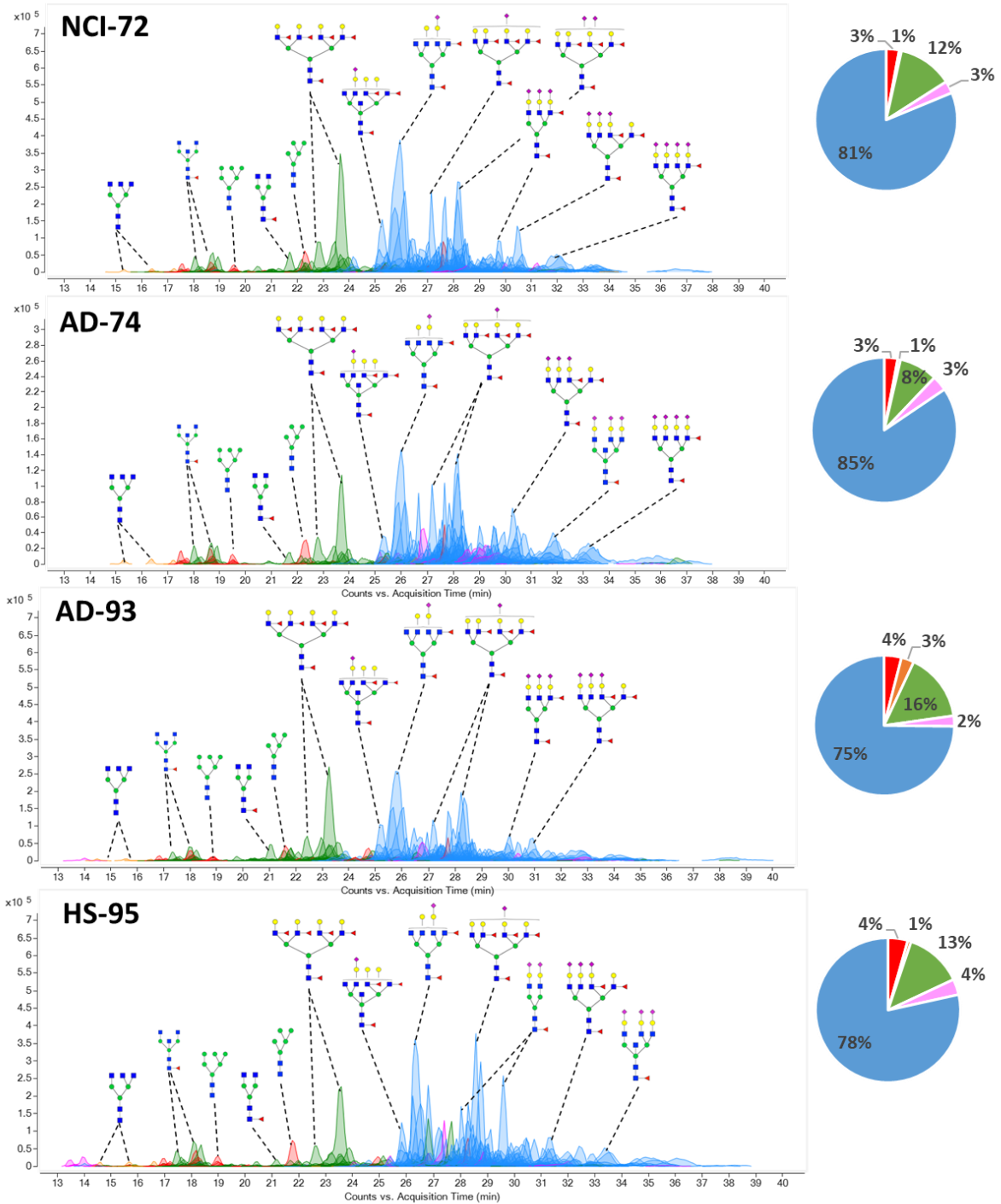


Fig. S1F.

N-Glycome of the Orbitofrontal Cortex.

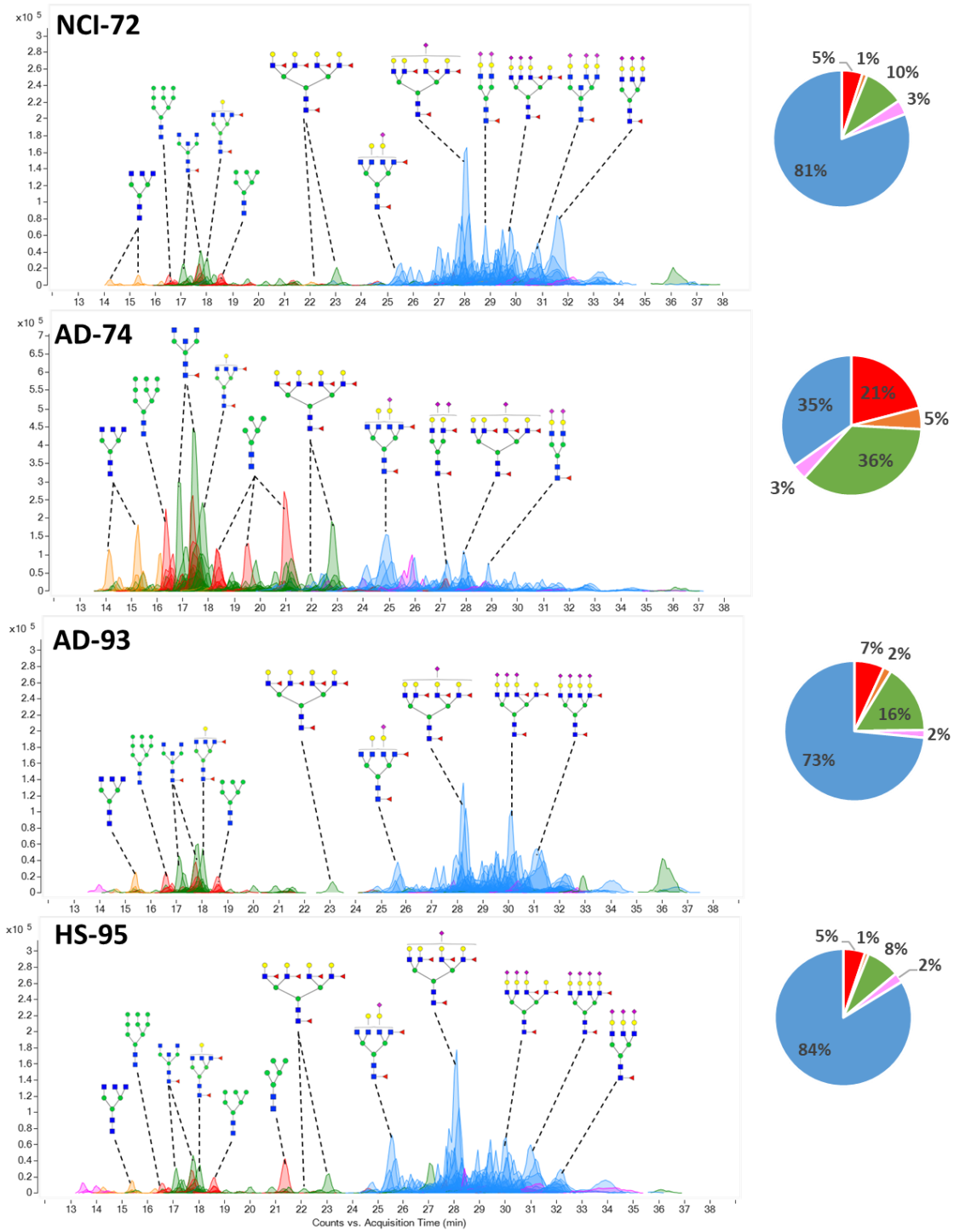


Fig. S1G.

N-Glycome of the Posterior Hippocampus.

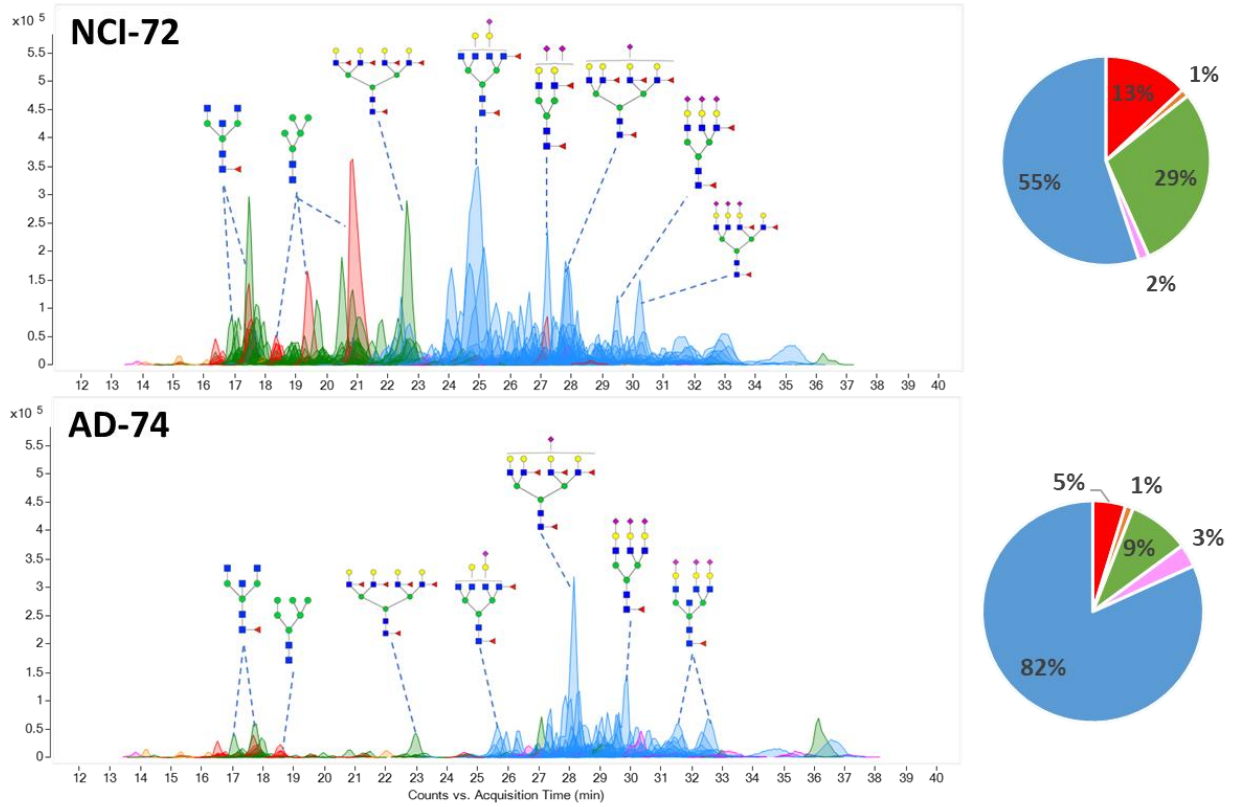


Fig. S1H.

N-Glycome of the Thalamus.

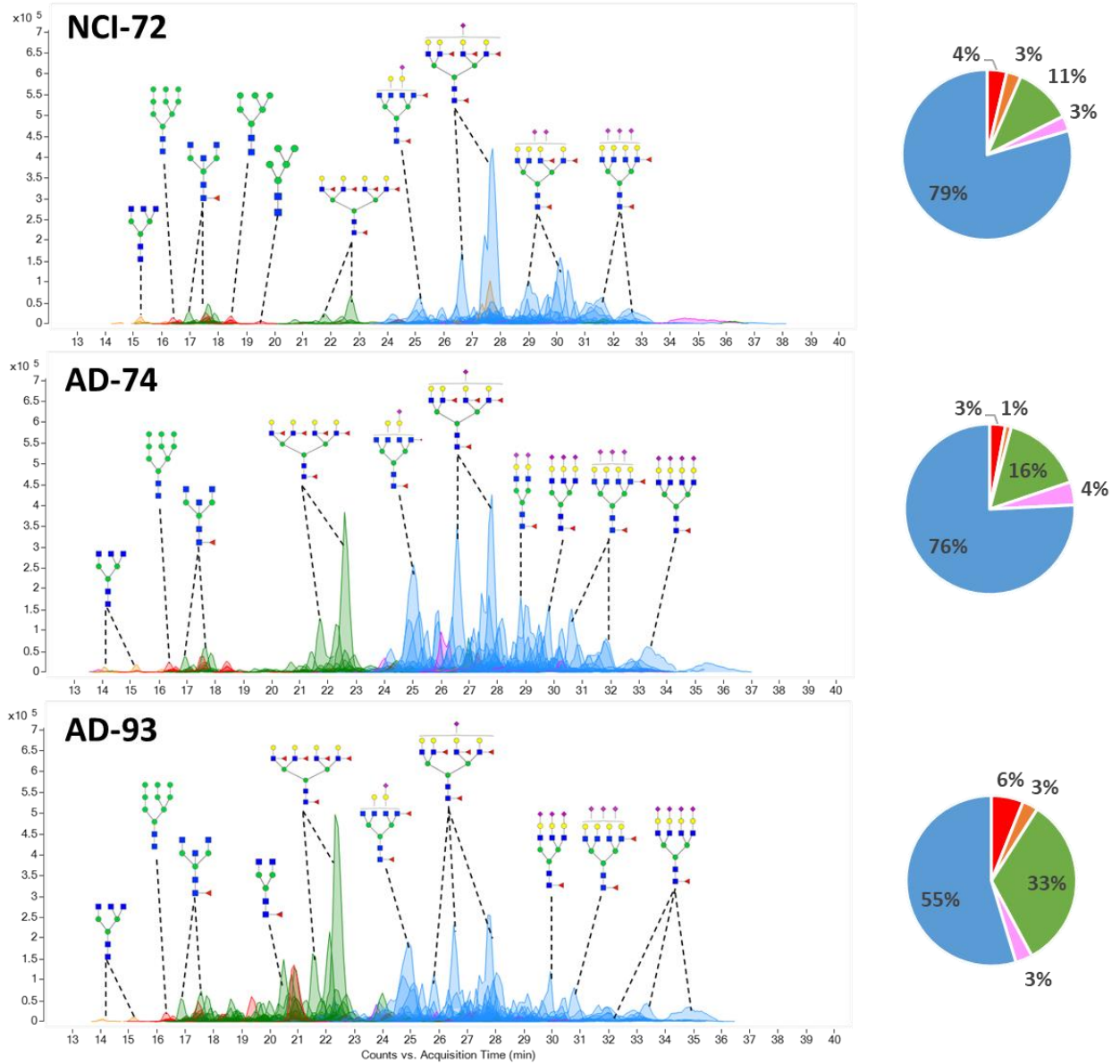


Fig. S1I.
N-Glycome of the Caudate Nucleus.

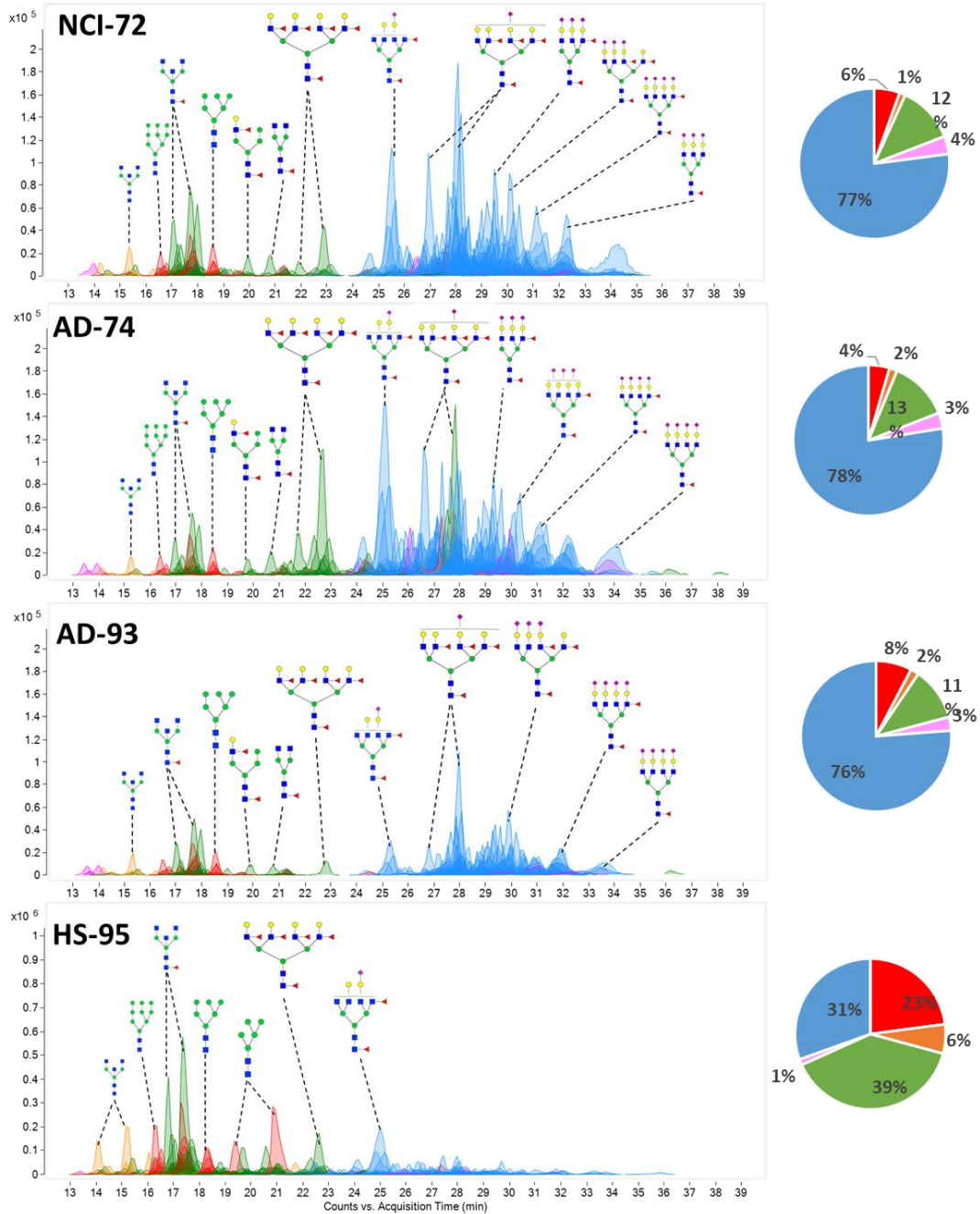


Fig. S1J.

N-Glycome of the Lateral Cerebellar Cortex.

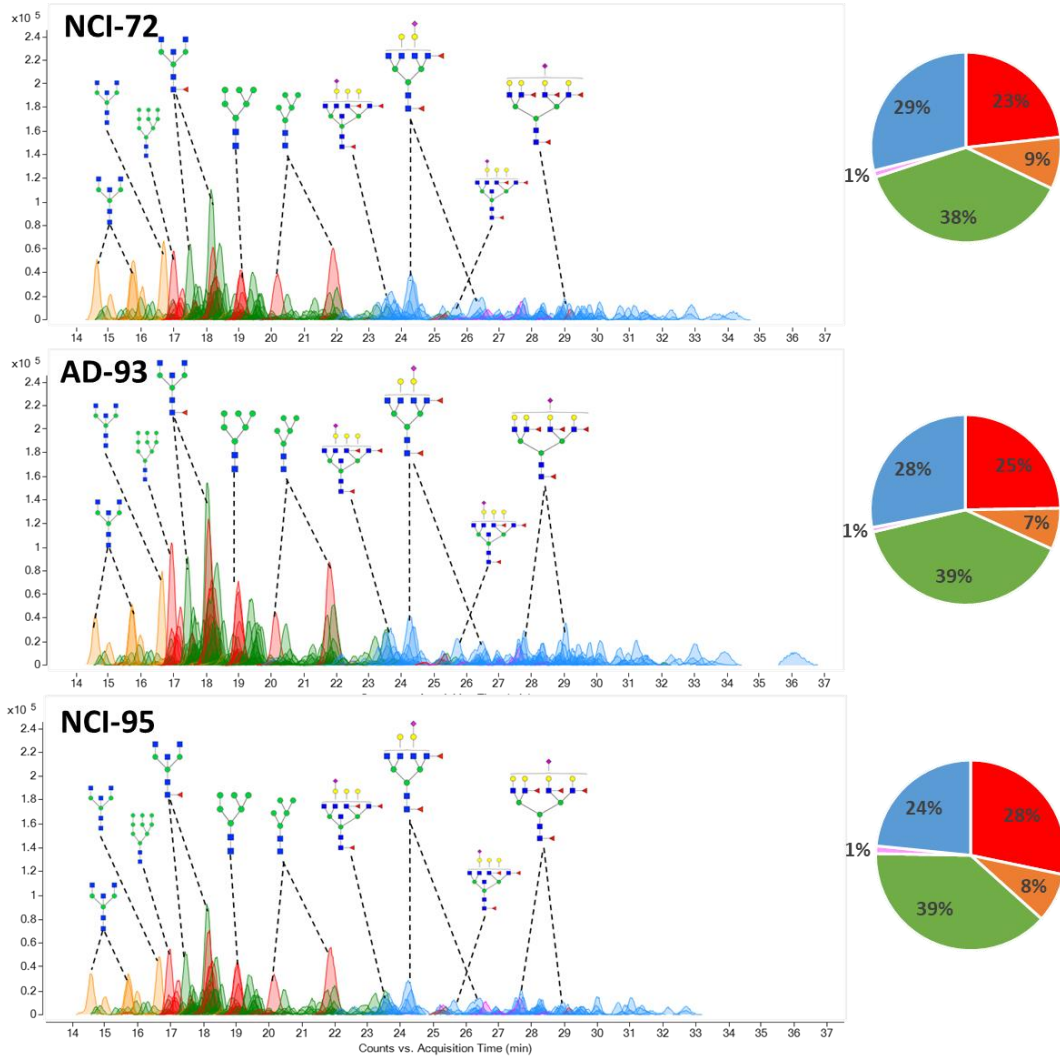


Fig. S1K.
N-Glycome of the Pons.

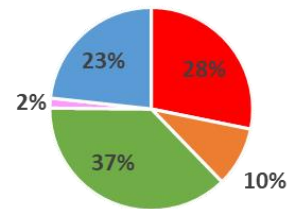
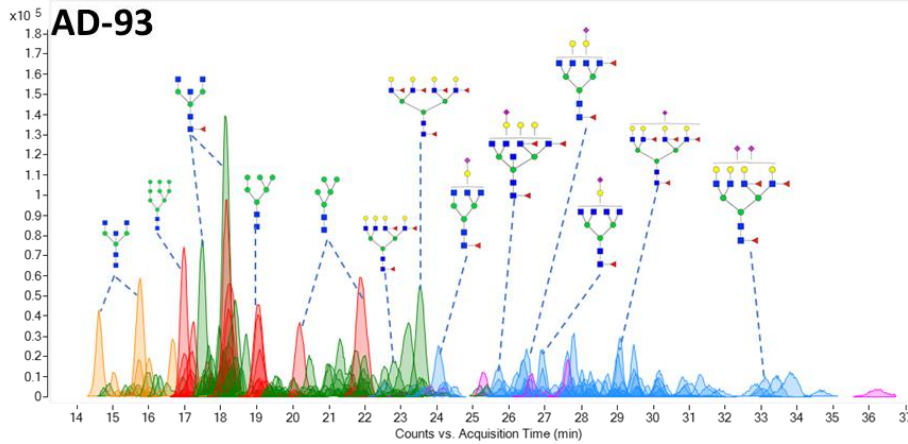
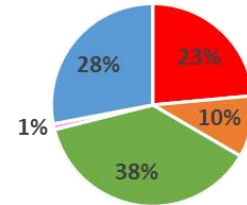
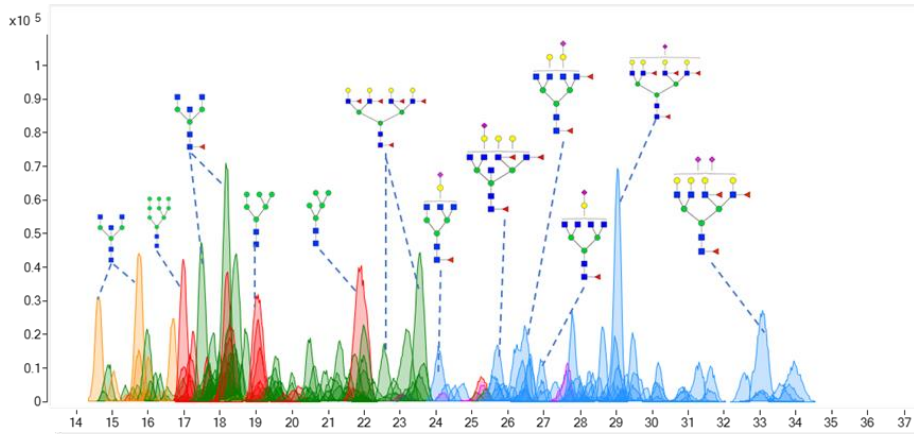


Fig. S2.

N-Glycans detected including isomers.

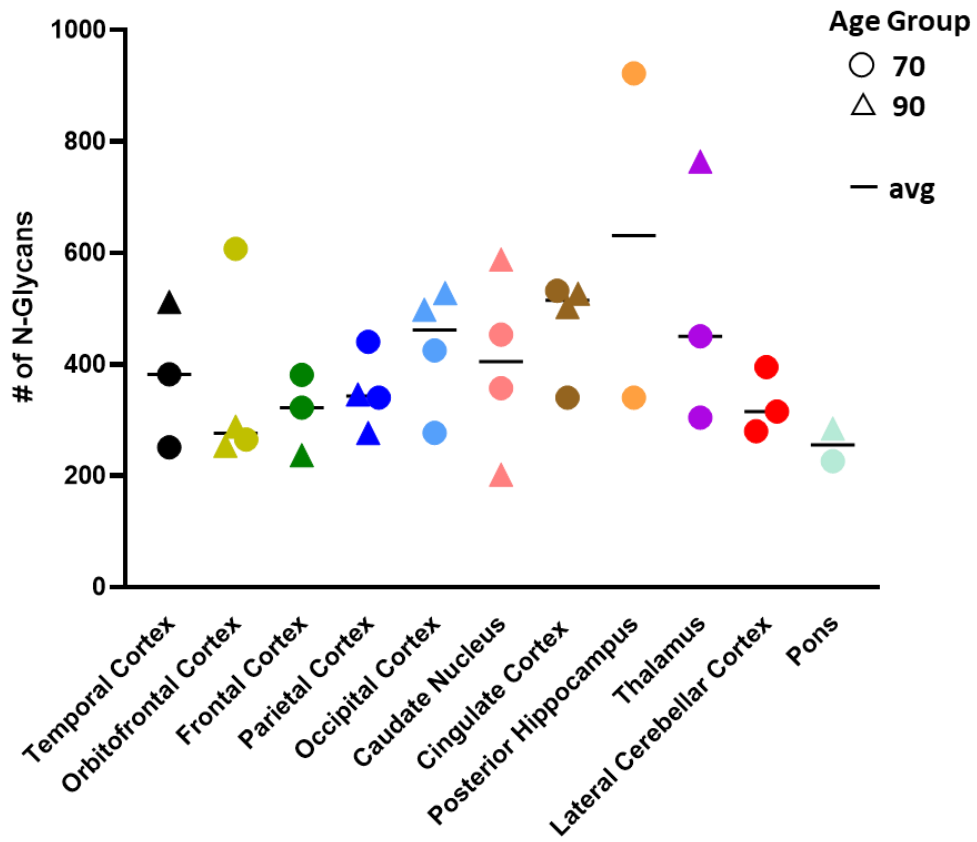


Fig. S3.

Structural analysis of N-glycans across all 11 brain regions.

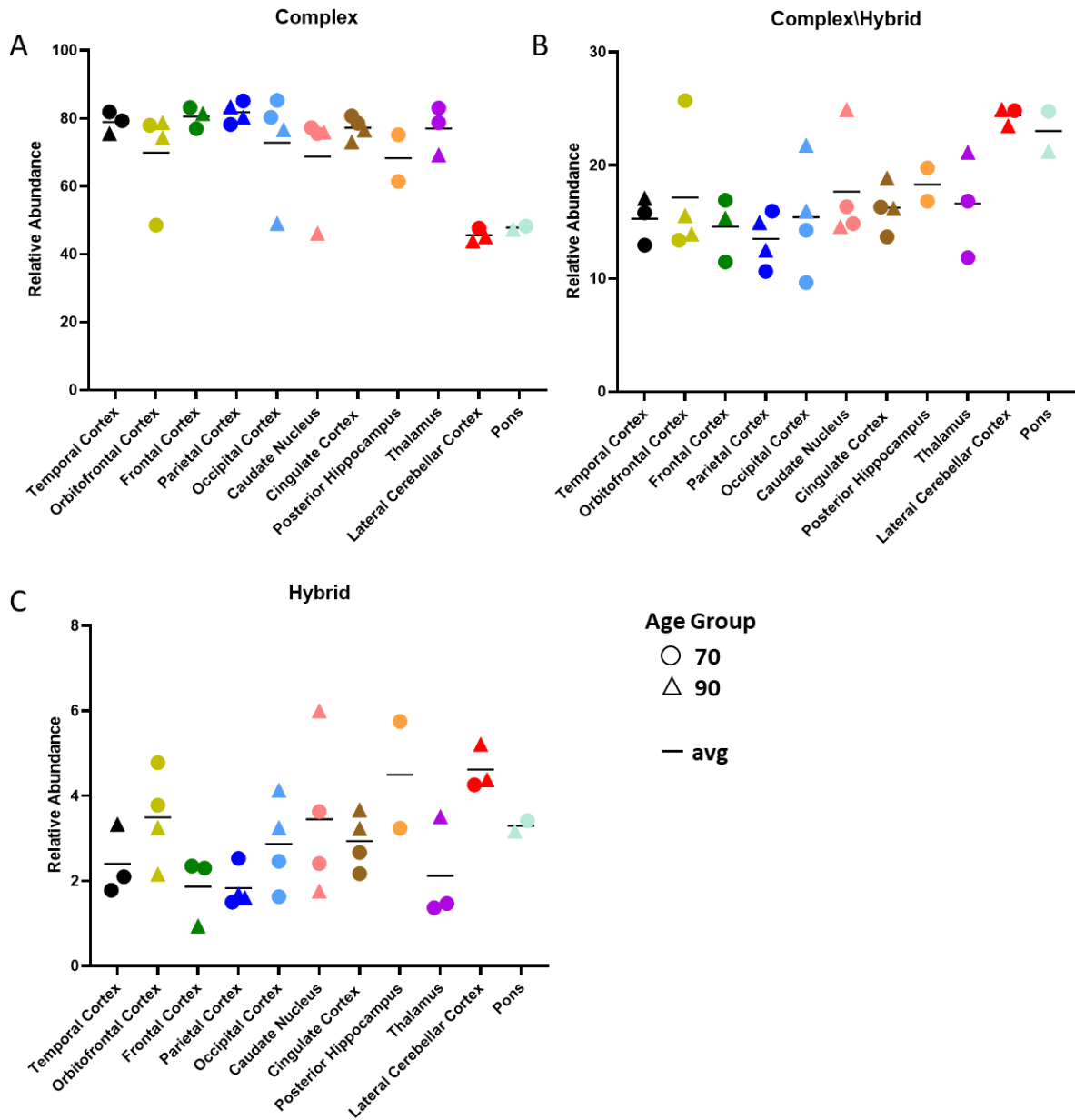


Fig. S4.

Heat map of the elderly human brain across 11 functional brain regions from four subjects.

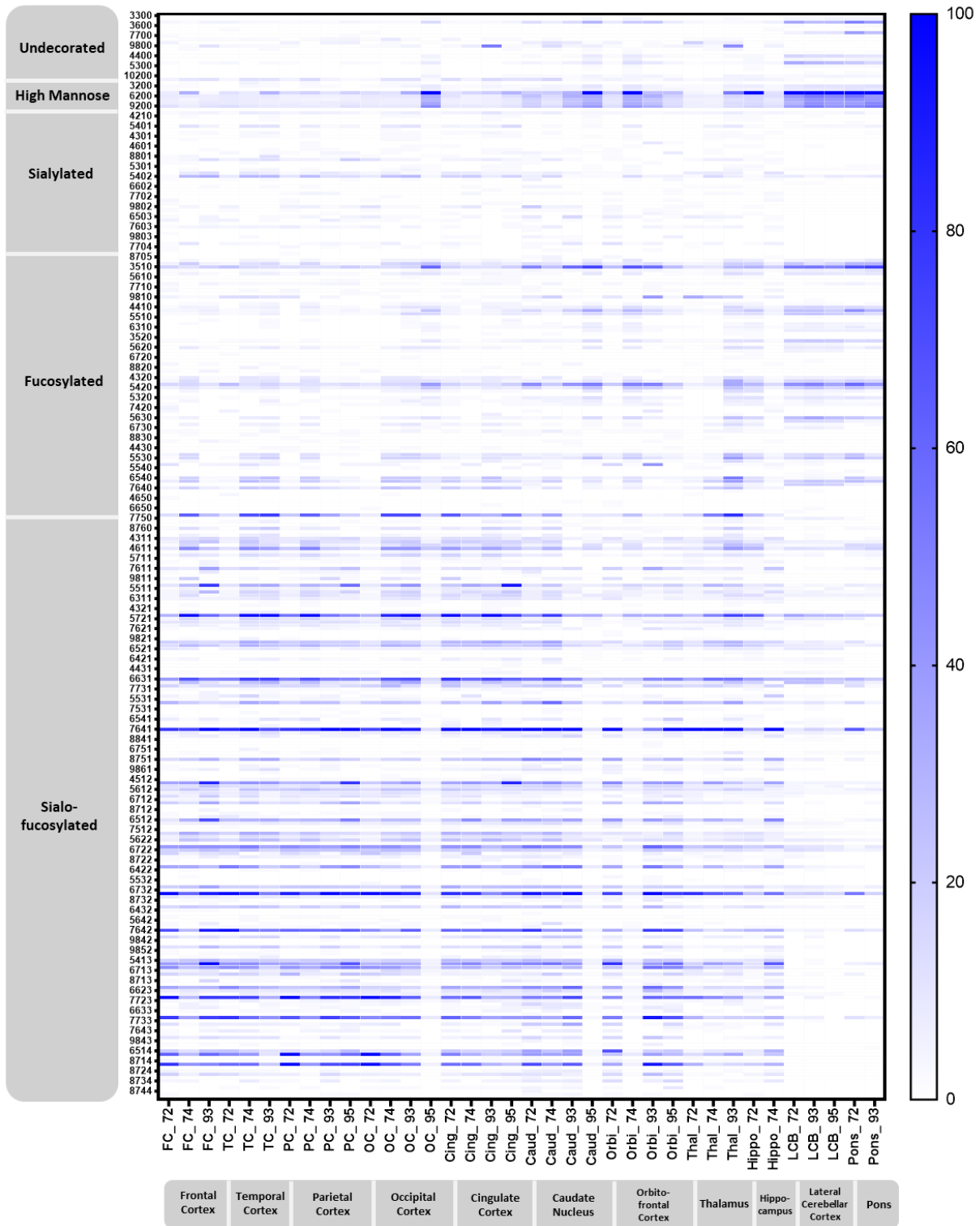
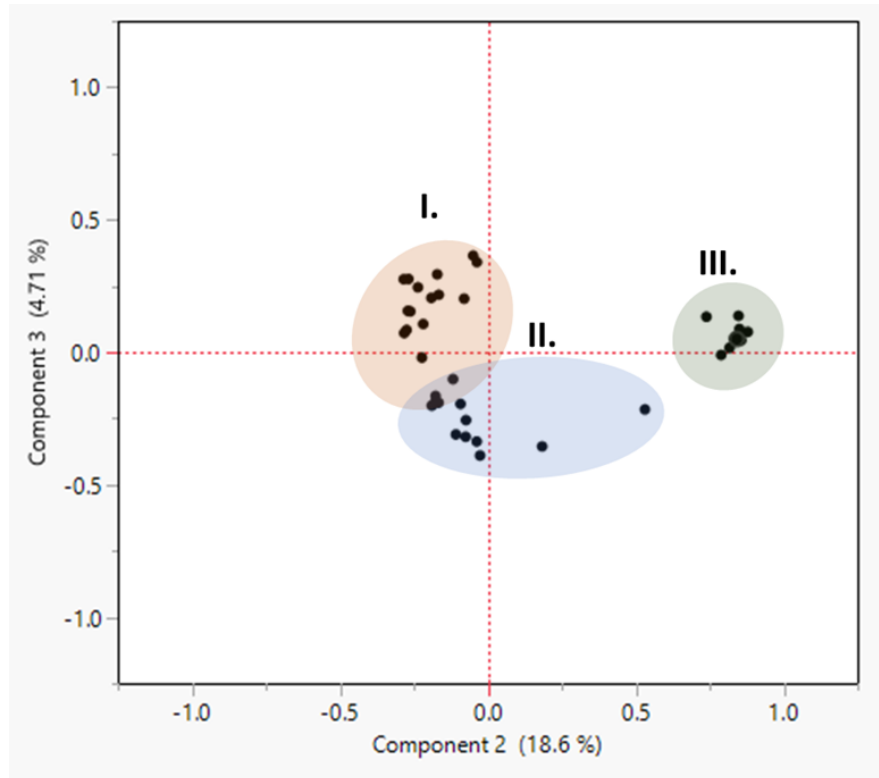


Fig. S5.

Region comparison based on N-glycan expression. Principal component analysis plot of human brain samples between 11 brain regions.



	NCI-72	AD-74	AD-93	HS-95
Cluster 1	Orbitofrontal cortex		Orbitofrontal cortex	Orbitofrontal cortex
	Caudate Nucleus	Caudate Nucleus	Caudate Nucleus	
	Temporal Cortex			Temporal Cortex
	Frontal Cortex		Frontal Cortex	Frontal Cortex
	Thalamus	Thalamus		
	Occipital Cortex			
	Parietal Cortex			Parietal Cortex
	Cingulate Cortex	Cingulate Cortex		
Cluster 2	Posterior Hippocampus	Posterior Hippocampus		
			Cingulate Cortex	Cingulate Cortex
		Temporal Cortex	Temporal Cortex	
		Occipital Cortex	Occipital Cortex	
		Frontal Cortex		
		Parietal Cortex		
Cluster 3	Pons		Pons	
	Lateral Cerebellar Cortex		Lateral Cerebellar Cortex	Lateral Cerebellar Cortex
				Caudate Nucleus
				Occipital Cortex
		Orbitofrontal cortex		

Fig. S6.

Comparison of the total membrane glycoproteins in the different regions.



Table S1.

Human brain subjects utilized in this study for both control, AD and HS samples across eleven different brain regions.

Labeled	APOE	AGE	SEX	PMI	BRAAK	NEUROPATH DX	TISSUE ANALYZED IN THIS STUDY
HS-95	E3/E3	95	M	4	1	<p>1. Hippocampal Sclerosis, left</p> <p>2. Ischemic brain injury due to small vessel disease</p> <ul style="list-style-type: none"> • Arteriosclerosis, moderate • White matter pallor • Multiple microinfarcts in external capsule <p>3. Old lacunar infarct in pons</p> <p>4. Ischemic tauopathy</p> <ul style="list-style-type: none"> • Astrocytic tau in anterior hippocampus • Astrocytic tau in visual cortex <p>5. Alzheimer's Disease Neuropathologic changes: A1, B1, C0. Low likelihood of AD according to the NIA-Alzheimer's Association Guideline</p> <ul style="list-style-type: none"> • Thal Phase I (out of 5) • Braak and Braak Stage I (out of VI) • CERAD 0 <p>COMMENTS: Clinical diagnosis of this 96 yr old subject was carrier of AD and dementia due to vascular factors early in 2005. No neuroimaging data was available at CPC except a CT scan from 2005. In 1997, the impression from MRI was possible subacute infarct in left anterior pons and small vessel ischemic disease. Although AD was a strong impression at CPC, the atypical memory symptoms described were raised as not consistent with AD. Pathologically, this is a case of hippocampal sclerosis as well as vascular brain damage due to small vessel disease (white matter damage, arteriosclerosis, etc.). Alzheimer disease pathology is not likely considered a contributing factor to the patient's dementia. Interestingly, there are tau2 immunoreactivity in the white matter astrocytes in the areas with white matter damage. This atypical tau accumulation is considered secondary to ischemic brain injury.</p>	<p>[03] Parietal cortex</p> <p>[04] Occipital cortex</p> <p>[05] Cingulate cortex</p> <p>[06] Orbitofrontal cortex</p> <p>[09] Caudate nucleus</p> <p>[10] Lateral cerebellar cortex (if available)</p> <p>—</p> <p>The following tissues were unavailable for sampling:</p> <p>[01] Frontal cortex</p> <p>[02] Temporal cortex</p> <p>[07] Posterior hippocampus</p> <p>[08] Thalamus</p> <p>[11] Pons</p>
AD-93	E3/E4	93	M	5	5	Incomplete	<p>[01] Frontal cortex</p> <p>[02] Temporal cortex</p> <p>[03] Parietal cortex</p> <p>[04] Occipital cortex</p> <p>[05] Cingulate cortex</p> <p>[06] Orbitofrontal cortex</p> <p>[08] Thalamus</p> <p>[09] Caudate nucleus</p> <p>[10] Lateral cerebellar cortex (if available)</p> <p>[11] Pons</p> <p>—</p> <p>The following tissues were unavailable for sampling:</p> <p>[07] Posterior hippocampus</p>
NCI-72	E3/E3	72	M	4	1	<p>1. Cerebrovascular disease</p> <ul style="list-style-type: none"> -Atherosclerosis, mild -Arteriosclerosis, mild -Old infarct in caudate nucleus -Multiple microhemorrhages in caudate nucleus -Infarct in lateral, inferior parietal/occipital cortex -Parietal and occipital patchy white matter pallor, moderate -Visual cortex white matter pallor, severe <p>2. Alzheimer's Disease neuropathologic change: A1, B1, C0. NIA-ALZHEIMER'S ASSOCIATION GUIDELINE: LOW LIKELIHOOD OF ALZHEIMER'S DISEASE</p> <ul style="list-style-type: none"> -Thal Phase 1 (out of 5) -Braak Stage I (out of VI) -CERAD score 0 (out of 3) 	<p>[01] Frontal cortex</p> <p>[02] Temporal cortex</p> <p>[03] Parietal cortex</p> <p>[04] Occipital cortex</p> <p>[05] Cingulate cortex</p> <p>[06] Orbitofrontal cortex</p> <p>[07] Posterior hippocampus</p> <p>[08] Thalamus</p> <p>[09] Caudate nucleus</p> <p>[10] Lateral cerebellar cortex</p> <p>[11] Pons</p>
AD-74	E3/E4	74	M	8	6	<p>1. ALZHEIMERIS DISEASE, SEVERE (CERAD FREQUENT PLAQUES, BRAAK AND BRAAK STAGE VI, NIA/REAGAN INSTITUTE DEFINITE AD)</p> <p>2. CEREBRAL AMYLOID ANGIOPATHY, GRADE II</p>	<p>[01] Frontal cortex</p> <p>[02] Temporal cortex</p> <p>[03] Parietal cortex</p> <p>[04] Occipital cortex</p> <p>[05] Cingulate cortex</p> <p>[06] Orbitofrontal cortex</p> <p>[07] Posterior hippocampus</p> <p>[08] Thalamus</p> <p>[09] Caudate nucleus</p> <p>—</p> <p>The following tissues were unavailable for sampling:</p> <p>[10] Lateral cerebellar cortex (if available)</p> <p>[11] Pons</p>

CHAPTER III

Glycosylation alterations across three pathological stages in the human brain of Alzheimer's disease patients

ABSTRACT

The cell surface glycocalyx displays a complex wealth of information found in the glycoproteins and glycolipids. The glycosylation present on the cell surface modulates a wide range of processes such as cell adhesion, migration, and proliferation. Emerging evidence suggests glycosylation influences neuronal processes such as neurite outgrowth. However, our understanding of the glycome alterations in a neurodegenerative disease such as Alzheimer's Disease are relatively poorly understood. The two pathological hallmarks in Alzheimer's Disease are associated with the accumulation of insoluble amyloid- β plaques and neurofibrillary tangles. The amyloid plaques and neurofibrillary tangles spread differently as the disease progresses mainly affecting the frontal and temporal lobes. In this work, we sought out to elucidate the glycome alterations in the human brain of Alzheimer's Disease subjects across the frontal cortex, temporal cortex, and lateral cerebellar cortex. The frontal cortex and temporal cortex are highly affected in the Alzheimer's disease neuropathology while the lateral cerebellar cortex is the least affected region. Preliminary data suggest spatial alteration in fucosylated and sialofucosylated N-glycans in Alzheimer's disease subjects. Glycolipid variations were also observed in the frontal cortex and temporal cortex, but not in the lateral cerebellar cortex. The work presented here can be a useful source of reference to further human brain glycome studies.

INTRODUCTION

Alzheimer's Disease is a progressive neurodegenerative disease with an estimated prevalence of 10-30% in the population greater than 65 years (1). Alzheimer's Disease can be categorized as familial (fAD) or sporadic (sAD). sAD is the most common type accounting for approximately 95% of all cases (2). The risk for developing sAD rely in genetic risk factors such as the $\epsilon 4$ allele of Apolipoprotein E (*APOE4*). On the other hand, fAD is caused by specific mutations in Presenilin 1 (*PSEN1*) or 2 (*PSEN2*) or Amyloid precursor protein (*APP*). The now questioned "A β cascade hypothesis" terms Alzheimer's Disease as an imbalance in the production and clearance of A β . While Alzheimer's Disease shares similar characteristics with other molecularly defined neurodegenerative diseases such as Parkinson's disease and the frontotemporal dementias, true diagnosis specific to Alzheimer's Disease is a challenge. It is often argued that Alzheimer's Disease is related to the normal brain ageing process (3). Research highlighting the different neurocognitive changes associated with normal aging and AD have been reported (4).

The two pathological hallmarks in AD are associated with the accumulation of insoluble amyloid- β plaques and in neurons aggregates of microtubule protein tau in neurofibrillary tangles (5). The amyloid plaque and neurofibrillary tangles spread differently as the disease progresses. Typically, the amyloid plaque deposition occurs originate in the frontal and temporal lobes before neurofibrillary tangles. The neurofibrillary tangles initiate in the temporal and hippocampus shown in **Figure 1**.

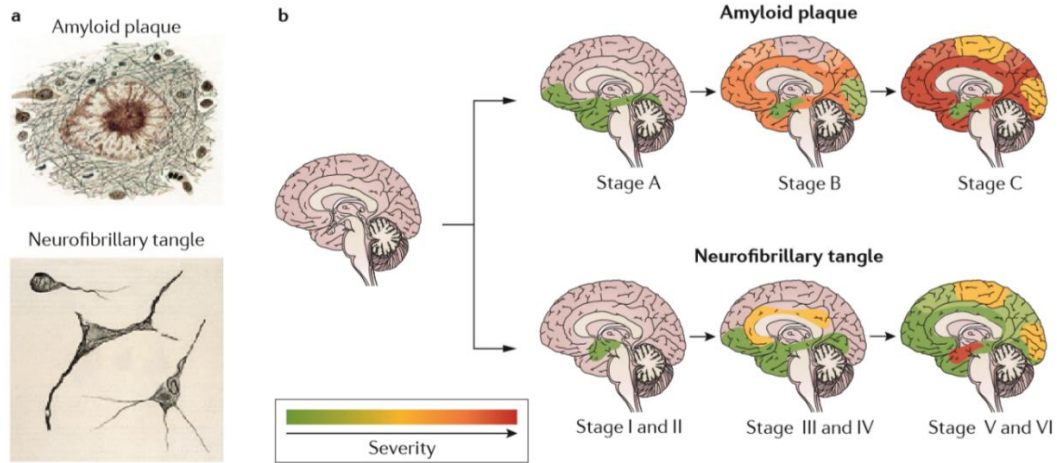


Figure 1: The amyloid plaques and neurofibrillary tangles affecting the brain differently as disease progresses. Adapted from ref. (1)

The focus of this study is placed in understanding the glycosylation alterations in three distinct human brain regions affected differently in the AD pathology. The lateral pre-frontal cortex involved in executive function is an area heavily affected in advanced AD especially by amyloid plaques. The medial temporal cortex is involved in early stages of AD especially by neurofibrillary tangles. While the lateral cerebellar cortex is the least involved in AD.

RESULTS AND DISCUSSION

N-Glyome alterations across three pathological stages in AD

To examine the regional variations in the neuro-glycome, this study focused on three distinct regions impacted differently in the AD neuropathology. The lateral cerebellar cortex regions contained 10 normal brain termed controls and seven AD autopsy confirmed regions. In the temporal cortex six control and nine AD regions were used while in the frontal cortex nine

brain regions were from the control group and 10 in the AD. The pathological diagnosis (Dx), sex, ethnicity, BRAAK, and the brain region obtained from each subject are shown in **Table S1**. Where the BRAAK stage classifies the degree of pathology in Alzheimer's disease. The abnormal tau protein detectable in the transentorhinal and entorhinal regions (stages I–II), in the limbic allocortex and adjoining neocortex (stages III–IV), or in the neocortex (stages V–VI).

The structural diversity of N-glycan expression in the lateral cerebellar cortex, temporal cortex and frontal cortex yielded more than 250 glycans including isomers. Regional variations were detected between different pathological stages of AD. N-Glycome profiles in the cerebellar cortex remain similar between control and AD subjects, while lower levels of sialofucosylation was observed in the temporal and frontal cortex relative to the other regions (blue in **Figure 2**). The other glycoforms included undecorated (orange), high mannose-type (red) sialylated-only (pink), and fucosylated-only (green). Interestingly, the presence of highly abundant sialofucosylated glycans is a unique glycomic character of the brain compared to other tissues and body fluids (9). For the frontal cortex, the most impacted region by the amyloid- β plaques and neurofibrillary tangles, the levels of sialofucosylation appear lower than other regions (**Figure 2**). Closer inspection of the statistically significant N-glycan compositions altered between control and AD subjects from the 250+ N-glycans monitored across the three distinct brain regions are found in **Table S2 -S4** and discussed below.

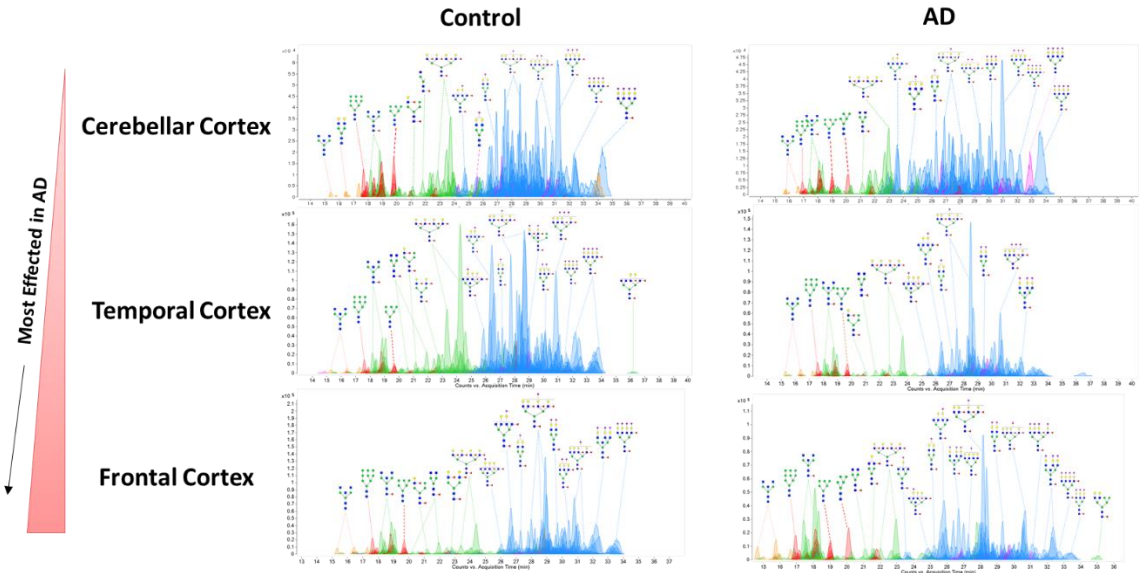


Figure 2: Extracted compound chromatograms (ECC) from the cerebellar cortex, temporal cortex and frontal cortex of control and AD subjects.

The neuro N-glycome of the lateral cerebellar cortex between control and AD subjects showed six varying glycans with statistically significant ($p < 0.05$) (**Figure 3A and Table S2**). Interestingly, the two most abundant N-glycans in this region were sialofucosylated with high degrees of terminal sialylation and represented by compositions $\text{Hex}_6\text{HexNAc}_5\text{Fuc}_1\text{NeuAc}_3$ and $\text{Hex}_7\text{HexNAc}_6\text{Fuc}_3\text{NeuAc}_3$. The frontal cortex showed distinct altered N-glycan expressions between control and AD. In this region, fucose containing N-glycans showed the largest variations. The tri-fucosylated sialofucosylated N-glycan with compositions $\text{Hex}_7\text{HexNAc}_6\text{Fuc}_3\text{NeuAc}_2$ and $\text{Hex}_6\text{HexNAc}_5\text{Fuc}_3\text{NeuAc}_1$ were among the most abundant and statistically significant N-glycans with $p < 0.05$, **Figure 3B and Table S3**. These highly fucosylated N-glycans were lower in the AD subjects compared to control subjects. Interestingly, the decrease in fucosylation observed in AD aligns with multiple studies suggesting the important roles of fucosylation in learning and memory (10–13). Studies have shown the usage of

exogenous L-fucose was able to enhance long-term potentiation (LTP), which is an electrophysiological model for measuring learning and memory (14–16). The fructosyltransferases have also been reported to increase during synaptogenesis (14).

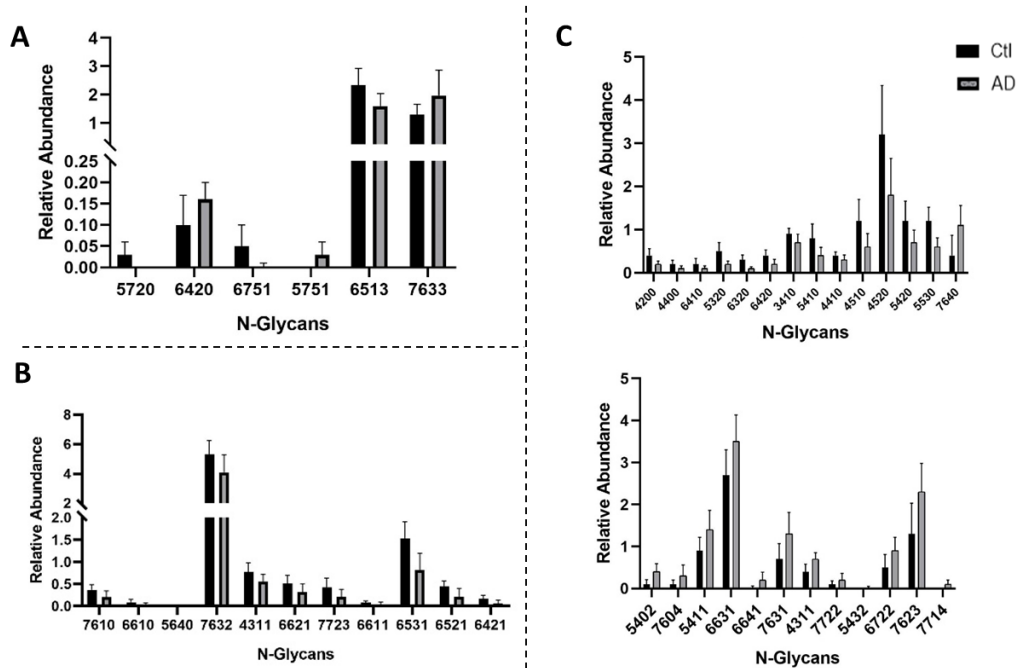


Figure 3: Region specific N-glycans of the lateral cerebellar cortex, frontal cortex, and temporal cortex. The statistically significant ($p < 0.05$) N-glycans found in the lateral cerebellar cortex (A), frontal cortex (B), and temporal cortex (C). The glycan composition four-digit number abbreviation is as follow where the first digit corresponds to Hex=Hexose, second digit corresponds to HexNAc=N-Acetylhexosamine, third digit corresponds to Fuc=Fucose, and the last digit corresponds to NeuAc= N-Acetylneuraminic Acid. The error bars correspond to biological replicate for (A) Ctl (N=10) and AD (N=7), (B), Ctl (N=6) and AD (N=9), and (C) Ctl (N=9) and AD (N=10).

The temporal cortex generated the most statistically significant number of N-glycan compositions between controls and AD subjects with a total of 26 distinct N-glycans **Figure 3C**, **Table S4**. The most abundant type was fucosylated-only N-glycans, or fucosylated N-glycan with no sialic acid moiety. The majority of these 12 fucosylated-only N-glycans decreased in AD compared to controls. However, the 10 sialofucosylated N-glycans showed the opposite effect and increased in AD subjects. This phenomenon can potentially indicate that sialofucosylated N-glycans compensate for the loss of fucosylation when fucosylated-only N-glycans is lower in AD subjects, as the source of fucosylation can be derived from either fucosylated-only or sialofucosylated type N-glycans.

Glycosphingolipid (GSL) alterations across three pathological stages in AD

The glycosphingolipidome results from a representative sample of a control and AD subject are displayed in **Figure 4**. Sialylated GSLs, termed gangliosides, were the most prominent across the three brain regions. Additionally, recent studies have shown the ganglioside metabolism closely associated with the pathology of AD. Specifically, a complex of GM1 (monosialotetrahexosylganglioside) and amyloid- β plaques termed “Ga β ” has been found to over accumulate solely in AD brains (17).

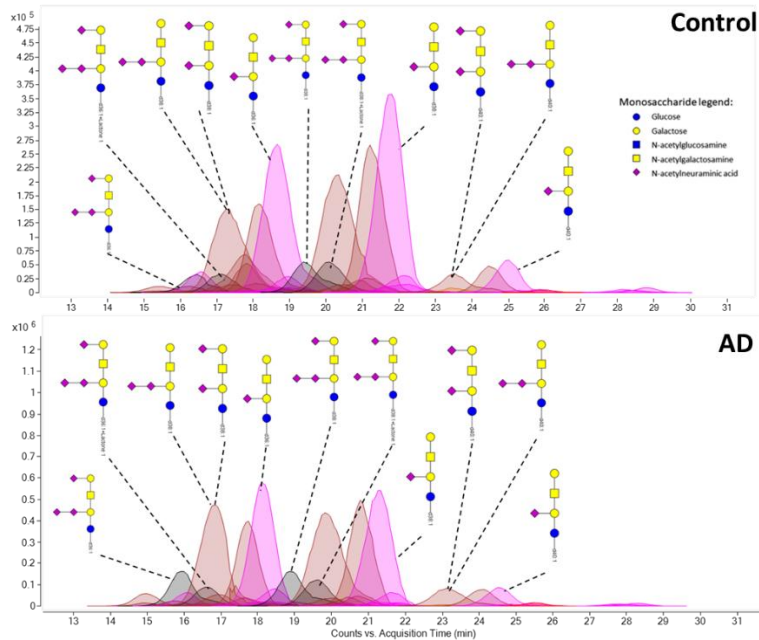


Figure 4: Representative (ECC) chromatograms of GSLs in control and AD subject. Peaks are annotated with schematic representations of their corresponding GSL structures.

Interestingly, in the frontal cortex a region most impacted by amyloid- β plaques, three gangliosides yielded a statistically significant increase in AD subjects, **Figure 5C**. While no significant difference was detected in the cerebellar cortex a region least affected in AD **Figure 5A**. The glycan component and the ceramide compositions were analyzed individually to determine whether changes were specific to one or the other. A startlingly small number of nine glycan compositions were found to compose the neuro-glycosphingolipidome, **Figure 5 A-C**. The putative structures of the glycan compositions shown here are believed to be the major contributors to the human brain GSL's aided by the known biosynthetic pathway (18). The three most abundant glycolipids were in the three brain regions were GM1, GD1 and GT1 **Figure 5 A-C**.

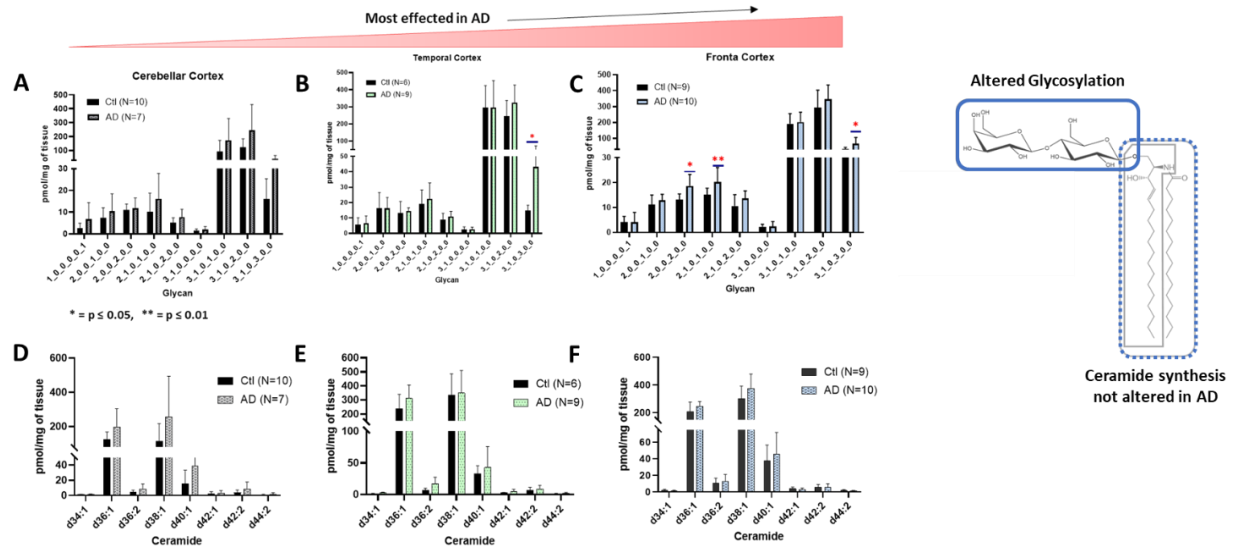


Figure 5: Normalized abundances of the glycosylation and ceramide composition in GSLs. Glycan decoration of the lateral cerebellar cortex (A), temporal cortex (B), and frontal cortex (C) are shown. The ceramide composition of the cerebellar cortex (D), temporal cortex (E), and frontal cortex (F) where the error bars correspond to biological replicates.

Variations in composition of the ceramide portions also yielded a small number of eight distinct compositions, **Figure 5 D-F**. The ceramide contains the number of hydroxyl groups, the degree of unsaturation, and the chain lengths of the spingoid and fatty acid. The three most expressed ceramides were d36:1, d38:1 and d40:1. Remarkably, the ceramide compositions across the three distinct brain regions showed no statistically significant difference between control and AD subjects. This indicates that the ceramide synthesis is highly regulated and not dependent in region or disease state, **Figure 5**.

CONCLUSION

The importance of glycosylation in the human brain has become apparent especially the alterations in a neurodegenerative disease like AD. This study encompassed the glycomic analyses of the spatial variation across the lateral cerebellar cortex, frontal cortex, and temporal cortex. The comprehensive analyses focuses on the neuro-N-glycome and glycolipidome across three pathological stages of AD. Interestingly, changes primarily attributed to sialylated and fucosylated N-glycans were extensively observed in regions highly affected in the AD neuropathology. In addition, our findings reveal statistically significant alterations in the glycan component of glycosphingolipids but no change in the ceramide portion for regions affected in AD pathology. Furthermore, this study contributes to valuable information on the human brain N-glycome and glycosphingolipidome of AD research.

METHODS

Cell membrane extraction from human brain tissue

All tissue samples were obtained from the UC Davis Alzheimer's Disease Research Center brain bank. Tissue samples were homogenized and resuspended in homogenization buffer containing 0.25 M sucrose, 20 mM HEPES-KOH (pH 7.4), and a 1:100 protease inhibitor cocktail mixture. Cells were lysed on ice using a probe sonicator operated with alternating on and off pulses of 5 and 10 s, respectively. Lysates were pelleted by centrifugation at 9000xg for 10 min to remove the nuclear fraction and cell debris. The supernatant was transferred to high-speed tubes, loaded onto a Beckman Optima TLX Ultra-centrifuge at 4°C, and centrifuged at 200,000 x g for 45 min in series to remove other nonmembrane subcellular fractions. The resulting cell membrane pellet was stored at - 20°C until further processing. Optimizations to this approach have been shown to generate a purified cell membrane pellet (6).

Enzymatic Release and Purification of N-Glycans

Proteins were suspended with 100 µL of 100 mM NH₄HCO₃ in 5 mM dithiothreitol and heated at 100°C for 10s to thermally denature the proteins. To release the glycans, 2 µL of peptide N-glycosidase F was added to the samples, followed by incubation in a microwave reaction at 60°C for 10 min to accelerate N-glycans release. Samples were incubated for 18 h at 37°C to hydrolyze the N-glycans. The reaction was quenched with 350 µL of water followed by ultracentrifugation at 200,000 x g to separate the N-glycans and the membrane fraction (MF) containing our lipids and de-glycosylated proteins. The released N-glycans were purified by solid-phase extraction using porous graphitized carbon (PGC) packed cartridges. The cartridges

were first equilibrated with nanopure water and a solution of 80% (v/v) acetonitrile and 0.05% (v/v) trifluoroacetic acid in water. The dried samples were solubilized, loaded onto the cartridge, and washed with nanopure water to remove salts and buffer. N-Glycans were eluted with a solution of 40% (v/v) acetonitrile and 0.05% (v/v) trifluoroacetic acid in water, then dried by vacuum centrifugation, and reconstituted in 30 μ l of water prior to mass spectrometric analysis.

Release and Purification of Glycosphingolipids

Palleted membrane fraction underwent a folch extraction following established procedure (7). In brief, samples were resuspended in a mixture of 3:8:4 (v/v/v) of water/methanol and chloroform. Samples were homogenized with sonication for 10 min, and centrifuged at 20,000 x g for 1 min. The supernatant was collected and 100 μ l of 0.1 M potassium chloride was added to isolate the methanol upper layer where enriched GSL's are found. The enriched GSL top layer was collected and dried under vacuum centrifugation. GSL's were purified using C8 solid phase extraction. Solid phase extraction C18 columns were activated with 1:1 methanol/water followed by 1:1 methanol/isopropanol. Conditioning with 1:1 methanol/water and elution with 1:1 methanol/isopropanol. Purified GSL's were dried down under vacuum at room temperature prior to LC-MS/MS analysis.

Glycomics Analysis by LC-MS/MS

Purified brain N-glycans were analyzed using an Agilent nano-LC/chip Q-ToF MS system. The nano-LC system employed a binary solvent consisting of A (0.1% formic acid in 3% acetonitrile in water (v/v)) and B (0.1% for-mic acid in 90% acetonitrile in water (v/v)). Samples were enriched and separated on the Agilent HPLC-Chip comprised of a 40 nL enrichment column and a 75 μ m x

43 mm ID analytical column both packed with porous graphitized carbon in 5 μm particle size. The sample was delivered by the capillary pump to the enrichment column at a flow rate of 3 $\mu\text{L min}^{-1}$ and separated on the analytical column by the nano-pump at a flow rate of 0.3 $\mu\text{L min}^{-1}$ with a gradient that was previously optimized for N-glycans: 0% B, 0-2.5 min; 0-16% B, 2.5-20 min; 16-44% B, 20-30 min; 44-100% B, 30-35 min; and 100% B, 35-45 min followed by pure A for 20 min of equilibration. MS spectra were acquired at 1.5 s per spectrum over a mass range of m/z 600–2000 in positive ionization mode. Mass inaccuracies were corrected with reference mass m/z of 1221.991.

N-Glycan compositions were identified using MS and MS/MS data as well as an in-house retrosynthetic library based on the mammalian N-glycan biosynthetic pathway. Deconvoluted masses were compared to theoretical masses using a mass tolerance of 20 ppm and a false discovery rate of 0.5% on the Agilent MassHunter software version B.7. Relative abundances were determined by integrating peak areas for observed glycan masses, averaging abundances from instrumental triplicates and normalizing to the summed peak areas of all glycans detected.

Purified GSL's were reconstituted in 100 μl solution of 1:1 methanol/water and analyzed using an Agilent nano-LC/chip Q-ToF MS system with a C18 microfluid chip. A binary gradient consisting of (A) 20 mM ammonium acetate and 0.1% acetic acid in water, and (B) 20 mM ammonium acetate and 0.1% acetic acid in 85:15 (v/v) methanol/isopropanol was used to separate the GSLs at a flow rate of 0.3 $\mu\text{l}/\text{min}$. Fragmentation was achieved by collision-induced dissociation (CID) with nitrogen gas at collision energies of around 25V. Data was processed with Agilent MassHunter B.08 software. GSL structures were determined based on m/z , RT, and

tandem data. Libraries were then created based on mass, RT, GSL composition and analyzed using MassHunter Software Profinder.

REFERENCES

1. C. L. Masters, *et al.*, Alzheimer's disease. *Nat. Rev. Dis. Prim.* **1**, 1–18 (2015).
2. H. Haukedal, K. K. Freude, Implications of Glycosylation in Alzheimer's Disease. *Front. Neurosci.* **14** (2021).
3. R. Tarawneh, Biomarkers: Our Path Towards a Cure for Alzheimer Disease. *Biomark. Insights* **15** (2020).
4. M. Toepper, Dissociating normal aging from Alzheimer's disease: A view from cognitive neuroscience. *J. Alzheimer's Dis.* **57**, 331–352 (2017).
5. F. Panza, M. Lozupone, D. Seripa, B. P. Imbimbo, Amyloid- β immunotherapy for alzheimer disease: Is it now a long shot? *Ann. Neurol.* **85**, 303–315 (2019).
6. Q. Li, Y. Xie, M. Wong, M. Barboza, C. B. Lebrilla, Comprehensive structural glycomic characterization of the glycocalyxes of cells and tissues. *Nat. Protoc.* **15** (2020).
7. M. Wong, G. Xu, D. Park, M. Barboza, C. B. Lebrilla, Intact glycosphingolipidomic analysis of the cell membrane during differentiation yields extensive glycan and lipid changes. *Sci. Rep.* **8**, 1–10 (2018).
8. H. Mi, *et al.*, PANTHER version 7: Improved phylogenetic trees, orthologs and collaboration with the Gene Ontology Consortium. *Nucleic Acids Res.* **38**, D204–D210 (2009).
9. J. Lee, *et al.*, Spatial and temporal diversity of glycome expression in mammalian brain. *Proc. Natl. Acad. Sci.* **117**, 28743–28753 (2020).
10. E. Bieberich, Synthesis, Processing, and Function of N-glycans in N-glycoproteins. *Adv Neurobiol* **9**, 47–70 (2014).
11. A. C. Vieira, *et al.*, Glycomic analysis of tear and saliva in ocular rosacea patients: The search for a biomarker. *Ocul. Surf.* **10**, 184–192 (2012).
12. D. Park, *et al.*, Enterocyte glycosylation is responsive to changes in extracellular

- conditions: implications for membrane functions. *Glycobiology* **27**, 847–860 (2017).
13. D. J. Becker, J. B. Lowe, Fucose: Biosynthesis and biological function in mammals. *Glycobiology* **13** (2003).
 14. H. E. Murrey, L. C. Hsieh-Wilson, The chemical neurobiology of carbohydrates. *Chem. Rev.* **108**, 1708–1731 (2008).
 15. E. Oliveros, *et al.*, Sialic acid and sialylated oligosaccharide supplementation during lactation improves learning and memory in rats. *Nutrients* **10** (2018).
 16. A. Dityatev, *et al.*, Polysialylated neural cell adhesion molecule promotes remodeling and formation of hippocampal synapses. *J. Neurosci.* **24**, 9372–9382 (2004).
 17. T. Ariga, M. P. McDonald, R. K. Yu, Role of ganglioside metabolism in the pathogenesis of Alzheimer's disease - A review. *J. Lipid Res.* **49**, 1157–1175 (2008).
 18. R. L. T. Schnaar, T. Kinoshita, Chapter 11 Glycosphingolipids. *Essentials Glycobiol. 3rd Ed.*, 1–11 (2017).

SUPPLEMENTARY DATA

Table S1: Human brain tissues of control and AD subjects used in this study. Corresponding parameters include sex, ethnicity, BRAAK score, and sections used lateral pre-frontal cortex (LPFC), lateral cerebellar cortex (LCbC), and medial temporal cortex (MTC).

PATHDX1	SEX	ETHNICITY	BRAAK	Sections
Normal Brain	M	White	2	LPFC LCbC
Normal Brain	M	White	0	LPFC LCbC MTC
Normal Brain	F	White	1	LPFC LCbC
Normal Brain	M	White	5	LPFC LCbC MTC
Normal Brain	F	White	1	LPFC LCbC
Normal Brain	F	White	2	LPFC LCbC MTC
Normal Brain	F	African American	3	LPFC LCbC MTC
Normal Brain	F	White	2	LPFC LCbC
Normal Brain	F	White	1	LPFC LCbC MTC
Normal Brain	F	White	2	LPFC LCbC MTC
Definite AD	M	White	4	LPFC MTC
Definite AD	F	White	5	LPFC LCbC MTC
Definite AD	F	White	5	LPFC MTC
Definite AD	M	African American	5	LPFC LCbC
Definite AD	M	White	6	LPFC LCbC MTC
Definite AD	F	White	5	LPFC LCbC
Definite AD	F	African American	6	LPFC LCbC MTC
Definite AD	F	Asian	6	LPFC LCbC MTC
Definite AD	F	White	6	LPFC LCbC MTC
Definite AD	M	White	6	LPFC MTC

Table S2: List of statistically significant ($p < 0.05$) N-glycans between the lateral cerebellar cortex between controls and AD subjects. N-glycan symbol key: yellow circles, galactose (Gal); green circles, mannose (Man); blue squares, N-acetylglucosamine (GlcNAc); red triangles, fucose (Fuc); purple diamonds, N-acetylneuraminic acid (Neu5Ac). Student's t test at confidence intervals of 95% and two-tailed p values, assuming unequal variance.

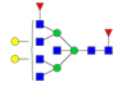
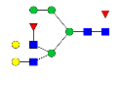
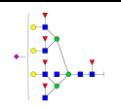
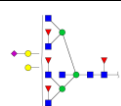
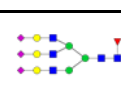
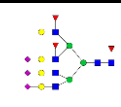





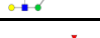





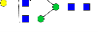

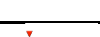

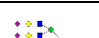










Glycan	Class	Structure	p value
5720	C-F		0.012
6420	H-F		0.044
6751	C-FS		0.039
5751	C-FS		0.011
6513	C-FS		0.014
7633	C-FS		0.044

Table S3: List of statistically significant ($p < 0.05$) N-glycans between the frontal cortex between controls and AD subjects. N-glycan symbol key: yellow circles, galactose (Gal); green circles, mannose (Man); blue squares, N-acetylglucosamine (GlcNAc); red triangles, fucose (Fuc); purple diamonds, N-acetylneuraminic acid (Neu5Ac). Student's t test at confidence intervals of 95% and two-tailed p values, assuming unequal variance.

Glycan	Class	Structure	p-value
7610	C-F		0.015
6610	C-F		0.013
5640	C-F		0.037
7632	C-FS		0.024
4311	C-FS		0.012
6621	C-FS		0.036
6611	C-FS		0.039
7723	C-FS		0.034
6531	CH-FS		0.001
6521	CH-FS		0.009
6421	H-FS		0.007

Table S4: List of statistically significant ($p < 0.05$) N-glycans between the temporal cortex between controls and AD subjects. N-glycan symbol key: yellow circles, galactose (Gal); green circles, mannose (Man); blue squares, N-acetylglucosamine (GlcNAc); red triangles, fucose (Fuc); purple diamonds, N-acetylneuraminic acid (Neu5Ac). Student's t test at confidence intervals of 95% and two-tailed p values, assuming unequal variance.

Glycan	Class	Structure	p value
4400	CH		0.032
4200	HM		0.037
5320	H-F		0.016
6420	H-F		0.008
6320	H-F		0.024
6410	H-F		0.047
5410	CH-F		0.036
5420	CH-F		0.047
4520	CH-F		0.027
4510	CH-F		0.030
4410	CH-F		0.014
5530	CH-F		0.004
7640	C-F		0.028
3410	C-F		0.038

5402	C-S		0.001
7604	C-S		0.036
5411	CH-FS		0.037
4311	C-FS		0.018
6631	C-FS		0.029
7631	C-FS		0.028
5432	C-FS		0.033
7623	C-FS		0.026
6641	C-FS		0.047
7714	C-FS		0.033
6722	C-FS		0.033
7722	C-FS		0.036

CHAPTER IV

Glycosylation alterations in serum of Alzheimer's disease patients show widespread changes in N- glycosylation of proteins related to immune function, inflammation, and lipoprotein metabolism

Abstract

There is an increased need for the development of novel blood-based biomarkers for early detection, prevention, or intervention in Alzheimer's Disease (AD), particularly in ethnically diverse cohorts. This study sought to determine whether serum glycopeptide analysis holds potential for identifying novel diagnostics and prognostics of AD.

The study involved 195 participants including 96 patients with an AD diagnosis and 99 controls with no cognitive deficit, with equal age and sex distribution, and including individuals of white, Hispanic, and African American ethnicity. Utilizing a validated analytical mass spectrometry method, we monitored the site-specific glycosylation of 52 serum glycoproteins. Data processing and both univariate and multivariate statistical analyses were performed to assess the discriminatory potential of serum glycopeptides.

Partial least squares discriminant analysis (PLS-DA) revealed that changes in overall sialylation and fucosylation of serum glycoproteins may be indicators of AD disease state. In particular, loss of fucosylation of immunoglobulin G1 (IgG1) and IgG2 were indicative of AD diagnosis. Individual glycopeptides analysis also found separation between the AD patients and normal controls, highlighting alterations in non-fucosylated, sialylated glycopeptides on complement proteins and apolipoprotein B. Of the 35 individual glycopeptides that were differentially expressed in AD patients compared with controls, 24 remained statistically significant after adjustment for age, sex, apolipoprotein E (APOE) genotype, body mass index (BMI), and ethnicity, and included proteins involved in immune function (e.g. immunoglobulins and acute phase proteins), as well as proteins involved in lipoproteins metabolism.

The results of this study suggest that serum glycoprofiling may be a promising approach for biomarker discovery to not just identify those at risk for AD but also potentially to identify novel intervention targets.

INTRODUCTION

Alzheimer's disease (AD) is a chronic neurodegenerative disease that begins decades before the onset of symptoms and discernible dementia [1]. Medications for the treatment for AD in the later stages of disease have been elusive with modern therapeutic approaches only being able to slow the progression of disease, but not prevent or reverse it [1]. The current techniques for AD detection rely on cerebrospinal fluid (CSF) and plasma biomarkers (e.g. the ratio of A β 42 to A β 40) and images from positron emission tomography (PET) to evaluate the extent of neurodegeneration in the brain. These methods are based on the hallmark characteristics of AD, namely amyloid-beta (A β) deposition - neurofibrillary tangles involving hyperphosphorylated tau, and neurodegeneration[2–4]. However, CSF-based biomarkers require invasive sample collection, while PET imaging-based detection is costly for screening purposes. Furthermore, these detection approaches are generally uninformative about how to intervene to prevent or slow the progression of the disease. Therefore, early actionable detection approaches that could lead to the development of new disease prevention strategies are urgently needed.

Glycosylation is a common post-translational modification that affects protein structure and function with diverse glycans. Multiple studies have revealed aberrant glycosylation in AD-related proteins, including amyloid precursor protein (APP), tau, Beta-secretase 1 (BACE1), and Nicastrin (NCSTN)[5–8]. Furthermore, dysregulated glycosylation in AD brains affects multiple biological processes, such as neuroinflammation, cell adhesion, and cell signaling [8]. Plasma glycan-based measurements have proven to be useful for the detection of other diseases including ovarian cancer, and breast cancer [9,10].

Modern liquid chromatography- mass spectrometry (LC-MS) analysis employing dynamic multiple reaction monitoring (dMRM) technology has enabled large-scale glycoproteomic profiling of blood. Here, we used an established MRM method to evaluate the potential for plasma or serum based glycoproteomic profiling as a viable biomarker approach for AD [11,12]. We used serum samples obtained from 96 AD patients and 99 age- and gender matched cognitively normal controls whose samples are part of the UC Davis Alzheimer's Disease Research Center biorepository, to quantify serum glycopeptides of the most abundant serum proteins, and determine the potential of serum glycoproteomic profiling as a novel biomarker approach for AD.

EXPERIMENTAL

Study Design

A power calculation was conducted on an exploratory set of samples involving 48 serum samples. Sample size calculation was performed prior to the study design as multiple two-sample T-tests with an FDR-adjusted rate of 0.05, and a K factor of 22. A sample size of 100 per group was determined to be an adequate number of participants for a power of 80%. In this study, samples from 195 total participants were analyzed, which included 99 participants with no cognitive deficit as per clinical diagnosis, and 96 participants with an AD diagnosis. All AD patients had a clinical AD diagnosis made within one year of the blood draw based on the UC Davis Alzheimer's Disease Research Center (ADRC) clinical diagnosis criteria. The diagnosis criteria for AD involved autopsy confirmed with BRAAK state four or higher with likelihood of AD moderate to high and the rest of whom were 'probable AD' based on ADRC clinical diagnosis criteria. The cohorts were selected to have equal percentages of males and females in both groups. In the control group, 50% of participants were male while in the AD group 51% were male. **Table 1**

summarized the demographic data of all participants including age, sex, BMI, APOE genotype, and ethnicity, among other parameters. Among AD patients, 13.3% were African American, 10% were Hispanic, and 77% were White. Among controls, 20% were African American, 27% were Hispanic, and 53% were White. The median age was 79 [IQR: 73-83] for AD patients and 78 [IQR:73-82] for the normal controls. The median body mass index (BMI) was 26.4 [IQR: 23.83-29.64] for AD patients and 27.70 [IQR: 25.34-31.01] for the normal controls.

Table 1 Demographics data of participants with Alzheimer's Disease and controls.

	Control	AD
n	99	96
Age (years) (median [IQR])	78[73-82]	79[78-83]
Gender=Male (%)	49 (49.5)	49 (51)
BMI (median [IQR])	27.7[25.3-31]	26.4[27-29.5]
APOE genotype		
e22 (%)	1(1.08)	0(0)
e23 (%)	13(14)	1(1.06)
e24 (%)	1(1.08)	3(3.19)
e33 (%)	55(59.1)	35(37.2)
e34 (%)	23(24.7)	42(44.7)
e44 (%)	0(0)	13(13.8)
APOE4 Positivity (%)	30 (30.3)	60 (62.5)
Ethnicity		
African American (%)	20(20.4)	12(12.5)
Hispanic (%)	26(26.5)	10(10.4)
White (%)	52(53.1)	74(77.1)
Verbal Memory Score (median [IQR])	0.5[-0.13-0.94]	-1.4[-1.3--1]
Executive Function Score (median [IQR])	0.15[-0.11-0.48]	-0.72[-0.63--0.47]
Semantic Memory Score (median [IQR])	0.66[-0.013-1.2]	-0.33[-0.42-0.17]
Spatial Score (median [IQR])	0.45[-0.11-0.82]	-0.51[-0.47-0.14]
CDR (median [IQR])	0[0-0.38]	4.5[5.3-7]
Total White Matter Hypertension (median [IQR])	5.7[2.7-13]	8.4[15-18]
Intracranial Volume (median [IQR])	1300[1200-1400]	1300[1300-1400]

Note:

Cognitive function scores and brain measurements had missing values in both groups. The number of data points for each measurement was listed in supplemental table 2.

Sample Preparation

Serum samples were processed using a well-established protocol employing a dynamic multiple reaction monitoring (dMRM) MS method [13]. Briefly, serum samples were reduced with dithiothreitol, alkylated with iodoacetamide, and digested with trypsin in a water bath at 37°C for 18 h. For glycopeptide quantitative analysis, tryptic digested samples were analyzed directly with no further enrichment. Serum samples were then spiked with a synthetic peptide standard for inter-batch reproducibility monitoring.

UPLC–ESI–QqQ–MS Analysis of Serum Glycoproteomic

The mixed samples were analyzed using an ultra high-performance liquid chromatography coupled to triple quadrupole mass spectrometry as previously described [12]. Briefly, 2 µL samples were injected and separated by an Agilent Eclipse plus C18 column (rapid resolution high definition (RRHD) 1.8µm, 2.1×150 mm) coupled with a C18 guard column (RRHD 1.8µm, 2.1×5 mm). An Agilent 1290 infinity LC system (Agilent Technologies, Santa Clara, CA) was used, and the separation was performed with a 70 min binary gradient consisting of solvent A of 3% acetonitrile, 0.1% formic acid, solvent B of 90% acetonitrile, and 0.1% formic acid in nano pure water (v/v) at a flow rate of 0.5mL/min. The UHPLC system was coupled to an Agilent 6490 triple quadrupole (QQQ) mass spectrometer (Agilent Technologies, Santa Clara, CA) with the MS conditions previously described [14]. The dMRM method used predetermined collision induced dissociation from previously determined study, however LC retention times were modified. A deep learning method PB-Net (Peak Boundary Neural Network) was used for fully automatic chromatographic peak integration [15]. Relative glycopeptide abundances were calculated using

the area under the curve of the glycopeptide peak and normalized to its reference non-glycosylated peptide as previously described [13].

Data Processing and Statistical Analysis

Instrument reproducibility was monitored with commercially available digested serum samples (Sigma-Aldrich) as quality controls. The digested serum pool was used as a quality control for monitoring MRM transitions every ten samples for a total of 20 technical replicates. A hierarchical clustering was then performed using the relative abundance of all glycopeptides with average linkage to detect any outlier samples. Samples were determined to be outliers at a branch cutoff at height 15.5 using hierarchical clustering and were removed from analysis. The coefficient of variation (CV) was calculated for all glycopeptides based on these pooled serum samples. Glycopeptides that were below the limit of quantitation for the instrument or with CV>30% were excluded from analysis. The naming convention of the glycopeptides used throughout the text follows the convention, Protein_Glycosite_Glycan. For example, IgG1_297_5510 reads Immunoglobulin G1 at glycosite N297 with N-glycan composition of Hex₍₅₎HexNAc₍₅₎Fuc₍₁₎Neu5Ac₍₀₎.

The fractions of sialylated and fucosylated peptides were calculated as the sum of relative glycopeptide abundances of non-, mono-, di-, or poly-glycosylated peptides relative to that of the total peptides. Relative glycopeptide abundances of individual glycopeptides and the fractions of sialylated and fucosylated peptides were used in subsequent analyses. All statistical analyses were performed using the R statistical package (R version 4.1.0). Linear models were constructed for univariate and multivariate analysis that included each potential covariate separately. Each simple multivariate model had one covariate at a time: glycopeptide abundance ~ Diagnosis +

covariate. These simple multivariate models were compared to the univariate model, which included diagnosis group as the only variable to evaluate the impact of these covariates on glycopeptide concentrations. Potential covariates included age, sex, ethnicity, presence of the ApoE4 allele, and BMI. Linear models with interaction terms were used to analyze the sex-by-AD diagnosis interaction and ethnicity-by-AD diagnosis interaction: glycopeptide abundance ~ diagnosis + sex + diagnosis * sex or glycopeptide abundance ~ diagnosis + ethnicity + Diagnosis * ethnicity. For sex-by-AD diagnosis interaction, a post hoc analysis was done to estimate the sex specific diagnosis effects on serum glycopeptide abundance.

Differential expression analysis was performed as linear models using the limma package in R. Coefficients related to diagnosis were tested according to the null hypothesis (being zero) using t-tests moderated in a Bayesian fashion. Raw p-values were then adjusted for multiple hypothesis testing using the Benjamini-Hochberg (HB) correction. The differences in glycopeptide abundance between normal control and AD are presented as natural log fold-change.

A partial least square discriminant analysis (PLS-DA) was performed to assess the discriminatory potential of serum glycopeptides. We scaled glycopeptide abundances to the variance of 1 and conducted leave-one-out cross-validation (LOOCV) to identify the best number of latent components using 1 through 20 with the train() function from the caret package. The importance of independent variables in the PLS-DA model was measured using variable importance in projection (VIP) scores. The testing set was used to evaluate the classification accuracy of the PLS-DA model developed with training. Spearman's correlation analysis was used to evaluate the association between glycopeptides, cognitive scores (SENAS scores) and clinical dementia rating (CDR).

RESULTS

A hierarchical clustering was first performed to target outlier samples that can result in false positives. The hierarchical clustering results show three outlier samples that were excluded from all further analysis (B10, C13, and A67) as shown in **Figure S1**. CVs were calculated for all 372 glycopeptides monitored in this mass spectrometry study and their distribution is listed in **Figure S2**. Of the 372 glycopeptides monitored 14 glycopeptides had CV values greater than 30% as listed in **Table S1**.

Fucosylated and Sialylated Glycopeptides in AD

Glycopeptides were grouped by their fucosylation and sialylation status separately. We then assessed whether the fucosylation and sialylation status of glycopeptides discriminates serum samples from AD patients and normal controls by looking at patterns of fucosylated and sialylated glycopeptides generated from PLS-DA analysis. The fucosylation and sialylation status of glycopeptides did not explicitly separate AD samples from normal controls with PLS-DA models (**Figure 1A and 1C**). However, the models show that several changes in overall sialylation and fucosylation of serum glycoproteins may be indicators of AD disease state. The PLS-DA model for fucosylation status had 12 glycopeptides with VIP scores > 1.5 . A VIP score > 1.5 is considered to enable discrimination between groups. Notably, non-fucosylated and mono-fucosylated immunoglobulin G1 (IgG1) and IgG2 had high contributions to the model with VIP score > 2 , indicating the fucosylation status of IgG1 and IgG2 may be potential biomarkers for AD (**Figure 1B**). The PLS-DA analysis for sialylation identified 19 glycopeptides with VIP scores > 1.5 , which includes inflammation response glycoproteins such as Kininogen-1 (KNG1) and immune response

glycoproteins such as Complement factor I (CFAI) as well as lipid metabolism glycoproteins Apolipoprotein C3 (APOC3) and Clusterin (CLUS) (**Figure 1D**).

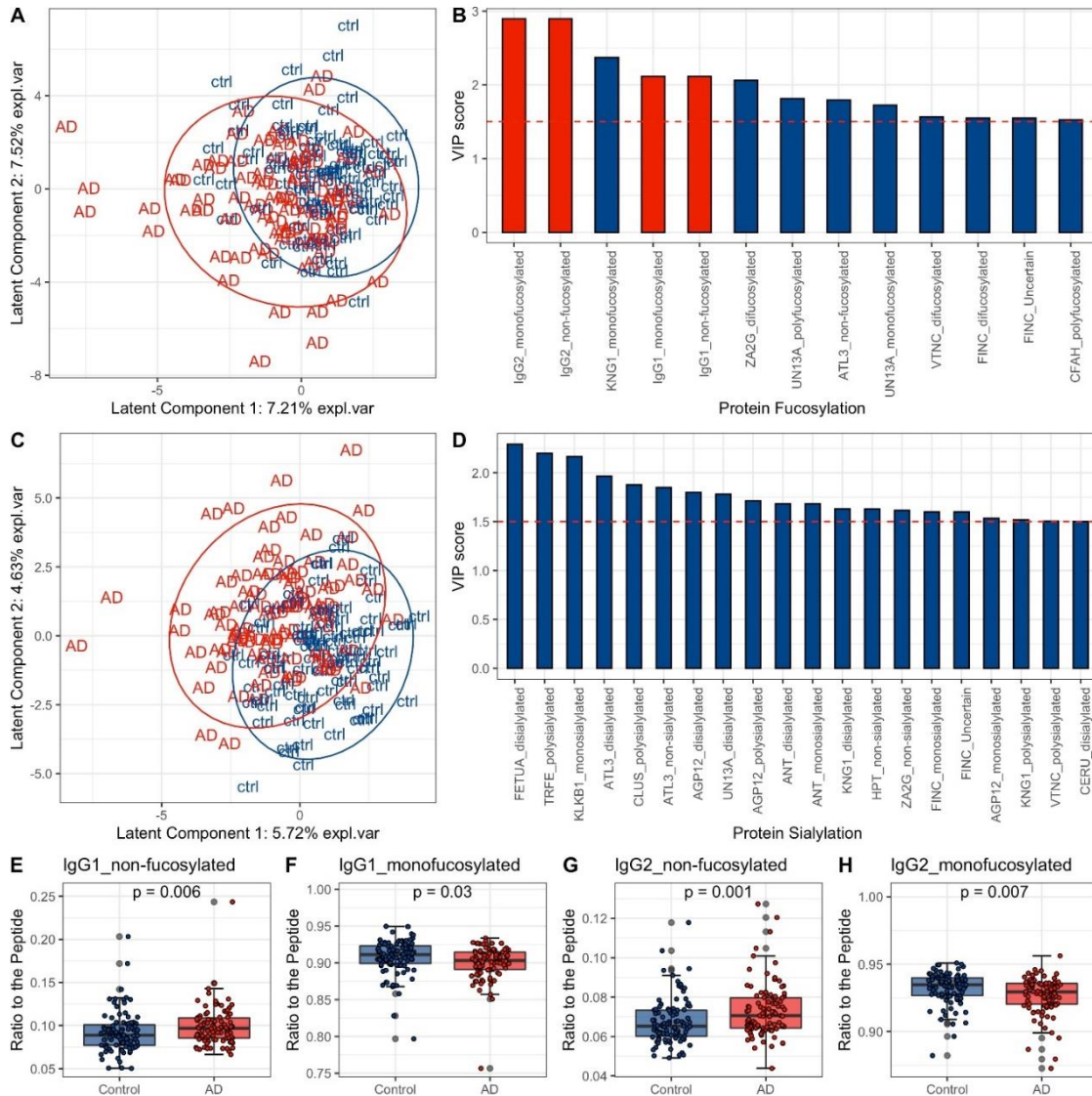


Figure 1: Changes in fucosylation and sialylation status in serum samples from patients with clinically diagnosed Alzheimer’s Disease (AD) compared to controls (ctrl) using partial least squares-discriminant analysis (PLS-DA). **A)** The scores plot shows the distribution of subjects across latent components 1 and 2 given the PLS-DA model for fucosylation status. **B)** Variables with variable importance in projection (VIP) scores ≥ 1.5 and their VIP scores in the PLS-DA model for fucosylation status. Variables colored in red are those selected for differential analysis and are visualized in E-H. **C)** The scores plot shows the distribution of participants across latent components 1 and 2 given the PLS-DA model for sialylation status. **D)** Variables with VIP scores ≥ 1.5 and their VIP scores in the PLS-DA model for sialylation status. **E-H)** Boxplots showing the

differences in abundance of non-fucosylated and monofucosylated immunoglobulin G1 (IgG1) and IgG2 proteins from control and AD samples.

Identification of Aberrant Fucosylated or Sialylated Glycopeptides in AD

The PLS-DA analysis for fucosylation and sialylation showed that AD and control samples were located in two clusters in the score plot with some overlap. We then identified fucosylated and sialylated glycopeptides that drive the discrimination for AD versus normal controls using differential analysis. For fucosylation, six statistically significant glycoproteins which correspond to 10 glycopeptides differed (P-values < 0.05) between AD and normal controls in the univariate model, including glycopeptides with high contribution to the fucosylation PLS-DA model (non-fucosylated IgG1, monofucosylated IgG1, non-fucosylated IgG2, monofucosylated IgG2, etc.) (**Figure 1E-H and Figure S3A**). For sialylation, eight proteins with 10 glycopeptides differed between AD and normal controls (**Figure S3B**).

Glycopeptide Signatures of AD

PLS-DA analysis was used to model the individual glycopeptide data and found separation between the AD patients and normal controls, though as with the fucosylation and sialylation data there was overlap between the groups (**Figure 2A**). The model had 51 glycopeptides that had a VIP score >1.5, including proteins involved in lipid metabolism (APOB, APOC3, APOH), immunity (IgG1, IgG2, IgM), and inflammation response (CO3, CFAI, VTNC, ANT) (**Figure 2B**). We then determined whether there were significant differences between patients and controls in the abundances of the glycopeptides that had high contribution to the PLS-DA model using differential analysis. CFAI_494_5402 and CO3_85_5200 were significantly increased and

APOB_983_5401 was significantly decreased in the AD patients compared to controls (P-values < 0.05). The three glycopeptides were all non-fucosylated (**Figure 2C-E**).

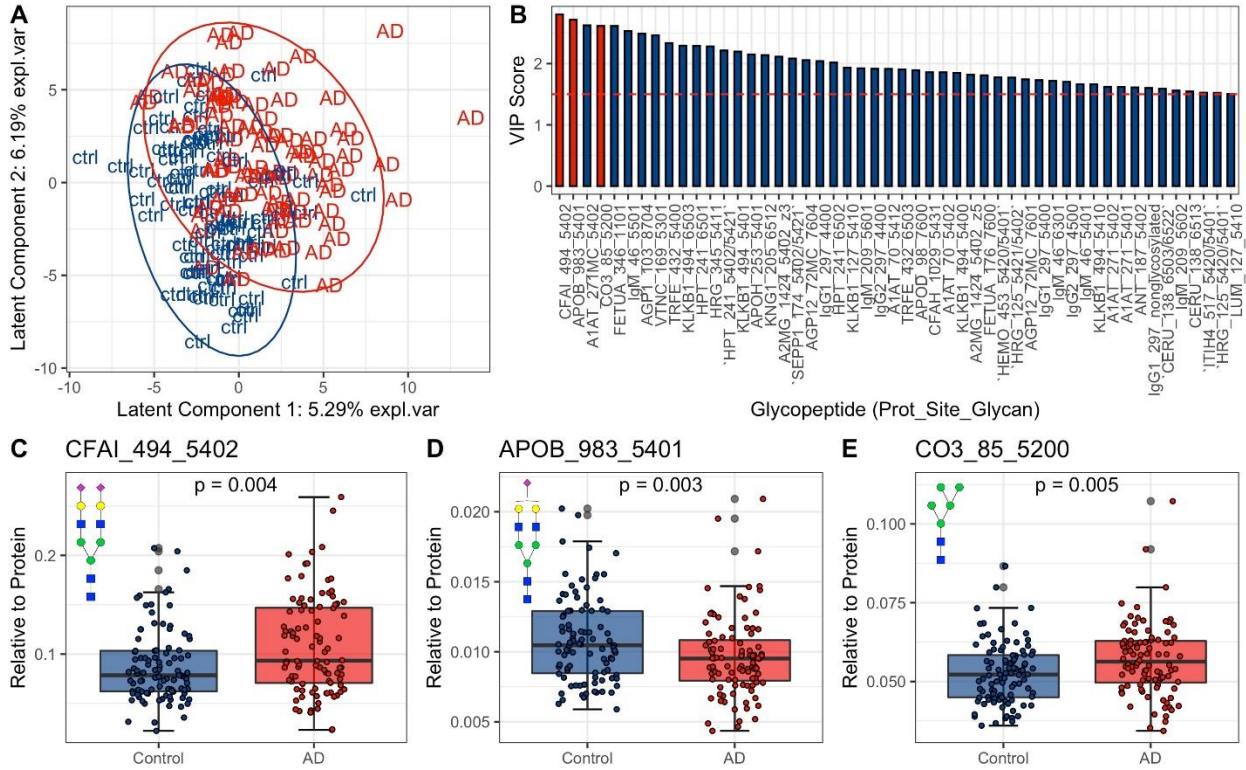


Figure 2: Changes in serum glycopeptide abundance in serum samples from Alzheimer's Disease patients compared to controls using PLS-DA. **A)** The scores plot shows the distribution of participants across latent components 1 and 2 given the PLS-DA model for glycopeptides. **B)** Variables with VIP scores ≥ 1.5 and their VIP scores. Variable colored in red are those selected for differential analysis and are visualized in C-E. **C-E)** Boxplots showing the differences in abundances of glycopeptides from control and Alzheimer's Disease (AD) samples. Protein abbreviations: complement factor I (CFAI), Apolipoprotein B (Apolipoprotein B) and Complement C3 (CO3). N-glycan symbol key: yellow circles, galactose (Gal); green circles, mannose (Man); blue squares, N-acetylglucosamine (GlcNAc); red triangles, fucose (Fuc); purple diamonds, N-acetylneuraminic acid (Neu5Ac).

Identification of Aberrant Glycopeptides in AD

We next performed differential analysis to identify which glycopeptide abundances differed in the serum of AD patients vs. normal controls. With the univariate model, among the 372 glycopeptide transitions monitored accounting for 53 out of the 57 glycoproteins, 35 glycopeptide abundances were altered in individuals with AD, including 19 upregulated glycopeptides and 16 downregulated glycopeptides (P-values < 0.05, **Figure 3A**). Among the 35 glycopeptides, which were differentially expressed in AD patients, most belong to proteins involved in immune function, including immunoglobulins and acute phase proteins such as alpha-1 antitrypsin (A1AT), alpha-2-macroglobulin (A2MG), alpha-1-acid-glycoprotein (AGP1), alpha-2-HS-glycoprotein (FETUA), and complement C3 (CO3). After adjusting for sex and age separately, these differences remain statistically significant. With the models adjusting for ethnicity, APOE4, and BMI separately the majority of the differentially expressed glycopeptides remained statistically significant; however, new differences were also detected in these multivariate models as shown in x-axis of **Figure 3A**. In the final multivariate model, all covariates including sex, age, ethnicity, APOE4 status, and BMI were included. This analysis yielded 24 significant AD-associated glycopeptides (**Figure 3A**). The glycopeptides with highest VIP scores in the PLS-DA model, such as CFAI_494_5402, APOB_983_5401, A1AT_271MC_5402, FETUA_346_1101, etc., also change significant across different linear models in the differential analysis (P-values < 0.05), indicating they are important in distinguishing AD patients from controls.

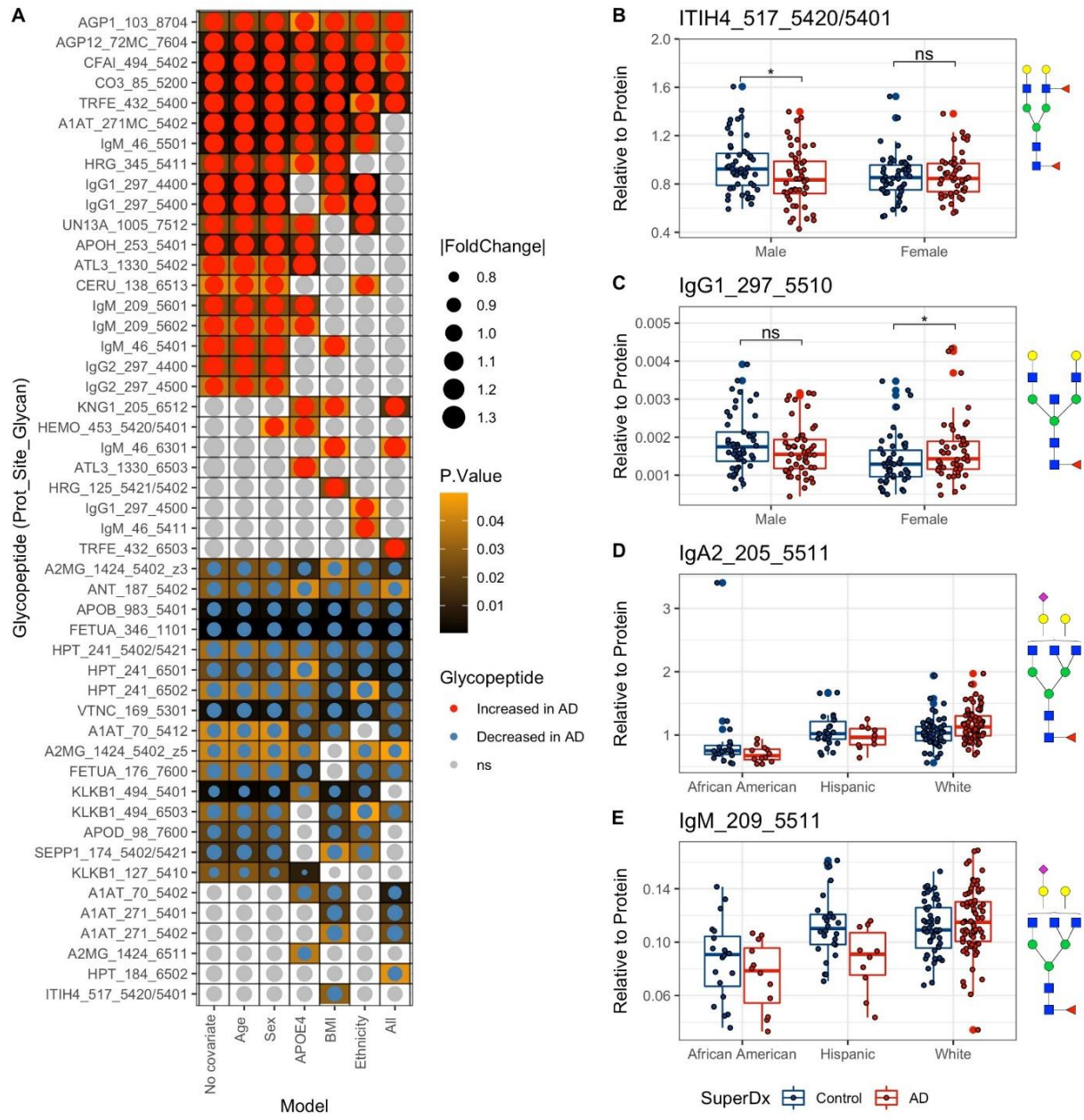


Figure 3: Differential analysis of glycopeptides and the impact of confounders on glycopeptide abundance. **A)** The heatmap shows glycopeptides significantly different in Alzheimer’s Disease patients compared to controls using univariate and multivariate linear regressions. The dot size shows the effect size (absolute fold change). Darker background color refers to smaller p-value (before multiple testing correction). **B-C)** The boxplot shows the sex specific diagnosis effects on serum glycopeptide abundance. Differences with p-value < 0.05 are denoted by asterisk, whereas differences with p>0.05 are denoted as “ns” (not significant). **D-E)** Boxplot showing the ethnicity specific diagnosis effects on serum glycopeptide abundance. Protein abbreviations: Inter-alpha-trypsin inhibitor heavy chain H1 (ITIH), Immunoglobulin G1 (IgG1), Immunoglobulin A2 (IgA2), and Immunoglobulin M (IgM). N-glycan symbol key: yellow circles, galactose (Gal); green circles,

mannose (Man); blue squares, N-acetylglucosamine (GlcNAc); red triangles, fucose (Fuc); purple diamonds, N- acetylneuraminic acid (Neu5Ac).

Potential Confounders

Factors including sex, ethnicity, age, BMI, and ApoE4 genotype had impacts on glycopeptide abundances in serum. Sex and ethnicity were the two major confounders that influenced glycopeptide abundance in controls and AD. We analyzed the contributions of sex and ethnicity on serum glycopeptide abundances as covariates in the linear regression models. Among 372 glycopeptides, 135 glycopeptide abundances differed by sex, including 50 that were significantly higher in females and 85 that were significantly higher in males (adjusted P-values < 0.05, **Figure S4 A**). Thirty-eight glycopeptides significantly differed across ethnicity groups, where KLKB1_127_5410 had the lowest P-value (adjusted P-values<0.05, **Figure S4 B-D**). The impacts of other confounders are showed in **Figure S4 E-G**.

Our study also provided the evidence of sex-by-AD diagnosis and ethnicity-by-AD diagnosis interactions. For example, ITIH4_517_5420/5401 was decreased in male AD patients vs. controls (P-value<0.05), but was not different in female AD patients vs. controls (**Figure 3B**). In contrast, IgG1_297_5510 was increased in AD female patients vs. controls (P-value<0.05), but was not different in male patients vs. controls (**Figure 3C**). For the ethnicity specific effects, Diagnosis had a different effect in glycopeptides such as IgA2 _201_5511, IgM _209_5511 depending on the ethnicity of subjects (**Figure 3, D&E**).

Associations Between Glycopeptides and Clinical Cognitive Scores

Correlation analysis revealed associations between cognitive score and glycopeptides that were important in discriminating AD patients and controls. For example, non-fucosylated

and monofucosylated IgG2, former increased and latter decreased in AD, were positively and negatively correlated with the CDR (**Figure 4, A&B**). The glycopeptide CO3_85_5200, which highly contributed to the PLS-DA model and was increased in AD patients vs. controls, was negatively associated with semantic score, and positively associated with CDR (**Figure 4, C&D**).

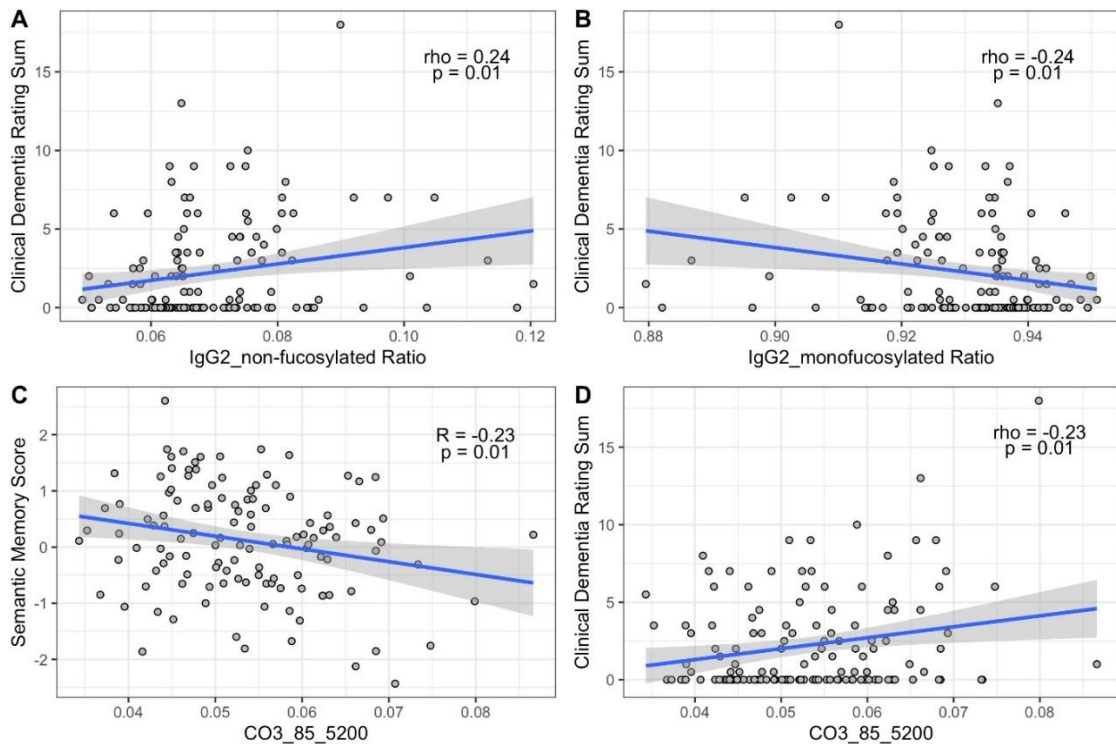


Figure 4: Correlations between glycopeptides and cognitive function measures. **A-B)** Correlations between clinical dementia rating (CDR) sum and IgG2 fucosylation status. **C-D)** Correlations between CO3_85_5200 and semantic memory score and CDR sum. Protein abbreviations: Immunoglobulin G2 (IgG2) and Complement C3 (CO3).

DISCUSSION

In this study we set out to determine whether serum-based glycopeptide analysis may be a useful approach for identifying novel actionable diagnostics for AD. Our results suggested that serum glycopeptide profiling is a promising approach for the development of new biomarkers. Even with mass spectrometry platform, which is not yet tailored for AD-specific glycan markers, and instead is an application of an existing platform developed originally for cancer diagnostics, our results indicate that glycopeptide profiling can uncover important underlying disease mechanisms and point to future biomarker development. The importance of the fucosylation status of IgG in discriminating between controls and AD patients stood out as an important finding (**Figure 1B**). As the most abundant antibody in human blood, the importance of IgG in inflammation, infections, metabolic health and autoimmunity is well established [16,17]. Specifically, an increased abundance of non-fucosylated IgG1 and IgG2 was observed in AD patients compared with controls (**Figure 1, E&G**). Previous investigations have associated dementia with IgG N-glycans, however this previous work lacked site-specific information and did not include a diverse cohort in the population selection [18]. The extent of IgG fucosylation and sialylation has been found previously to be associated with the pro- vs. anti-inflammatory signaling of IgG, with non-fucosylated and non-sialylated IgG preferentially binding to pro-inflammatory Fc γ receptors [19]. Additionally, PLS-DA analysis of glycopeptides was able to separate AD patients from controls (**Figure 2A**) and proteins with VIP score >1.5 also involved immunoglobulins IgG1, IgG2, IgA and IgM among others (**Figure 2B**). Overall, the results highlight the dysregulation of glycosylation of immune response proteins, particularly immunoglobulins, in AD pathology. Other glycopeptides with VIP score >1.5 included proteins involved in lipid

metabolism (APOB, APOC3, APOH) and inflammation response (CO3, CFAI, VTNC, ANT) (**Figure 2B**). For example, the mono-sialylated glycopeptide APOB_N983_5401 was decreased in AD patients compared to controls (**Figure 2D**). Previous studies have shown a relationship between the glycosylation state of lipoprotein-associated proteins and the pro-inflammatory capacity and functionality of their lipoprotein carrier [20,21].

The univariate model showed 35 altered glycopeptide abundances in AD patients from the 372 glycopeptide transitions monitored (**Figure 3A**). All altered proteins are involved in immune function and immune response, including immunoglobulins and acute phase proteins. Interestingly, all immunoglobulin glycopeptides were observed to be increase in AD patients. The study cohort involved equal numbers of males and females, and equal average age in both groups, thus when adjusting for sex and age all glycopeptide remained statistically significant as expected. Age and sex are the covariates that are typically accounted for in biomarker discovery; however, our study suggests that ethnicity is also an important variable that can contribute to variability (**Figure 3A, D & E**). Research on racial disparities in biomarkers for AD has shown that analyses of molecular biomarkers of AD should adjust for race. Given the low sample size for participants of different ethnic groups in this preliminary study, we were not able to fully explore the contribution of ethnicity to the variability in serum glycopeptide profiles. However, our results indicate that serum glycoprofiling may be an exceptionally useful tool for the development of biomarkers in a disease such as AD, in which ethnic-specific differences in disease pathophysiology and biomarker profiles are marked. For example, a differential effect on total tau and phosphorylated tau181 has been shown to differ in African American individuals compared to white individuals [22]. Our data revealed that certain glycopeptides such as

KLKB1_127_5410 strongly distinguished between AD patients and controls only in African American participants, but not in Caucasian or Hispanic participants. These findings highlighted the potential for the development of glycan-based diagnostics that have the ability to identify individuals at risk of developing AD across a broad diversity of individuals (**Figure S4, B-D**).

Of note, our data revealed that non-fucosylated IgG2 was positively correlated with CDR, while mono-fucosylated IgG2 was negatively correlated with CDR (**Figure 4 A and B**). This result suggests a direct relationship between immunoglobulin fucosylation and clinical measures of cognitive function loss. Likewise, a non-sialylated, non-fucosylated glycopeptide of was also positively correlated with CDR CO3 (**Figure 4C**), highlighting the loss of fucosylation and sialylation at specific sites of immune-related proteins as a potential mediator and/or biomarker of AD. Major challenges in the development of blood-based biomarkers for AD include a high degree of patient heterogeneity and the potential existence of multiple clinical phenotypes [23–25]. Importantly, new biomarkers are needed not just for diagnostic purposes, but also for determining prognosis and monitoring therapeutic efficacy. In this pilot work, we sought to determine whether serum-based glycoprofiling may be a useful approach to address these critical questions in the field.

CONCLUSION

Our work for the first time utilized a previously developed MRM analytical method to monitor glycan alterations in serum glycoproteins in a site-specific manner to determine whether serum glycoprofiling can discriminate between AD patients and controls, but also simultaneously point to potential therapeutic approaches to prevent, treat, or reverse AD. Our results suggested that serum glycoprofiling may indeed be a powerful biomarker discovery platform that can be

harnessed to identify new markers in diverse cohorts and new therapeutic targets, particularly those focused on immune-related mechanisms. Future studies including a larger sample size, particularly in ethnically diverse cohorts powered to account for age, sex, and ethnicity, are needed to develop glycan-based biomarkers for AD. Further work to refine the transitions monitored by the MRM method that are specific to AD would improve the sensitivity and specificity of the biomarkers.

References

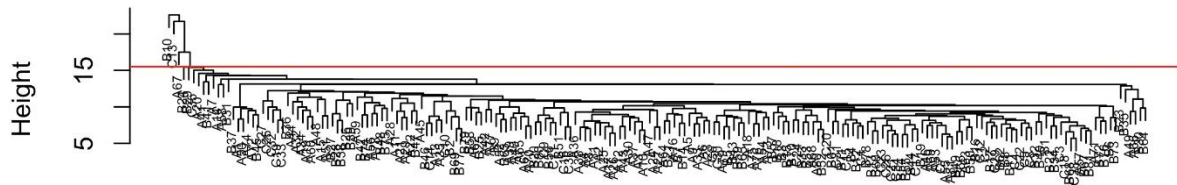
- [1] Association A. 2021 ALZHEIMER ' S DISEASE FACTS AND FIGURES Race , Ethnicity and Alzheimer ' s in America. *Alzheimers Dement* 2021;13:1–104.
- [2] Jack CR, Bennett DA, Blennow K, Carrillo MC, Dunn B, Haeberlein SB, et al. NIA-AA Research Framework: Toward a biological definition of Alzheimer's disease. *Alzheimer's Dement* 2018;14:535–62. <https://doi.org/10.1016/j.jalz.2018.02.018>.
- [3] McKhann GM, Knopman DS, Chertkow H, Hyman BT, Jack CR, Kawas CH, et al. The diagnosis of dementia due to Alzheimer's disease: Recommendations from the National Institute on Aging-Alzheimer's Association workgroups on diagnostic guidelines for Alzheimer's disease. *Alzheimer's Dement* 2011;7:263–9. <https://doi.org/10.1016/j.jalz.2011.03.005>.
- [4] Molinuevo JL, Ayton S, Batrla R, Bednar MM, Bittner T, Cummings J, et al. Current state of Alzheimer's fluid biomarkers. *Acta Neuropathol* 2018. <https://doi.org/10.1007/s00401-018-1932-x>.
- [5] Akasaka-Manyu K, Manyu H. The role of APP o-glycosylation in Alzheimer's disease. *Biomolecules* 2020;10:1–14. <https://doi.org/10.3390/biom10111569>.
- [6] Schedin-Weiss S, Winblad B, Tjernberg LO. The role of protein glycosylation in Alzheimer disease. *FEBS J* 2014;281:46–62. <https://doi.org/10.1111/febs.12590>.
- [7] Schedin-Weiss S, Gaunitz S, Sui P, Chen Q, Haslam SM, Blennow K, et al. Glycan biomarkers for Alzheimer disease correlate with T-tau and P-tau in cerebrospinal fluid in subjective cognitive impairment. *FEBS J* 2020;287:3221–34. <https://doi.org/10.1111/febs.15197>.
- [8] Zhang Q, Ma C, Chin LS, Li L. Integrative glycoproteomics reveals protein n-glycosylation aberrations and glycoproteomic network alterations in Alzheimer's disease. *Sci Adv* 2020;6:1–19. <https://doi.org/10.1126/sciadv.abc5802>.
- [9] Kirmiz C, Li B, An HJ, Clowers BH, Chew HK, Lam KS, et al. A serum glycomics approach to

- breast cancer biomarkers. *Mol Cell Proteomics* 2007;6:43–55.
<https://doi.org/10.1074/mcp.M600171-MCP200>.
- [10] Ruhaak LR, Kim K, Stroble C, Taylor SL, Hong Q, Miyamoto S, et al. Protein-Specific Differential Glycosylation of Immunoglobulins in Serum of Ovarian Cancer Patients. *J Proteome Res* 2016;15:1002–10. <https://doi.org/10.1021/acs.jproteome.5b01071>.
- [11] Hong Q, Lebrilla CB, Miyamoto S, Ruhaak LR. Absolute Quantitation of Immunoglobulin G and Its Glycoforms Using Multiple Reaction Monitoring. *Anal Chem* 2013;85.
<https://doi.org/10.1021/ac4009995>.
- [12] Hong Q, Ruhaak LR, Stroble C, Parker E, Huang J, Maverakis E, et al. A Method for Comprehensive Glycosite-Mapping and Direct Quantitation of Serum Glycoproteins. *J Proteome Res* 2015;14:5179–92. <https://doi.org/10.1021/acs.jproteome.5b00756>.
- [13] Li Q, Kailemia MJ, Merleev AA, Xu G, Serie D, Danan LM, et al. Site-Specific Glycosylation Quantitation of 50 Serum Glycoproteins Enhanced by Predictive Glycopeptidomics for Improved Disease Biomarker Discovery. *Anal Chem* 2019;91:5433–45.
<https://doi.org/10.1021/acs.analchem.9b00776>.
- [14] Hong Q, Lebrilla CB, Miyamoto S, Ruhaak LR. Absolute quantitation of immunoglobulin G and its glycoforms using multiple reaction monitoring. *Anal Chem* 2013;85:8585–93.
<https://doi.org/10.1021/ac4009995>.
- [15] Wu Z, Serie D, Xu G, Zou J. PB-Net: Automatic peak integration by sequential deep learning for multiple reaction monitoring. *J Proteomics* 2020;223:103820.
<https://doi.org/10.1016/j.jprot.2020.103820>.
- [16] Biermann MHC, Griffante G, Podolska MJ, Boeltz S, Stürmer J, Muñoz LE, et al. Sweet but dangerous - The role of immunoglobulin G glycosylation in autoimmunity and inflammation. *Lupus* 2016;25:934–42. <https://doi.org/10.1177/0961203316640368>.
- [17] Plomp R, Ruhaak LR, Uh HW, Reiding KR, Selman M, Houwing-Duistermaat JJ, et al. Subclass-specific IgG glycosylation is associated with markers of inflammation and

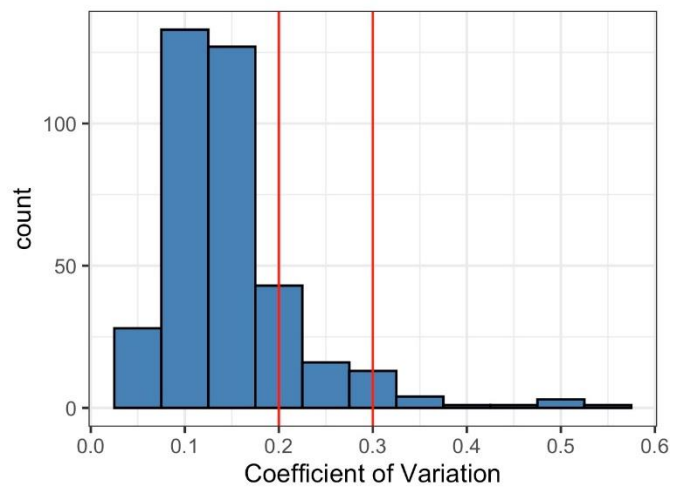
- metabolic health. *Sci Rep* 2017;7:1–10. <https://doi.org/10.1038/s41598-017-12495-0>.
- [18] Zhang X, Yuan H, Lyu J, Meng X, Tian Q, Li Y, et al. Association of dementia with immunoglobulin G N-glycans in a Chinese Han Population. *Npj Aging Mech Dis* 2021;7:1–12. <https://doi.org/10.1038/s41514-021-00055-w>.
- [19] Maverakis E, Kim K, Shimoda M, Gershwin ME, Patel F, Wilken R, et al. Glycans in the immune system and The Altered Glycan Theory of Autoimmunity: A critical review. *J Autoimmun* 2015;57:1–13. <https://doi.org/10.1016/j.jaut.2014.12.002>.
- [20] Krishnan S, Shimoda M, Sacchi R, Kailemia MJ, Luxardi G, Kaysen GA, et al. HDL glycoprotein composition and site-specific glycosylation differentiates between clinical groups and affects IL-6 secretion in lipopolysaccharide-stimulated monocytes. *Sci Rep* 2017;7:1–15. <https://doi.org/10.1038/srep43728>.
- [21] Zhu C, Wong M, Li Q, Sawrey-Kubicek L, Beals E, Rhodes CH, et al. Site-Specific Glycoprofiles of HDL-Associated ApoE are Correlated with HDL Functional Capacity and Unaffected by Short-Term Diet. *J Proteome Res* 2019;18:3977–84. <https://doi.org/10.1021/acs.jproteome.9b00450>.
- [22] Morris JC, Schindler SE, McCue LM, Moulder KL, Benzinger TLS, Cruchaga C, et al. Assessment of Racial Disparities in Biomarkers for Alzheimer Disease. *JAMA Neurol* 2019;76:264–73. <https://doi.org/10.1001/jamaneurol.2018.4249>.
- [23] Hampel H, O’Bryant SE, Molinuevo JL, Zetterberg H, Masters CL, Lista S, et al. Blood-based biomarkers for Alzheimer disease: mapping the road to the clinic. *Nat Rev Neurol* 2018;14:639–52. <https://doi.org/10.1038/s41582-018-0079-7>.
- [24] Tarawneh R. Biomarkers: Our Path Towards a Cure for Alzheimer Disease. *Biomark Insights* 2020;15. <https://doi.org/10.1177/1177271920976367>.
- [25] Henriksen K, Bryant SEO, Hampel H, Trojanowski JQ, Montine TJ, Wyss-coray T, et al. The future of blood-based biomarkers for Alzheimer ’ s disease. *Alzheimer’s Dement* 2014;10:115–31.

SUPPLEMENTARY DATA

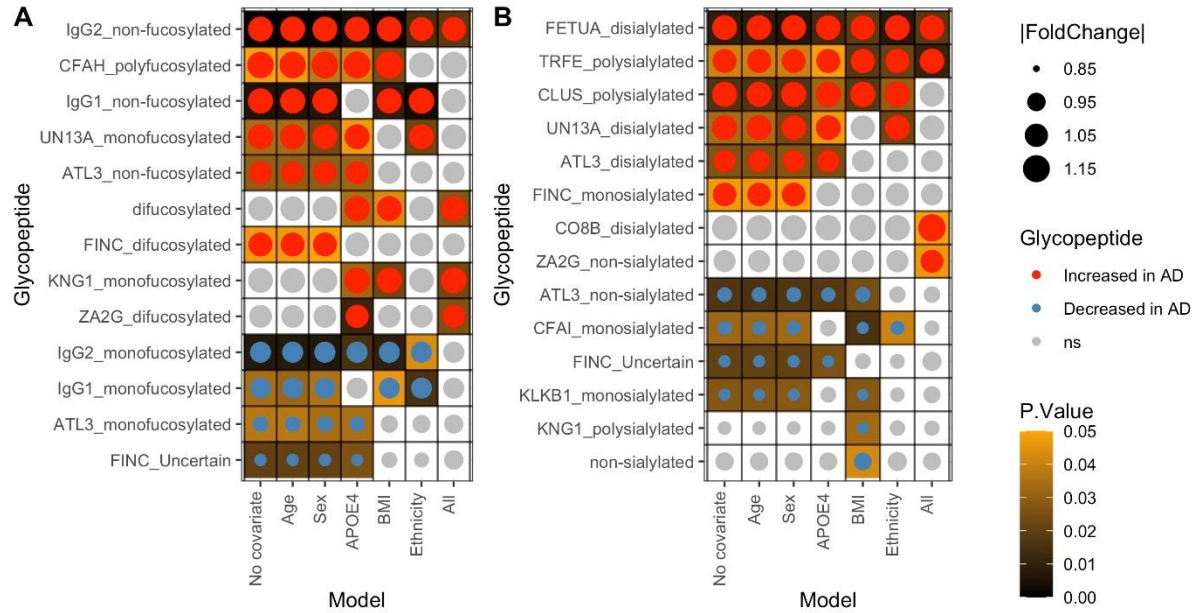
Glycopeptide Sample Clustering to Detect Outliers



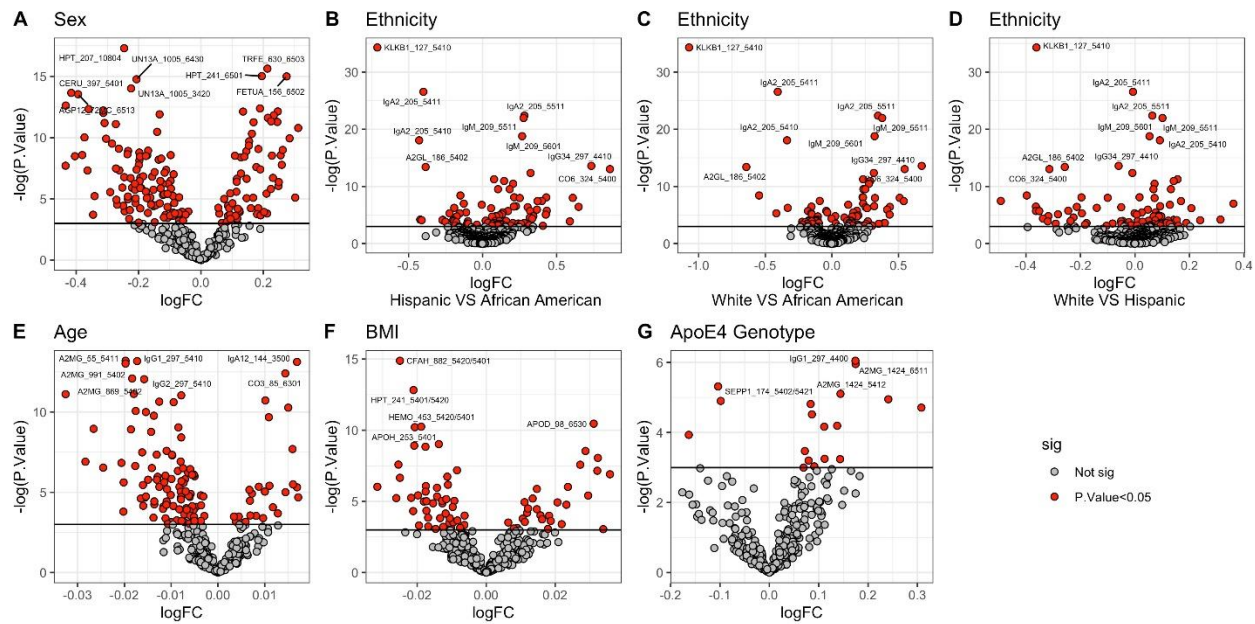
Supplementary Figure S1: Glycopeptide sample outliers identified from hierarchical clustering.



Supplementary Figure S2: The distribution of the CV's of glycopeptides. The red vertical lines show the cutoff at 0.2 (20%) and 0.3 (30%).



Supplemental Figure S3: Differential analysis on the fucosylated and sialylated status of glycopeptides. **A-B)** Heatmaps presented the glycopeptides that differed in AD and control in at least one linear model ($p < 0.05$) by their fucosylation status (**A**) and sialylation status (**B**). The dot size indicates the fold change of the glycopeptide in AD compared to control. Dot color indicates glycoproteins in the serum of AD patients that were down- (blue), upregulated (red), or not significantly changed (grey) compared to controls. The darkness of the background color shows the P-value.



Supplemental Figure S4: The impact of potential confounders on glycopeptide abundance. Red dots showed glycopeptides impacted by each confounder ($p < 0.05$), while grey dots were glycopeptides not impacted. **A)** Volcano plot showing the impact of sex on glycopeptides. Positive and negative log-fold changes indicate that the serum glycopeptide abundances in AD patients were higher or lower in females than males. The glycopeptides with $-\log(P\text{-value}) > 13$ were labeled. **B-D)** Volcano plot showing the impact of ethnicity on glycopeptides with pairwise comparison. The glycopeptides with $-\log(P\text{-value}) > 13$ were labeled. **E)** Volcano plot showing the impact of age on glycopeptides. The glycopeptides with $-\log(P\text{-value}) > 12$ were labeled. **F)** Volcano plot showing the impact of BMI on glycopeptides. The glycopeptides with $-\log(P\text{-value}) > 10$ were labeled. **G)** Volcano plot showing the impact of ApoE4 genotype on glycopeptides. Positive and negative log-fold changes indicate that the serum glycopeptide abundances in AD patients were higher or lower in ApoE4 positive individuals than ApoE4 negative ones. The glycopeptides with $-\log(P\text{-value}) > 5$ were labeled.

Glycopeptide	CV%
A1AT_70_5402	52
A1AT_70_5412	49
A2MG_247_5200	32
A2MG_247_5401_z4	35
A2MG_247_5402	37
AGP12_72MC_6503	34
AGP12_72MC_7604	35
APOC3_74_1210	57
APOC3_74_1300	47
CERU_397_6411	31
CFAI_494_5402	48
HPT_184_5400	31
HPT_241_5412	32
IgM_209_4601	38

Supplementary Table S1: The glycopeptides with CV over 30%.

	Normal	AD
Verbal Memory Score	84	50
Executive Function Score	84	54
Semantic Memory Score	70	54
Spatial Score	69	46
CDR	82	52
Total White Matter Hypertension	61	46
Intracranial Volume	61	46

Supplementary Table S2: The number of data points of cognitive function measurements.